INVESTIGATION OF

DIFFERENTIALLY EXPRESSED GENES BY RNA-SEQ IN

DUCKS (*Anas platyrhynchos*) INFECTED WITH PABV-2

A Thesis

by

ZOE GARNETT KOLKHORST

Submitted to the Office of Graduate and Professional Studies of
Texas A&M University
in partial fulfillment of the requirements for the degree of

MASTER OF SCIENCE

Chair of Committee,	Jeffrey M.B. Musser
Committee Members,	Ian R. Tizard
	Noushin Ghaffari
Head of Department,	Ramesh Vemulapalli

August 2018

Major Subject: Biomedical Sciences

ABSTRACT

Parrot bornaviruses are the etiological agents of proventricular dilatation disease (PDD), a fatal neurologic and gastrointestinal disease in birds. The virus is non-cytopathic, and the clinical presentation associated with the disease is due to inflammation and resulting injuries to the nerves. Mechanisms by which the virus evades and alters the immune system, thus producing disease, are not fully elucidated. To investigate disease caused by parrot bornavirus infections, RNA-seq was used to identify differentially expressed genes in the brains of non-infected (control) and parrot bornavirus 2 (PaBV-2) infected mallard ducks. Our hypothesis was that ducks infected, *in ovo*, with PaBV-2 differentially express genes associated with the immune system as compared to non-infected ducks. Mallard eggs were inoculated *in ovo* with PaBV-2 at day 5 of incubation, with control eggs sham inoculated with diluent without virus. At 83 ($\pm$ 2) days post-hatch, ducks were euthanized; serum and cerebellum was collected and stored at -80°C until assayed. RNA from the cerebellar samples was sequenced, then RNA expression was quantified and compared between the groups. Differentially expressed genes with a significant difference ($P < 0.01$) between the infected and normal control ducks and a greater than or equal 4-fold change in expression were analyzed using Database for Annotation, Visualization, and Integrated Discovery and Kyoto Encyclopedia of Genes and Genome pathway database. From the samples, 18,146 genes were identified. Using the criteria of a $P < 0.01$ and a greater than or equal 4-fold change in expression, 41 genes had decreased expression and 9 genes had increased expression in the PaBV-2 infected ducks as compared to control ducks

ACKNOWLEDGEMENTS

I would like to thank my committee chair and committee members, Dr. Jeffrey Musser, Dr. Noushin Ghaffari, Dr. Ian Tizard, and Dr. Yawei Ni, for mentorship and support throughout my research. Additionally, I would like to thank Paulina Escandon, who was always ready with advice in developing my thesis.

CONTRIBUTORS AND FUNDING SOURCES

This work was supported by a dissertation committee consisting of Clinical Professor Musser, Professor Tizard and Dr. Ni of the Department of Veterinary Pathobiology and Dr. Ghaffari of the Center for Bioinformatics and Genomic Systems Engineering, Texas A&M AgriLife Research.

Viral infection of duck eggs, raising of ducks, and sample collection was assisted by Dr. Heatley, Dr. de Araujo, Serene Yu, Debra Turner, and Paulina Escandon. The RNA-Seq data was provided by Texas A&M AgriLife Genomics and Bioinformatics Services (TxGen).

All other work conducted for the dissertation was completed by the student independently.

Graduate study was supported by The Schubot Exotic Bird Health Center of the College of Veterinary Medicine and Biomedical Sciences at Texas A&M University, Dr. Ian Tizard, and Dr. Jeffrey MB Musser.

NOMENCLATURE

Anpl-DRA	*Anas platyrhynchos* MHC class II alpha chain
Anpl-U	*Anas platyrhynchos* MHC class I alpha chain
B2M	Beta-2-microglobulin
BDV	Borna disease virus
C	Control duck (C1, C2, C3)
CD74	Cluster of differentiation 74
CS	Clinical signs duck
CTSS	Cathepsin S
DAVID	Database for Annotation, Visualization, and Integrated Discovery
DEG	Differentially Expressed Genes
EIF2AK2	Eukaryotic translation initiation factor 2 alpha kinase 2
ELISA	Enzyme-linked immunosorbent assay
GO	Gene Ontology
I	Infected duck (I1, I2)
IFN	Interferon
IRF	Interferon regulatory factor
Jak/STAT	Janus kinases/signal transducer and activator of transcription
KEGG	Kyoto Encyclopedia of Genes and Genome
MHC I	Major histocompatibility complex class I
MHC II	Major histocompatibility complex class II
MX	Interferon-induced myxovirus resistance ynamin like GTPase

NGS	Next Generation Sequencing
PaBV	Parrot Bornavirus
PDD	Proventricular Dilatation disease
PKR	Protein kinase RNA-activated (another name for EIF2AK2)
PRR	Pattern recognition receptor
qRT-PCR	Quantitative reverse transcription polymerase chain reaction
RIG-I	Retinoic acid-inducible gene I
RNA-Seq	RNA sequence
RSAD2	Viperin
RT-PCR	Reverse transcription polymerase chain reaction
STAT	Signal transducer and activator of transcription gene
SARS-CoV	Severe acute respiratory syndrome coronavirus
TANK	Traf family member associated-activator NF-κB
TAP	Transporter associated with antigen processing
TLR	Toll-like receptor
TNF	Tumor necrosis factor
TRIM25	Tripartite motif containing 25 gene
WaBV	Waterbird Bornavirus

TABLE OF CONTENTS

Page

LIST OF FIGURES

LIST OF TABLES

CHAPTER I

INTRODUCTION AND LITERATURE REVIEW

1.1. General Virus information

1.1.1 Parrot Bornavirus

Parrot Bornavirus (previously termed Avian bornavirus), in the Family *Bornaviridae,* are the etiological agents of proventricular dilatation disease (PDD), a fatal gastrointestinal and neurological condition of captive and wild birds. [1, 2] *Bornaviridae* are enveloped, non-segmented, negative sense RNA viruses that replicate inside the nucleus. *Bornaviridae* is comprised of eight species: *Elapid 1 bornavirus* found in reptiles, *Mammalian 1 bornavirus* and *Mammalian 2 bornavirus* (also known as *variegated squirrel bornavirus 1*) found in mammals, and five species that infect birds: *Psittaciform 1 bornavirus, Psittaciform 2 bornavirus, Passeriform 1 bornavirus, Passeriform 2 bornavirus,* and *Waterbird 1 bornavirus.* [3-6] The species of bornavirus associated with PDD are *Psittaciform 1 bornavirus,* which includes parrot bornavirus 1, 2, 3, 4, and 5 (PaBV-1, -2, -3, -4, and -5), and *Psittaciform 2 bornavirus,* which includes parrot bornavirus 5 (PaBV-5). [7]

It should be noted that across different studies the nomenclature for avian bornavirus, first identified in 2008, is still evolving. As such, the nomenclature of avian bornaviruses is inconsistent when reviewing the history and literature. In an attempt for clarity in this manuscript, all literature focuses on parrot bornaviruses (PaBV), unless noted as otherwise.

1.1.2. History of Parrot Bornavirus

Parrot bornavirus was determined to be the causative agent of PDD in 2008. Using isolates from PDD cases, investigations determined that PaBV was a new divergent form of bornavirus. [8, 9] Both investigations used next generation technology and BLAST, and are the first PaBV experiments to use NGS technology.[8, 9] Parrot bornavirus was confirmed as the etiologic agent of PDD when Gray et al. (2010) followed Koch's postulates and induced PDD in conures from PaBV infected brain samples of confirmed PDD case birds. [1]

1.2. PaBV and the Immune system

Cell cultures infected with PaBV have an ability to inhibit the production of type I interferons, essentially evading the activation of the innate immune system. [10] However, experimental infections of parrots trigger an inflammatory response. It was hypothesized that this inflammation may be due to the antibodies attacking the nervous system, similar to Guillain-Barre syndrome. This is still to be determined, as inoculation of PaBV brain gangliosides does not induce clinical PDD symptoms. [11] A second hypothesis is that infection of the nervous system by PaBV triggers an innate inflammatory response damaging the nerves, as PaBV has been consistently isolated from the damaged nerves in PDD cases. [12-17]

1.2.1. PaBV Pathology

Experimental routes of transmission, such as intramuscular, intravenous, and intracerebellar, are able to produce infection, histopathological lesions, and clinical PDD.[18-21] Parrot bornavirus infections have also been vertically transmitted.[14, 22-25] Non-invasive routes that produce a robust infection are still to be determined. [26] Even if infection with PaBV is successful, an infected host may never develop PDD.[2, 18, 26-31] Parrot bornavirus antigens are shown to have broad distribution in infected birds. Antigens are consistently detected in the brain, spinal cord, heart, gastrointestinal system, adrenal gland, and kidneys by PCR and immunohistological tests. [27, 30, 32, 33]

1.2.2. Techniques used for PaBV research

Parrot Bornavirus can replicate in duck embryonic fibroblasts and quail cell cultures.[33-35] Reverse transcription-PCR (RT-PCR) is the most common detection protocol due to its ability to detect small amounts of viral RNA, however little information other than possible viral protein distribution can be extrapolated from these results. Reverse transcription-PCR is routinely used in conjunction with immunohistochemistry and immunocytochemistry, both of which are less sensitive than RT-PCR but allow researchers to visualize viral load and viral distribution.[27] Quantitative reverse transcription-polymerase chain reaction (qRT-PCR) allows for the quantification of viral amount. Parrot bornavirus antibodies can be successfully detected by western blot, immunoblotting, and enzyme-linked immunosorbent assay (ELISA). Western blot assays are particularly useful in determining if a bird has been exposed to PaBV.

[36] However, western blot protocols are lengthy. Immunoblotting and ELISA, for the detection of antibodies against PaBV, are not used as widely at RT-PCR or immunohistochemistry, which detect the PaBV antigen.[37, 38] For visualization of viral distribution, immunofluorescence and immunohistochemistry protocols are used, and have been used frequently in the study of PaBV. [28, 39] For each of these protocols, detection target should be taken into consideration, as it has been shown that birds can shed PaBV or have antibodies against it, but may not develop clinical PDD. [29, 36] References for protocols used are in table 1.

Table 1. Protocol Reference Table

Category	Protocol	Reference
Molecular Techniques	Tissue extraction of PaBV RNA	50
	RT-PCR	7, 50
	Agarose gel electrophoresis	50
Viral isolation techniques	Growing PaBV in DEF	44, 46, 50
	PaBV isolation from tissues	50
	Serial dilution of PaBV	50
	Quantitate PaBV in a culture	48
Serologic Techniques	Western blot	10, 51
	ELISA	10, 47, 48, 51
	Immunohistochemistry	10, 47, 48, 51

1.2.3. History of PaBV Research

Investigators used high throughput sequencing to isolate the PaBV genome from confirmed cases of PDD when first confirming if PaBV was the etiologic agent of PDD. Reverse transcription-PCR was used to confirm that the viral genome isolated from confirmed cases of clinical PDD matched viral sequences in experimentally infected PDD cases. [8, 9]

Kistler et al. (2008) were the first to identify a novel bornavirus as a causative agent of PDD. [8] Using a high throughput assay, ABV (subsequently named PaBV) was found in naturally occurring cases of clinical PDD but not found in non-clinical birds. [8] At roughly the same time, Honkavuori et al. (2008), found by pyrosequencing of cDNA from the tissues of 2 macaws and one Amazon parrot that had clinical PDD, two novel strains of bornavirus in the birds' brain, proventriculus, and adrenal gland. [9] Gray et al. (2010) used Koch's postulates to connect these novel bornaviruses, PaBV, as the etiological agent of PDD. [1]

Experimental inoculation with PaBV is a useful method to study the pathology of PDD. However, the use of large parrots, such as macaws, Amazons and African Greys that are naturally susceptible to naturally occurring PDD is not practical due to many reasons: expense, emotional value, and endangered statue of some large parrots. Gancz et al. (2009) induced histopathological lesions and clinical manifestation of PDD in cockatiels (*Nymphicus hollandicus*) when brain homogenates containing avian bornavirus 4 were inoculated by multiple routes (intramuscular, intraocular, intranasal, and oral). [40] Subsequently, cockatiels have become the main species used for PaBV studies, including those studying natural infection routes, pathogenesis, and analysis of different PaBV strains. [19, 26, 41, 42] Other bird species, usually collections of species at aviaries, used successfully to investigate parrot

bornavirus include: conures, lovebirds, macaws, African greys, and cockatoos. [37, 43] Monk parakeets and budgerigars have been resistant to experimental infection by PaBV. [1]

Recently, PaBV has been isolated from waterfowl, and some passerines, naturally occurring in the wild. [13, 21, 23, 29, 34, 44, 45] However, the use of these birds as a research model is limited, as most of the studies have been from hunter-collected samples. [13, 17, 29, 34, 44] Parrot bornavirus 2 and parrot bornavirus 4 are the species used most in research as they are the species most often isolated from naturally occurring clinical PDD cases, most prevalent species occurring in North America and Europe, and have consistently produced histopathological lesions and clinical PDD in experimentally infected birds. [14, 15, 41, 43, 46]

1.3. Proventricular Dilatation Disease

In parrots, PDD is classified as a disease that affects the neurological and gastrointestinal system. Neurologic symptoms include general weakness, ataxia, declining proprioception, seizures, and blindness. Histopathology findings of lymphoplasmacytic inflammations throughout the nervous system, with lesions involving the ganglia of the enteric system, constitutes a definitive diagnoses of PDD. [2, 18, 42] Gastrointestinal symptoms include weight loss, regurgitation, passage of undigested food, and delayed crop emptying. As the name of the disease suggests, affected birds have a dilated proventriculus with thinning walls due to impaction theorized to be caused by damage to the enteric nervous system. [18, 42] These symptoms occur in acute PDD. Parrot bornavirus has been shown to be an etiological agent of PDD, but birds can be infected with PaBV without clinical signs of PDD,

otherwise known as carriers. [1, 2, 42, 47] As mentioned previously, there is broad tissue distribution of PaBV antigens in infected birds with the production of PaBV antibodies, but a definitive diagnosis of PDD is only made when lymphocytic ganglioneuritis is found in the enteric nervous system, thus PDD confirmation is a post-mortem diagnosis. [17, 33, 36, 48]

Waterfowl throughout northern America are infected with waterbird bornavirus (WaBV), and WaBV does not seem to cause clinical PDD in parrots. [13, 17, 29] It is speculated that WaBV may cause a neurological disease similar to PDD, however, most of the studies of WaBV use brains that are from birds that were found dead or hunter collected, so there is no observation of symptoms. [23, 29, 34, 44, 49, 50] Lesions typical of PDD cases are seen in the brains of waterfowl, however as mentioned earlier, to confirmation is based upon lymphocytic infiltration of the enteric ganglia and these tissues are not routinely available. [13, 18, 42] It remains to be seen if waterfowl infected with PaBV would show PDD like symptoms, as the similar lesions occur from both PaBV and WaBV.

1.4. Studies into PaBV Pathology

The pathology of how PaBV is able to cause PDD is not linear. There are accounts of birds being infected with PaBV, determined through PCR or western blot, but they don't develop PDD. [27, 29, 36, 48] Additionally, infection detection is not always consistent, with cloacal swabs being the most inconsistent and brain samples being consistently positive across multiple PaBV studies. [27, 31, 51] Furthermore, not all bird species develop clinical PDD following infection. [8, 9, 40, 52] While some birds remain fully asymptomatic, other birds that were consistently negative for PaBV may develop PDD and die quickly after contracting

PaBV. [27, 29, 48] As for treating PDD, at this time there is no proven efficacious treatment for infection or for reducing viral shedding. Most treatments reduce the severity of PDD symptoms. [2, 18] Most symptomatic treatments use non-steroidal anti-inflammation drugs, as PDD symptoms are theorized to be a result of inflammation to PaBV replicating in the neurons. NSAIDS effectiveness is variable, as PDD can increase in severity with the use of Meloxicam compared to the relative success of Celecoxib. [2, 53] There is some evidence that conjugation of ABV proteins with New Castle disease and a modified vaccinia virus can resist PDD development, however, this is still in development. [54] Overall, there is a dearth of information on the mechanisms by which PaBV produces disease. Therefore, incorporating next generation sequencing technology would add another aspect that could elucidate the pathology of PaBV, in particular the host-virus interactions.

1.5. Gene Expression Changes: Viral Infection

To survive in a host some viruses have the ability to hijack a cell's regulation of gene expression. It is unknown if PaBV uses this strategy to cause disease, but this may be elucidated by using next generation sequencing (NGS) technology. Next generation sequencing technology has been used in PaBV studies to determine novel species, but the full capacity of this technology has not been explored. [8, 9, 40, 55] For instance, NGS technology has been used to determine new species of PaBV that infects waterfowl and passerines. [8, 9, 34, 56]

Using NGS technology to study bird viruses is not unprecedented and has been successful in revealing viral-host interactions. Most of these studies are of chickens and those

diseases that harm chicken meat and egg production. Response to stressors such as heat, growth rate, and even exposure to ammonia in chickens have shown to cause changes to gene regulation. [57-59] Viral and bacterial infection of chickens, including influenza A and avian pathogenic *E. coli*, have been shown to cause changes to gene regulation that induce a disease in chickens. [60-63] For instance, avian influenza virus studies suggested that infection was correlated to changes in cell signaling pathways, viral response pathways, and cellular protein production. [64-67] Additionally, differentially expressed genes caused by coronavirus infection of apparently healthy chickens supported evidence that the virus is able to escape recognition by the immune system. [61, 68]

These viral studies are not limited to chickens. Ducks are the alternative bird of choice in chicken production studies as most of their genome is available to use for analysis. [69-72] There are multiple studies on differentially expressed genes occurring when ducks are infected with viruses. [55, 73-77] For instance, ducks are used in influenza A studies; ducks are a reservoir species whereas chickens develop the disease. [78] There are multiple precedents of sequencing technology being used to investigate host-virus interactions in respect to gene expression. Parrot bornavirus is not one of those precedents, but Borna disease virus (BDV) has been analyzed with next generation technology. Studies in rats infected with BDV have differentially expressed genes associated with the kynurenine pathway causing neurodegeneration.[79] Essentially, differential gene expression is able to suggest effects that a virus may have on cellular gene expression, thus elucidating mechanisms that allow for the survival and replication of the virus within the host.

1.6. History of RNA-Seq

Most experiments before next generation technology used microarrays which gave a snapshot of gene expression at one point in time. Unlike NGS, microarrays allowed researchers to visualize gene regulation. However, microarrays are limited to amount of RNA it can hybridize as it has a linear dynamic range.[80, 81] Next generation technology has a larger dynamic range, can analyze large amounts of data, and is relatively quick and cheap as compared to microarrays. Additionally, NGS is not exclusive, any researcher with enough storage space and an internet connection can have access to multiple free bioinformatics tools available online. [80-83] Finally, as mentioned earlier, NGS technology has a better dynamic range than microarrays. Even short sequence fragments are able to be detected in the genome, unlike microarray. Additionally, using RNA-Seq, an NGS tool, allows researchers to analyze multiple different cellular operations like meiotic differentiation, the occurrence of rapid cellular proliferation, responses to environmental stressors and even the discovery of mutant RNA. [80, 81]

1.6.1. Next Generation Sequencing Technology Limitations

There are some limitations to NGS abilities. For instance, large data outputs of genetic information will need a large storage capacity to perform statistical analysis and normalization. Without the analysis, the data is not useable. Parsing out significant data points from a large data output may require additional technical help from bioinformaticists. Technical knowledge of types of sequencing analysis, most available software, and overall computer knowledge is necessary to fully extrapolate all significant data from the output of NGS. [84]

1.6.2. Methodology of Next Generation Sequencing

Most NGS projects outsource sequencing, and get back the output of genetic data. Previously, all projects that used next generation technology were exclusive to organizations that had the technology and the technical knowledge to analyze genetic data. Now researchers can have access to online software capable of exacting statistical analysis on genetic information without having advanced knowledge of coding languages or statistics. [81-83, 85] One popular method of sequencing samples is with technology produced by Illumina. (Illumina HiSeq 4000, Illumina, Inc., San Diego, CA) Companies such as this have helped drive down the cost of sequencing and helped streamline the sequencing process. [82, 83, 86, 87]

While sequencing can be outsourced, preparation of the samples is not. For RNA-Seq, RNA is extracted, isolated, and purified. The purity of the RNA sample is key to avoiding errors in sequencing. To keep purity and avoid RNA degradation, it is recommended that samples are frozen once obtained either by keeping it in a freezer or immediately freezing a sample with liquid nitrogen. [82] After sequencing and qualitative reads are performed and the researcher receives the data output, the data is ready for analysis. There are many types of software available for analysis, and one with a consumer friendly interface is CLC Genomics Workbench. (CLC Bio Genomic Workbench, Qiagen Inc.) CLC Genomics Workbench is a collection of analysis software necessary for different sequencing tasks. [88] For instance, for RNA-Seq, CLC Genomics Workbench has incorporated the EdgeR Bioconductor package which statistically analyzes and normalizes expression data. [89, 90] Additionally, this package introduces the least amount of bias during normalization. [89, 91-93] Once

normalized, the genetic data can be analyzed by online tools like the Database for Annotation, Visualization, and Integrated Discovery (DAVID), and the Kyoto Encyclopedia of Genes and Genomes (KEGG) database to discover gene information including biological functions and pathways.[94-98]

1.6.3. RNA-Seq and Infectious Disease

The NGS technology, RNA-Seq, is effective at creating expression profiles to determine differentially expressed genes. This type of analysis, called differential gene expression (DEG) analysis, is a suitable approach to identify changes in gene transcription when viruses alter cellular regulation, and may indicate how PaBV is able to cause pathology. This type of analysis is also regularly used in the study of infectious avian diseases instead of microarrays. [61, 62, 66, 67] RNA-Seq of PaBV has been used to determine new strains, but not for DEG analysis. Other types of viruses have previously used DEG to infer possible host-virus interactions. Nervous necrosis virus upregulates genes related to the innate immune system in brain cells, and it is theorized that genes like lectins and chemokine ligand 2 (CCL-2) were regulators of regulation. [99] Muscovy ducks infected with reovirus had upregulation of transcription factor regulators, and signaling pathway receptors including the retinoic acid-inducible gene I (RIG-I)-like and toll-like receptors. [73, 100] In chickens, DEG analysis indicated a correlation between immune recognition evasion by the avian influenza virus and gene expression of infected cells. [67] In respect to ducks and infectious viruses, the transcriptome of different ducks has been analyzed for infections of influenza A virus, avian paramyxovirus, and avian coronavirus to understand the diversity of such viruses in mallard

duck populations. [74, 101] Using RNA-Seq to perform DEG on PaBV infected animals may provide insight into the pathology of a PaBV infection and PDD.

1.7. Precedents in PaBV Pathology

There is no dearth of pathological theories of a PaBV infection. One theory is that PaBV is autoimmune, and similar to Gulliarn-Barre syndrome in presentation. However, this may not be the case as autoantibodies against gangliosides do not cause symptoms or lesions similar a typical PDD case. [1, 2, 11, 18] However, there is evidence that PaBV has a transient autoimmune response to myelin and brain gangliosides when infected with PaBV as detected by western blot. [18] Cellular pathology of the virus has been visualized using immunofluorescence of PaBV infected cells which shows the virus occupying the nucleus of duck embryonic fibroblasts. [31, 39] This method is also used to detect PaBV infection in other animal cells, as indicated by a viral loaded nucleus. [12] In developing PaBV detection methods, the pathology of PaBV is further elucidated. During the development of PCR for PaBV, it was found that viral proteins could be broadly distributed in tissues and even in feather shafts, but not in the blood. [102] Additionally, PCR testing of cloacal swabs found that viral shedding was an inconsistent detection method for confirming viral infection, as the virus can be infrequently and inconsistently shed. [29, 31, 51] This raises the question in the difference between clinical PDD cases and asymptomatic cases of PaBV infection. The development western blot was able to elucidate immune response to PaBV. Western blot has shown that birds do develop antibodies against the nucleoprotein (N-protein) and phosphoprotein (P-protein) of PaBV, and that birds can be seropositive due to exposure to the

virus. [36] Unlike PCR, western blot is able to detect proteins in blood. [36] However, western blot is not frequently used as a detection method due to time required to perform the protocol. Overall, the development of PaBV detection methods have been significant in elucidating PaBV pathology but do not give insight into host-virus interaction on a genetic level as RNA-Seq may be able to do.

1.8. RNA-Seq and PaBV

To the best of our knowledge, there is not a precedent of DEG being performed on PaBV infected animals to elucidate virus-host interaction effects on gene expression. Proventricular dilatation disease (PDD) can present with neurological symptoms, and PaBV does infect neurological cells, but it is only theorized how PaBV causes inflammation to induce such neurological symptoms. [1, 18] The virus is non-cytopathic, therefore damage is not due to direct viral destruction of cells, and additionally, there is no evidence of an autoimmune response to infected neurological cells causing the symptomatic neurological signs. [17, 18] The theory of inflammation is based upon previously mentioned detection methods, which do not give insight into virus-host cell interactions unlike RNA-Seq and subsequent DEG analysis. RNA-Seq and DEG analysis quantify transcripts and create gene expression profiles of sampled tissues. If these tissues sampled were from the cerebellum of a clinical PDD case bird, then determination of differentially expressed genes would be insightful, as the cerebellum has been shown to have a high load of PaBV in PDD cases. [27, 52] Essentially, RNA-Seq paired with DEG analysis is able to give insight into PaBV's pathology that previous viral detection methods are not capable of doing.

1.8.1. Reference Genome: PaBV and Ducks

Few avian species are vulnerable to a PaBV infection and have a quality annotated genome necessary for RNA-Seq. This is because few psittacine genomes have been sequenced, and fewer have been annotated for genes. However, the mallard duck does have a quality annotated genome. [69, 70, 74, 103-118] Additionally, mallard ducks have been shown to become infected with WaBV, a species of virus similar to PaBV. [23, 27, 29, 34] Therefore, for a preliminary test to see if there is any significance to using RNA sequencing on PaBV infected birds, the mallard duck is the most reasonable choice

1.9. Hypothesis and Objectives

Our hypothesis is that ducks infected, *in ovo*, with PaBV-2 have differentially expressed genes associated with the immune system as compared to non-infected ducks. Objectives to test our hypothesis will be:

1. to determine baseline gene expression, using RNA-Seq technology, in the cerebellum of uninfected control ducks;
2. to identify genes expressed, using RNA-Seq technology, in ducks infected with PaBV-2; and,
3. to analyze differential gene expression to identify dysregulated genes in PaBV-2 infected ducks as compared to uninfected ducks.

CHAPTER II

MATERIALS AND METHODS

2.1. Objective 1: Create a baseline gene expression on cerebellum of uninfected ducks

Mallard (*Anas platyrhynchos*) eggs were obtained from a commercial farm (Metzer Farms, Gonzales, CA). Eggs were incubated at 37.5° C at 55-60% relative humidity. At 5 days incubation, the eggs were injected with the 0.1 ml inoculation solution without PaBV-2. The inoculation solution was made from duck embryo fibroblast cells grown in media that were freeze-thawed 3 times, centrifuged, and the diluent collected as the inoculation solution. On day 83 ($\pm$ 2) post-hatching, ducks (n=3), C1, C2, and C3, were euthanized and necropsied. Cerebellum and hindbrain samples were collected and stored in 1.5mL microcentrifuge tube at -80°C until assayed. To determine infections status, cerebellum and hindbrain were assayed by RT-PCR using an M-protein sequence primer. Serum taken during necropsy was assayed by western blot for the presence of antibodies to viral N-protein, the immunodominant epitope in avian bornaviruses.

Samples of cerebellum were processed for RNA isolation by utilizing a commercial RNA isolation product (NucleoSpin® RNA Plus, Macheney-Nagel Inc., Bethlehem, PA). RNA isolation followed product protocol (Appendix A. Fig A1) with minor modifications noted here. Briefly, 550uL of LBP Buffer was added to 30uL of sample and fully homogenized by pellet mixer (VWR® Disposable Pellet Mixers and Cordless Motor, VWR International, Radnor, PA). Samples were incubated at room temperature for 10 minutes, examined for complete homogenization, and if not fully homogenized, 100 uL of additional

LBP buffer was added and the sample was homogenized again. Full homogenization was necessary as tissue can disrupt proper gDNA removal and lead to contamination of the final RNA isolate. The sample was then loaded on a NucleoSpin® gDNA Removal Column (Macheney-Nagel Inc.), centrifuged for 30 second at 11000x g, and the eluent collected. The eluent was then combined with 100uL of RNA Binding Solution and run through a NucleoSpin® RNA Plus Column and centrifuged for 15 seconds at 11000x g. The column was washed with Buffer WB1 solution (Macheney-Nagel Inc.) and then two additional washes with the Buffer WB2 (Macheney-Nagel Inc.). A final wash with the Buffer WB2 was done and the column was centrifuged twice for 2 minutes at 11000x g. The RNA was eluted from the column by adding 50uL of RNAse free H_2O (Macheney-Nagel Inc.), centrifuging for 1 minute at 11000x g, and collecting the eluent. The eluent, containing the isolated RNA, was stored at -80°C. For each sample, the process was done in triplicate to obtain biological replicates for RNA-Seq to account for biological variation across samples.

Eluted RNA samples were assayed for purity and concentration using a commercial product (NanoDrop 2000, ThermoFisher Scientific, Houston, TX) using the standard product protocol; purity needed to be 260/280 and 260/230 absorbance ratios above 1.8 and concentration above 100 ng/uL. The device was blanked using the same RNAse free H_2O used to elute samples during RNA isolation. .

Samples were then diluted, with RNAse free H_2O, to a concentration of 45 ng/uL, a criteria for RNA-Seq. The samples were submitted to Texas A&M AgriLife Genomics and Bioinformatics Services (TxGen) for RNA-Seq by Illumina TruSeq RNA library preparation protocol using the Hiseq 4000 platform.

2.2. Objective 2: Identify genes expressed in cerebellum of ducks infected with PaBV-2

Eggs and the environment for egg incubation is described in Objective 1. At 5 days incubation, the eggs were injected *in ovo* with 0.1mL of PaBV-2 inoculation solution containing $8x10^{-6}$ focus forming units (FFU). The inoculation solution was made from duck embryo fibroblast cells infected with PaBV-2, allowed to grow for 5 days, then freeze-thawed 3 times, centrifuged, and the diluent collected as the virus inoculation solution. Infected ducks, (n=3) I1, I2, and I3, were euthanized on day 83 ($\pm$ 2) post-hatch. Samples were collected, processed, and analyzed exactly as samples in Objective 1. If any clinical PDD-like symptoms were observed in a duck, additional tissues were taken for RT-PCR and histopathology (Appendix A. Table A1).

2.3. Objective 3: Use bioinformatics software to analyze the differential gene expression found between uninfected and PaBV-2 infected ducks

Raw data from the RNA-Seq run was compressed into a .tar file by Texas A&M AgriLife Genomics and Bioinformatics Services (TxGen). These files were then unpacked using 7-zip software and imported to the bioinformatics software, CLC Bio genomic workbench (Qiagen Inc.)(Appendix A. Fig.A3). [119] The raw RNA sequences were then mapped to a mallard duck reference genome release 1.0. The reference genome sequences were obtained from the ftp site developed by the National Center for Biotechnology Information (NCBI GenBank, National Center for Biotechnology Information, Bathesda, MD). [120] Mallard duck genome is still under construction, therefore, the detailed information such

as chromosome level sequences are not available yet. The current consensus genome consists of long sequences generated by assembly process, as well as annotation information to locate the recognized genes on these sequences. In order to generate the gene expression profiles for samples, the RNA-Seq output sequences, called reads, were mapped to the mallard duck reference release 1.0, using the CLC Bio genomics workbench "RNA-Seq Analysis" tool (Appendix A. Fig. A4). [119] The CLC Bio genomic workbench provides a plug in, "Annotating with GFF file", for incorporating the annotation information into the duck genome (Appendix A. Fig.A5). [119] Alignment of RNA-Seq reads to the mallard duck annotated reference genome, which was elaborated above, resulted in average 50% of genes mappings (Appendix A. Table A2). As a test, we used chicken reference genome for alignment and the mapping percentages were considerably lower. Comparatively, these results are valuable in studying the genes causing the disease as there is no reference genome for parrots that are susceptible to a PaBV infection. For each RNA-Seq mapping run, we used the following settings:

Mapping Type: Gene Regions; Mismatch cost: 2; Insertion Cost: 3; Length fraction: 0.85; Similarity fraction: 0.85; Global Alignment: yes; Strand specific: both; Maximum # of hits: 1; Count paired reads as 2: no; Expression Value: RPKM; Calculate RPKM for gene without transcript: no; Create report: yes

Normal reads checks were performed after mapping to check for consistency in mapping results (Appendix A. Table A3). Mapping reads to the genome generates expression values for each gene that was provided in the annotation file. Upon completion of alignments,

we used the “Setting Up an Experiment” tool in CLC Bio genomics workbench to organize the mapping results into comparable groups (Appendix A. Fig. A6).[119] The comparisons between infected (I1, I2, CS) and control groups (C1, C2, C3) with 3 biological replicates were set up using the following parameters:

Expression Value level: As set on samples; Expression value column: As set on samples; Experiment Type: Two group comparison; Number of samples in experiment: Varies

To normalize the data from these experiments, statistical analysis was performed using the CLC Bio software called, “Empirical Analysis of DGE” (Appendix A. Fig. A7). [119] The DGE stands for Digital Gene Expression, and it is used to account for difference between sequencing outputs of samples, such as different output amount. This criteria is set for each DGE analysis:

Total Count filter cutoff: 5.0; Estimate tagwise dispersions: Yes; Comparisons: All Pairs Bonferroni corrected: Yes; FDR corrected: Yes

In the next step, “Empirical analysis of DGE” tool was employed to compare the gene expression among the group. The previous experiments were used in this analysis. The “Empirical analysis of DGE” tool implements the two groups tested for significance based on the edgeR package of R. [119]

To select the most significant genes, the “Empirical analysis of DGE” performs multiple comparisons. There are methods to correct for multiple testing and CLC uses

Bonferroni and False Discovery Rate (FDR). [119] In this study we chose the expressions based on the Bonferroni p-value, as it is more conservative than the FDR p-value. Tables of genes that are both significant and either upregulated or downregulated were further analyzed to identify gene functions based on previously published articles, NCBI's e!Ensembl (National Center for Biotechnology Information, Bethesda, MD), and GenBank (National Center for Biotechnology Information) as the gene catalogues. [121, 122] To analyze biological function and pathways of these differentially expressed genes, the gene I.D.'s from Genbank (National Center for Biotechnology Information) were uploaded on to the Database for Annotation, Visualization, and Integrated Discovery (DAVID) and the Kyoto Encyclopedia of Genes and Genome (KEGG) pathway database. [94-98] Finally, the most significant genes were analyzed to determine if significance is constant for each infected duck.

CHAPTER III

RESULTS

3.1. Infection confirmation of ducks

For control ducks, no viral genetic material was detected in the cerebellum or hindbrain; PCR results were negative. No antibodies against the PaBV-2 viral N-protein was detected by western blot (Table 2).

One duck became severely ataxic and was euthanized on day 65 (supplementary materials contains video of ataxic signs). This duck is subsequently referred to as clinical signs (CS) duck. Additional tissues taken from and additional observation of the CS duck can be found in appendix B.

All infected ducks were positive for PaBV-2 by RT-PCR (Figure 1). Only 2 infected ducks were positive for antibodies against the viral N-protein from western blot, I1 and CS (Table 2).

Table 2. PCR and Western Blot Results of Sampled Ducks. After necropsy, brain tissue and serum were taken for testing. Control ducks are labeled as C1, C2, and C3. Infected ducks are labeled as I1 and I2. The clinical signs duck is labeled as CS. (Appendix B. Table B2. CS duck detailed PCR results)

Test	Sample	Control			Infected		
		C1	**C2**	**C3**	**I1**	**I2**	**CS**
Western Blot	Serum	-	-	-	+	-	+
	Cerebellum	-	-	-	+	+	+

PCR	Hindbrain	-	-	-	+	+	+

3.2. Host expression profile after PaBV-2 infection

The analysis identified 18,146 genes. Comparing control to infected ducks, 231 genes were significantly ($P < 0.01$) differentially expressed. Of these 231 significantly differentially expressed genes, 49 genes had greater than or equal to a 4-fold change in expression; 41 had at least a 4-fold decrease in expression and 8 had at least a 4-fold increase in expression (Table 3). Eleven genes had a fold change $\geq |100|$; 9 were down regulated and included 4 C-C motif chemokine genes (LOC101800938, LOC101800921, LOC101791569, LOC101791385), interferon-induced myxovirus resistance dynamin like GTPase (MX), viperin (RSAD2), placenta specific 8 (PLAC8), interferon-induced protein with tetratricopeptide repeats (LOC101797569), and interferon-induced alpha-inducible protein (LOC101794704), while the 2 upregulated genes included transcription factor BTF3 (BTF3) and 60s ribosomal protein L37 (LOC106020377).

Since neurological clinical signs in a PaBV-2 infected duck is unprecedented, a second expression profile was created to compare the differential expression in the clinical sign duck to the control ducks (C1, C2, C3). Out of the identified 18,142 genes, 185 genes were significantly ($P < 0.01$) differentially expressed. Of these 185 genes, 71 had a greater than or equal to 4-fold change; 54 had at least a 4-fold decrease in expression and 17 had at least a 4-fold increase in expression (Table 4). Eight genes had a fold change $\geq |100|$; 6 were downregulated and included C-C motif chemokine 4-like (LOC101800938), interferon-induced myxovirus resistance dynamin like GTPase (MX), viperin (RSAD2), interferon-induced protein with tetratricopeptide repeats (LOC101797569), interferon alpha-inducible protein

(LOC101794704), and prolactin-releasing peptide receptor (LOC101801882). Upregulated genes included 60s ribosomal protein (LOC106020377), and transcription factor BTF3 (BTF3). The full table of genes with a $P \leq 0.01$ is depicted in Appendix B.

Figure 1. Image of PCR Results. From left to right, after the PCR ladder are control duck results, PCR controls, and cerebellum results for I1 and I2. After the second ladder is the cerebellum result for the clinical sign duck, followed by the second set of PCR controls.

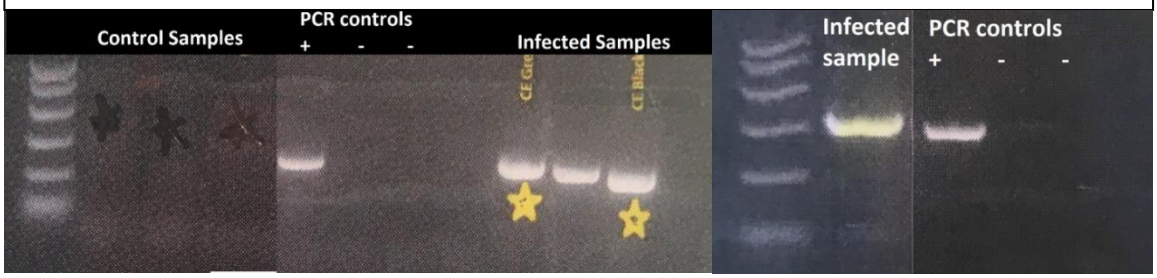

Table 3. Significantly Differentially Expressed Genes of Infected Ducks vs. Control Ducks. (Additional information found in supplementary attached files)

	Feature ID	GeneID	Gene Symbol	Gene Description	Fold change	P-value
Downregulated	Anapl_12933	101794704	LOC101794704	interferon alpha-inducible protein 27-like protein 2B	-366	1.91E-116
	Anapl_18401	101797569	LOC101797569	interferon-induced protein with tetratricopeptide repeats 5	-285	0.00E+00
	Anapl_04893	101800938	LOC101800938	C-C motif chemokine 4-like	-250	1.85E-59
	Anapl_18425	101800921	LOC101800921	C-C motif chemokine 4	-154	4.18E-39
	Anapl_01687	101791569	LOC101791569	C-C motif chemokine 4-like	-152	2.88E-37
	Anapl_13350	101793492	MX	interferon-induced GTP-binding protein Mx-like	-139	8.24E-57
	Anapl_14386	101791352	RSAD2	viperin, radical S-adenosyl methionine domain containing 2	-120	1.91E-52
	Anapl_01685	101791385	LOC101791385	C-C motif chemokine 5-like	-115	5.56E-37
	Anapl_05957	101791974	PLAC8	placenta specific 8	-114	1.80E-92
	Anapl_08494	101795904	IRF7	interferon regulatory factor 7	-99	6.97E-87
	Anapl_14385	101790338	CMPK2	cytidine/uridine monophosphate kinase 2	-58	9.49E-44
	Anapl_02580	101793511	SAMD9L	sterile alpha motif domain-containing protein 9-like	-48	1.69E-48
	Anapl_13382	101798516	EIF2AK2	interferon induced eukaryotic translation initiation factor 2 alp	-42	6.18E-39
	Anapl_03170	101800860	SAMD9L	sterile alpha motif domain-containing protein 9-like	-38	8.65E-73
	Anapl_19105	101790497	Anpl-U	class I histocompatibility antigen, F10 alpha chain	-31	3.10E-48
	Anapl_16041	101797680	TAP1	transporter 1	-29	1.09E-42
	Anapl_06165	110351393	SRGN	serglycin	-29	2.01E-28
	Anapl_18444	101805361	PLVAP	plasmalemma vesicle associated protein	-24	2.48E-88
	Anapl_09160	101796142	LOC101796142	interferon regulatory factor 4-like	-21	4.74E-35
	Anapl_03154	101791574	TRIM25	tripartite motif containing 25	-20	1.21E-74
	Anapl_03165	106014788	RNF135	ring finger protein 135	-18	4.41E-31
	Anapl_17300	101799633	IRF1	interferon regulatory factor 1	-12	6.73E-73
	Anapl_16039	101797091	TAP2	transporter 2	-11	2.04E-46
	Anapl_01734	101799108	B2M	beta-2-microglobulin	-11	5.22E-74
	Anapl_00935	101798744	PARP14	poly [ADP-ribose] polymerase 14	-11	2.81E-29
	Anapl_09935	101790771	TLR3	toll like receptor 3	-10	2.19E-18
	Anapl_04378	101803758	C1QA	complement C1q A chain	-9	6.41E-36
	Anapl_12048	101803806	USP18	ubiquitin specific peptidase 18	-9	2.05E-49
	Anapl_10110	101789908	LOC101789908	poly [ADP-ribose] polymerase 14	-8	1.93E-65
	Anapl_04377	101803105	C1QB	complement C1q B chain	-7	3.25E-33
	Anapl_02056	101801059	MOV10	Mov10 RISC complex RNA helicase	-7	1.50E-18
	Anapl_17425	101789604	LOC101789604	class II histocompatibility antigen, B-L beta chain	-7	1.78E-25
	Anapl_10146	101797758	NMI	N-myc and STAT interactor	-7	1.34E-47
	Anapl_09516	101794564	CTSS	cathepsin S	-6	1.93E-21
	Anapl_10109	101789724	PARP9	poly(ADP-ribose) polymerase family member 9	-6	5.28E-24
	Anapl_07454	101796809	LOC101796809	probable E3 ubiquitin-protein ligase HERC3	-6	8.98E-31
	Anapl_17310	101795567	LOC101795567	CD48 antigen	-6	1.72E-21
	Anapl_05113	101803982	TMEM140	transmembrane protein 140	-5	3.36E-43
	Anapl_17426	101804845	Anpl-DRA	HLA class II histocompatibility antigen, DR alpha chain	-5	2.65E-18
	Anapl_05503	101802002	MORN3	MORN repeat containing 3	-4	2.26E-22
	Anapl_03156	101797577	SCPEP1	serine carboxypeptidase 1	-4	3.09E-18
Upregulated						
	Anapl_18398	101793310	LOC101793310	transitional endoplasmic reticulum ATPase	10	2.15E-31
	Anapl_18322	101803793	LOC101803793	E3 SUMO-protein ligase PIAS2	27	2.52E-19
	Anapl_18875	101801464	LOC101801464	AN1-type zinc finger protein 5	46	4.54E-22
	Anapl_18543	101798222	LOC101798222	transitional endoplasmic reticulum ATPase	51	1.13E-70
	Anapl_18555	101791000	LOC101791000	heterogeneous nuclear ribonucleoprotein K	54	7.84E-88
	Anapl_19040	101795174	LOC101795174	vasculin	63	1.81E-30
	Anapl_18963	106020377	LOC106020377	60S ribosomal protein L37-like	173	1.46E-88
	Anapl_18574	101790838	BTF3	transcription factor BTF3	255	5.86E-77

Table 4. Significantly Differentially Expressed Genes of Clinical Sign Duck vs Control Ducks. (Additional information found in supplementary attached files)

	Feature ID	Gene ID	Gene Symbol	Gene Description	Fold change	P-value
Downregulated	Anapl_16761	101801882	LOC101801882	prolactin-releasing peptide receptor	-1191	5.21E-137
	Anapl_12933	101794704	LOC101794704	interferon alpha-inducible protein 27-like protein 2B	-362	1.09E-79
	Anapl_18401	101797569	LOC101797569	interferon-induced protein with tetratricopeptide repeats 5	-286	9.38E-307
	Anapl_14386	101791352	RSAD2	viperin	-150	3.64E-76
	Anapl_13350	101793492	MX	interferon-induced GTP-binding protein Mx-like	-149	1.14E-37
	Anapl_04893	101800938	LOC101800938	C-C motif chemokine 4-like	-135	2.8E-44
	Anapl_05957	101791974	PLAC8	placenta specific 8	-92	1.53E-65
	Anapl_12350	101791431	IFITM1	interferon-induced transmembrane protein 1	-83	2.01E-15
	Anapl_08494	101795904	IRF7	interferon regulatory factor 7	-77	3.13E-61
	Anapl_18425	101800921	LOC101800921	uncharacterized LOC101800921	-62	5.44E-31
	Anapl_02580	101793511	SAMD9	sterile alpha motif domain-containing protein 9	-56	1.63E-38
	Anapl_13644	101804721	LYZ	lysozyme	-54	2.5E-130
	Anapl_14385	101790338	CMPK2	cytidine/uridine monophosphate kinase 2	-50	1.88E-20
	Anapl_13382	101798516	EIF2AK2	eukaryotic translation initiation factor 2 alpha kinase 2	-42	5.62E-24
	Anapl_01685	101791385	LOC101791385	C-C motif chemokine 5-like	-35	8.38E-83
	Anapl_03170	101800860	SAMD9L	sterile alpha motif domain-containing protein 9-like	-30	3.32E-41
	Anapl_01687	101791569	LOC101791569	C-C motif chemokine 4-like	-28	2.73E-64
	Anapl_19105	101790497	Anpl-U	class I histocompatibility antigen	-27	7.93E-22
	Anapl_12150	101790417	DDX60	DExD/H-box helicase 60	-24	0.00867
	Anapl_18444	101805361	PLVAP	plasmalemma vesicle associated protein	-22	1E-76
	Anapl_16041	101797680	TAP1	transporter 1	-20	3.88E-18
	Anapl_03154	101791574	TRIM25	tripartite motif containing 25	-18	5.65E-46
	Anapl_09160	101796142	LOC101796142	interferon regulatory factor 4-like	-18	1.11E-18
	Anapl_06633	101798767	SELP	P-selectin	-15	0.00000089
	Anapl_18689	101797093	LOC101797093	uncharacterized LOC101797093	-15	1.44E-68
	Anapl_01734	101799108	B2M	beta-2-microglobulin	-12	0
	Anapl_03165	106014788	RNF135	ring finger protein 135	-11	9.6E-19
	Anapl_06165	110351393	SRGN	serglycin	-11	1.14E-12
	Anapl_02737	101791571	LOC101791571	uncharacterized LOC101791571	-11	9.21E-31
	Anapl_12048	101803806	USP18	ubiquitin specific peptidase 18	-10	9.32E-62
	Anapl_04499	101798590	LOC101798590	C-factor	-10	0.000152
	Anapl_17300	101799633	IRF1	interferon regulatory factor 1	-10	3.21E-50
	Anapl_10830	101794086	LOC101794086	Avidin	-10	0.000454
	Anapl_00935	101798744	PARP14	poly [ADP-ribose] polymerase 14	-9	2.4E-11
	Anapl_16039	101797091	TAP2	transporter 2	-8	8.69E-37
	Anapl_10110	101789908	LOC101789908	poly [ADP-ribose] polymerase 14	-8	1.25E-40
	Anapl_05044	101799009	TNNC1	troponin C1	-8	0.000000163
	Anapl_12082	101801672	STC2	stanniocalcin 2	-8	2.08E-11
	Anapl_09935	101790771	TLR3	toll like receptor 3	-7	0.00405
	Anapl_18328	101794524	LOC101794524	desmin	-7	1.72E-14
	Anapl_12194	101792676	KRT15	keratin	-6	0.0000016
	Anapl_17040	101797128	LOC101797128	interferon-induced, double-stranded RNA-activated protein kinase-like	-6	1.68E-31
	Anapl_07454	101796809	LOC101796809	probable E3 ubiquitin-protein ligase HERC3	-6	8.13E-21
	Anapl_18133	101789989	DES	desmin	-6	0.0000061
	Anapl_18492	101804236	LOC101804236	interferon-induced double-stranded RNA-activated protein kinase	-5	9.25E-25
	Anapl_10146	101797758	NMI	N-myc and STAT interactor	-5	4.4E-38
	Anapl_06658	101804116	FMO5	dimethylaniline monooxygenase [N-oxide-forming] 5	-5	3.53E-09
	Anapl_05113	101803982	TMEM140	transmembrane protein 140	-5	3.37E-23
	Anapl_10109	101789724	PARP9	poly(ADP-ribose) polymerase family member 9	-5	0.00000591
	Anapl_04378	101803758	C1QA	complement C1q A chain	-4	1.2E-35
	Anapl_05119	101804899	MGP	matrix Gla protein	-4	0.000000162
	Anapl_04377	101803105	C1QB	complement C1q B chain	-4	1.67E-27
	Anapl_05503	101802002	MORN3	MORN repeat containing 3	-4	4.07E-08
	Anapl_02710	101792273	ANXA2	annexin A2	-4	0.00000494
Upregulated						
	Anapl_09237	101802278	HEBP2	heme binding protein 2	4	1.48E-12
	Anapl_07161	106017883	LOC106017883	uncharacterized LOC106017883	4	0.000104
	Anapl_15348	101802855	CAMK1G	calcium/calmodulin dependent protein kinase IG	4	0.000000211
	Anapl_03384	101789775	NPPA	natriuretic peptide A	4	0.00249
	Anapl_00326	101795529	PLLP	plasmolipin	4	2.87E-22
	Anapl_07480	101792989	FA2H	fatty acid 2-hydroxylase	4	0.00314
	Anapl_02114	101797223	APOD	apolipoprotein D	4	4.45E-08
	Anapl_13900	101797552	GNG13	G protein subunit gamma 13	4	4.8E-13
	Anapl_18398	101793310	LOC101793310	transitional endoplasmic reticulum ATPase	10	1.05E-10
	Anapl_18322	101803793	LOC101803793	E3 SUMO-protein ligase PIAS2	16	0.0016
	Anapl_18555	101791000	LOC101791000	heterogeneous nuclear ribonucleoprotein K	38	8.42E-36
	Anapl_19040	101795174	LOC101795174	vasculin	41	8.93E-09
	Anapl_18360	101793809	LOC101793809	ras GTPase-activating protein 1	50	0.00491
	Anapl_18543	101798222	LOC101798222	transitional endoplasmic reticulum ATPase	52	5.78E-28
	Anapl_18875	101801464	LOC101801464	AN1-type zinc finger protein 5	66	0.0000278
	Anapl_18963	106020377	LOC106020377	60S ribosomal protein L37-like	201	6.68E-36
	Anapl_18574	101790838	BTF3	transcription factor BTF3	258	1.07E-30

3.3. Gene Ontology of PaBV-2 infected ducks

To examine the correlation between differentially expressed genes and infection-induced biological processes, table 3 was uploaded onto the Database for Annotation, Visualization, and Integrated Discovery (DAVID). [94, 95] A cutoff of $P \leq 0.01$ was set for Gene Ontology (GO) term enrichment. Results of the GO term enrichment indicated that two biological process groups were affected: immune system and cellular response to another organism (Figure 2). Immune system processes included immune response (15 genes), antigen processing and presentation (6 genes), response to chemical (12 genes), response to external stimulus (9 genes), immune effector process (5 genes), positive regulation of immune system process (5 genes), and regulation of immune system response (6 genes). Cellular response to another organism processes included multi-organism cellular process (6 genes), interspecies interaction between organisms (6 genes), response to other organism (6 genes), response to biotic stimulus (6 genes), and negative regulation of multi-organism process (3 genes). Individual genes of the 49 differentially expressed genes associated with the GO term biological process are shown in figure 3.

Figure 2. Enriched Biological Process GO Terms of 49 Differentially Expressed Genes from Infected Ducks. Only enriched terms with a $P \leq 0.01$ and a fold change $\geq |4|$ were used. Each section represents a GO term biological process, and the number of gene hits are next to each term. A gene can be included in more than one GO term biological process. Supplementary table 1 contains tables of genes associated with each depicted GO term. Genes for each labeled GO term are depicted in the table below.

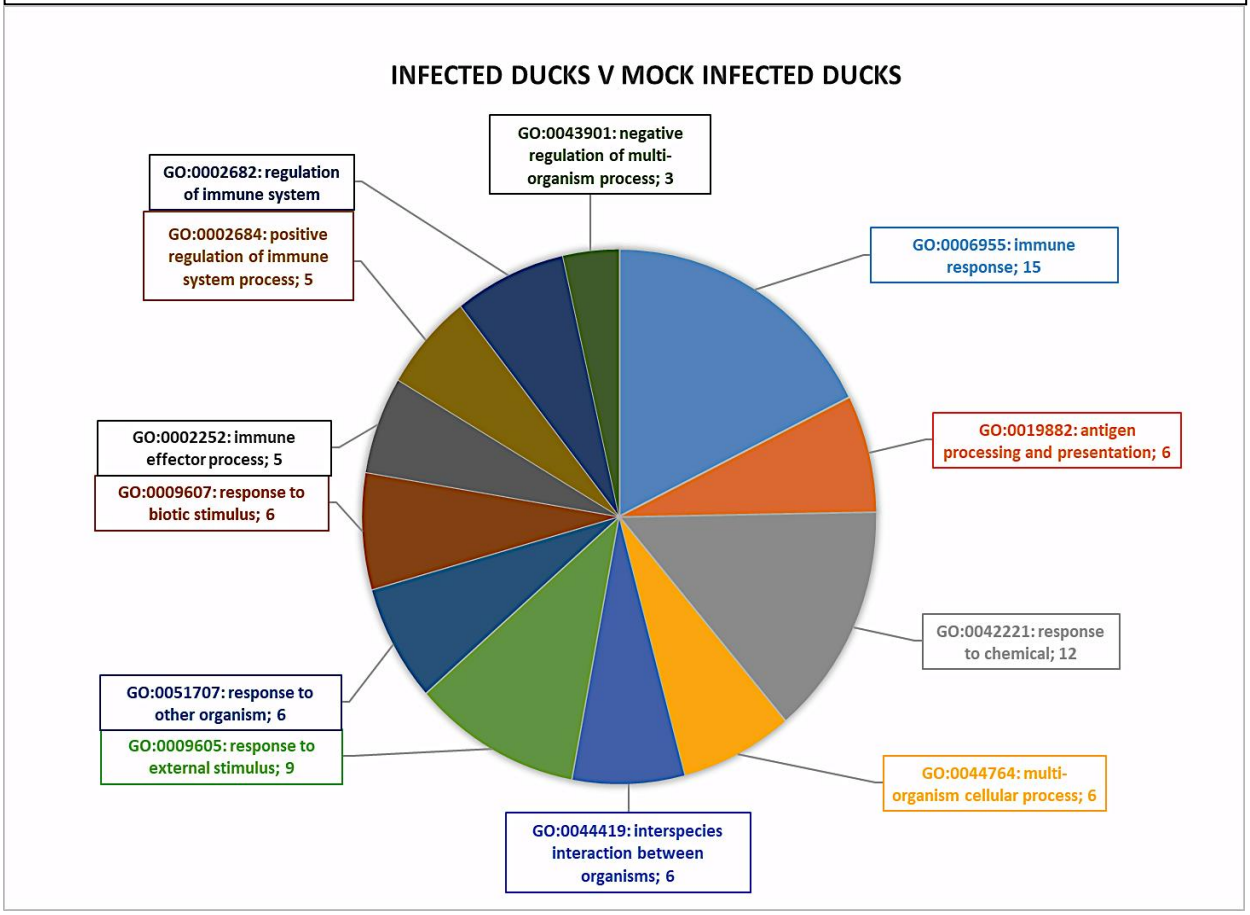

Figure 3. Genes Associated with Each Depicted GO Term. Genes for each labeled GO term are depicted in the table below.

GO:0019882: antigen processing and presentation		GO:0051707: response to other organism		GO:0043901: negative regulation of multi-organism process
LOC101804845	LOC101789604	B2M	RSAD2	EIF2AK2
B2M	TAP1	EIF2AK2	TLR3	RSAD2
CTSS	TAP2	IRF1	TAP2	TRIM25

GO:0009605: response to external stimulus		GO:0044419: interspecies interaction between organisms		GO:0044764: multi-organism cellular process	
LOC101791569	B2M	EIF2AK2	TLR3	EIF2AK2	TLR3
LOC101800938	EIF2AK2	IRF1	TAP1	IRF1	TAP1
LOC101791385	IRF1	RSAD2	TRIM25	RSAD2	TRIM25

GO:0009607: response to biotic stimulus		GO:0002252: immune effector process		GO:0002684: positive regulation of immune system process	
B2M	RSAD2	B2M	TLR3	B2M	TLR3
EIF2AK2	TLR3	IRF1	TAP2	IRF1	TAP2
IRF1	TAP2	RSAD2		RSAD2	

GO:0006955: immune response		GO:0042221: response to chemical		GO:0002682: regulation of immune system process	
LOC101791569	EIF2AK2	LOC101791569	EIF2AK2	B2M	RSAD2
LOC101800938	IRF1	LOC101800938	IRF1	IRF1	TLR3
LOC101791385	PARP9	LOC101791385	PARP9	PARP9	TAP2
LOC101804845	RSAD2	NMI	TLR3		
NMI	TLR3	B2M	TAP2		
B2M	TAP2	CTSS	USP18		
CTSS	TRIM25				
LOC101789604					

3.4. Major genes and pathways of PaBV-2 infection in duck brain

Using the information from the comparisons between infected and control duck expression profiles and from GO enrichment, fifteen genes, based on their dysregulation and their function in both the cellular response to other organism and the immune system response, were selected for pathway analysis (Table 5).

Table 5. Top 15 Selected Genes. Fold changes depicted are taken from the same values on Table 3.

Feature ID	Gene Symbol	Gene Description	Fold Change
Anapl_01687	LOC101791569	C-C motif chemokine 4-like	-152
Anapl_13350	MX	interferon-induced GTP-binding protein Mx-like	-139
Anapl_14386	RSAD2	viperin, radical S-adenosyl methionine domain containing 2	-120
Anapl_08494	IRF7	interferon regulatory factor 7	-99
Anapl_13382	EIF2AK2	interferon induced eukaryotic translation initiation factor 2 alpha kinase 2	-42
Anapl_19105	Anpl-U	class I histocompatibility antigen, F10 alpha chain	-31
Anapl_16041	TAP1	transporter 1	-29
Anapl_03154	TRIM25	tripartite motif containing 25	-20
Anapl_17300	IRF1	interferon regulatory factor 1	-12
Anapl_16039	TAP2	transporter 2	-11
Anapl_01734	B2M	beta-2-microglobulin	-11
Anapl_09935	TLR3	toll like receptor 3	-10
Anapl_17425	LOC101789604	class II histocompatibility antigen, B-L beta chain	-7
Anapl_09516	CTSS	cathepsin S	-6
Anapl_17426	Anpl-DRA	HLA class II histocompatibility antigen, DR alpha chain	-5

The genes were uploaded onto the Kyoto Encyclopedia of Genes and Genome (KEGG) pathway database. [96-98] Of the 20 pathways with hits for the duck in KEGG, two are pathways from viral infection and five pathways are part of the immune response. Viral infection pathways include the duck Influenza A pathway (8 genes), and the duck herpes

simplex infection pathway (8 genes). Pathways of the immune response included the toll-like receptor signaling pathway (3 genes), necroptosis pathway (2 genes), RIG-I-like receptor signaling pathway (2 genes), the cytosolic DNA-sensing pathway (2 genes), and the intestinal immune network for IgA production pathway (2 genes). Pathways and their correlating genes are depicted on table 6.

Table 6. KEGG Pathway Analysis Results. Each pathway, number of gene hits, and genes in each pathway are depicted.

		TLR3	toll like receptor 3
		RSAD2	radical S-adenosyl methionine domain containing 2
		TRIM25	tripartite motif containing 25
		MX	interferon-induced GTP-binding protein Mx-like
		IRF7	interferon regulatory factor 7
		EIF2AK2	eukaryotic translation initiation factor 2 alpha kinase 2
		Anpl-DRA	HLA class II histocompatibility antigen, DR alpha chain
apla05168	Herpes simplex infection (8)	LOC101789604	class II histocompatibility antigen, B-L beta chain
		Anpl-U	class I histocompatibility antigen, F10 alpha chain
		TLR3	toll like receptor 3
		IRF7	interferon regulatory factor 7
		TAP2	transporter 2, ATP binding cassette subfamily B member
		TAP1	transporter 1, ATP binding cassette subfamily B member
		EIF2AK2	eukaryotic translation initiation factor 2 alpha kinase 2
		Anpl-DRA	HLA class II histocompatibility antigen, DR alpha chain
apla04145	Phagosome (6)	LOC101789604	class II histocompatibility antigen, B-L beta chain
		Anpl-U	class I histocompatibility antigen, F10 alpha chain
		CTSS	cathepsin S
		TAP2	transporter 2, ATP binding cassette subfamily B member
		TAP1	transporter 1, ATP binding cassette subfamily B member
		Anpl-DRA	HLA class II histocompatibility antigen, DR alpha chain
apla04514	Cell adhesion molecules (CAMs) (3)	LOC101789604	class II histocompatibility antigen, B-L beta chain
		Anpl-U	class I histocompatibility antigen, F10 alpha chain
		Anpl-DRA	HLA class II histocompatibility antigen, DR alpha chain
apla04620	Toll-like receptor signaling pathway (3)	TLR3	toll like receptor 3
		LOC101791569	C-C motif chemokine 4-like
		IRF7	interferon regulatory factor 7
apla04217	Necroptosis (2)	TLR3	toll like receptor 3
		EIF2AK2	eukaryotic translation initiation factor 2 alpha kinase 2
apla04623	Cytosolic DNA-sensing pathway (2)	LOC101791569	C-C motif chemokine 4-like
		IRF7	interferon regulatory factor 7
apla04622	RIG-I-like receptor signaling pathway (2)	TRIM25	tripartite motif containing 25
		IRF7	interferon regulatory factor 7
apla02010	ABC transporters (2)	TAP2	transporter 2, ATP binding cassette subfamily B member
		TAP1	transporter 1, ATP binding cassette subfamily B member
apla04672	Intestinal immune network for IgA production (2)	LOC101789604	class II histocompatibility antigen, B-L beta chain
		Anpl-DRA	HLA class II histocompatibility antigen, DR alpha chain
apla04625	C-type lectin receptor signaling pathway (1)	IRF1	interferon regulatory factor 1
apla04621	NOD-like receptor signaling pathway (1)	IRF7	interferon regulatory factor 7
apla04218	Cellular senescence (1)	Anpl-U	class I histocompatibility antigen, F10 alpha chain
apla04141	Protein processing in endoplasmic reticulum (1)	EIF2AK2	eukaryotic translation initiation factor 2 alpha kinase 2
apla04144	Endocytosis (1)	Anpl-U	class I histocompatibility antigen, F10 alpha chain
apla04060	Cytokine-cytokine receptor interaction (1)	LOC101791569	C-C motif chemokine 4-like
apla05132	Salmonella infection (1)	LOC101791569	C-C motif chemokine 4-like
apla04210	Apoptosis (1)	CTSS	cathepsin S
apla04142	Lysosome (1)	CTSS	cathepsin S

CHAPTER IV

DISCUSSION

4.1. Discussion on selected down-regulated genes related to the immune response

4.1.1. Pattern Recognition Receptor Signaling and Interferon Induction

Tripartite motif containing 25 (TRIM25), toll-like receptor 3 (TLR3), Interferon regulatory factor 7 (IRF7) and interferon regulatory factor 1 (IRF1) genes are regulators of the innate immune response against viruses and are downregulated in PaBV-2 infection.

4.1.1.1. Tripartite Motif Containing 25

Tripartite motif containing 25 (TRIM25) gene is necessary for activation of the RIG-I signaling pathway, a pattern recognition receptor (PRR) (Figure 4). Genetic mutations that disrupt TRIM25 function have downstream effects of decreasing signaling by RIG-I and IFN induction, and of antiviral activity. [123, 124] The non-structural protein 1 and nucleoproteins of Influenza A and SARS-CoV, respectively, bind TRIM25 to inhibit ubiquitination and activation of RIG-I in cell culture studies. [125, 126] Unlike these viruses, TRIM25 is inhibited by the binding with the subgenomic RNA of dengue virus. [127] Interestingly, of all the selected genes in our study, TRIM25 is unique in that the downstream effected RIG-1 gene is lacking in the chicken. This lack of RIG-I signaling pathway may be a reason why avian influenza is more virulent in chickens than in ducks and maybe a contributing factor in why mallard ducks are a reservoir species for avian influenza. [128] Additionally, borna disease

viruses (BDV) are able to evade the RIG-I signaling pathway as the 5' end triphosphate group is replaced with a monophosphate group during BDV genomic replication, and this end triphosphate is not recognized by the RIG-I receptor. [129]

4.1.1.2. Toll-like Receptor 3

Toll-like Receptor 3 (TLR3) is an endosomal receptor that is shown to be expressed in the neurons of ducks. [130, 131] Viral RNA recognition by TLR3 activates the toll-like receptor pathway in avian species (Figure 4). [132] Toll-like receptor 3 is implicated in multiple neurotropic viruses as it is expressed on nerve cells and is able to induce the expression of type I interferons and proinflammatory chemoattractants. Viruses hijack TLR3 and can either inhibit or enhance inflammation of the nervous system through TLR3 control. [131] West Nile virus is able to inhibit TLR3 signaling and subsequently type I interferon expression in cell culture. However in vivo, TLR3 signaling and the subsequent expression of type I interferons increases the permeability of the blood-brain barrier and facilitates West Nile virus entry into and infection of the brain. [133-136] In an infection by herpes simplex virus, the downregulation of TLR3 in mice brains increases the vulnerability of astrocytes to infection. [137] However, TLR3 can also be hijacked for viral replication. TLR3 is upregulated in response to infection by rabies virus in mice. [138] This is due to TLR3 being expressed on the inclusion bodies, called Negri Bodies, during rabies virus infection. However, when TLR3 is absent in knockout mice, Negri bodies fail to form and mice are rabies resistant. [139, 140] It should be noted that TLR3 is unique among toll-like receptors. TLR3 expression is upregulated by type I interferons (IFNα and IFNβ) in the central nervous

system. This is unlike most toll-like receptors that upregulate relative to viral load. Researchers postulate that this may aid in making cells more sensitive to neighboring infected cells in the central nervous system. [138]

4.1.1.3. Interferon Regulatory Factor 7

Both the toll-like receptor pathway and the RIG-I receptor pathway activate interferon regulatory factors to induce the expression of type I interferons. Interferon regulatory factor 7 (IRF7) is activated downstream of both the RIG-I and toll-like receptor signaling pathway (Figure 4). Interferon regulatory factor 7 forms a homodimer or heterodimer with IRF3 located in the cytosol. IRF7 is able to activate both IFNα and IFNβ, while IRF3 activates IFNβ, and both are constitutively expressed in cells. [141] Once activated by pattern recognition receptor signaling pathways, IRF7 and IRF3 migrate to the nucleus and bind to the type I interferon promoter regions to express IFNα and IFNβ. [140, 142] However, IRF7 is the main regulator of type I IFN gene expression. In IRF7 knockout mice, severity of West Nile virus infection of mice was greater than that of IRF3 knockout mice. In addition to an increased severity, IRF7 knockout mice had an expanded tissue tropism, increased viral load, and earlier entry into the central nervous system by West Nile virus than the IRF3 knockout mice. [141] This is not entirely unexpected as IRF7 induced interferons are able to induce the expression of over 300 genes including signal transducer and activator of transcription 1 (STAT1), class I major histocompatibility complex (MHC I), and interferon-induced myxovirus resistance dynamin like GTPase (MX). [143, 144] Both rabies and borna disease virus are able to inhibit IRF7, and subsequently inhibit the induced antiviral state of a host cell, by different viral proteins (Figure

5). The phosphoprotein protein (P-protein) of rabies virus is able to block phosphorylation of IRF3 and IRF7 via the regulatory proteins proteins Traf family member associated-activator NF-κB (TANK) binding kinase-1 and inhibitor of nuclear factor kappa B kinase ϵ, respectively. This effectively inhibits expression of type I interferon genes. [140, 145] Interferon regulatory factor 7 is inhibited by the BDV nucleoprotein in oligodendroglia cells; however the mechanism of inhibition is unknown. IRF3 is inhibited by the BDV phosphoprotein because this protein is a competitive inhibitor of IRF3 to the TANK binging protein 1 binding site (Figure 5). [129, 136, 146-148]

Figure 4. Relationships between Top 15 Chosen Genes. Genes in maroon boxes are from the list of the top 15 chosen genes. Grey ovals represent genes that are not part of the top 15 selected genes, but are involved in the top 15 gene downstream relationships. Arrows represent downstream relationships.

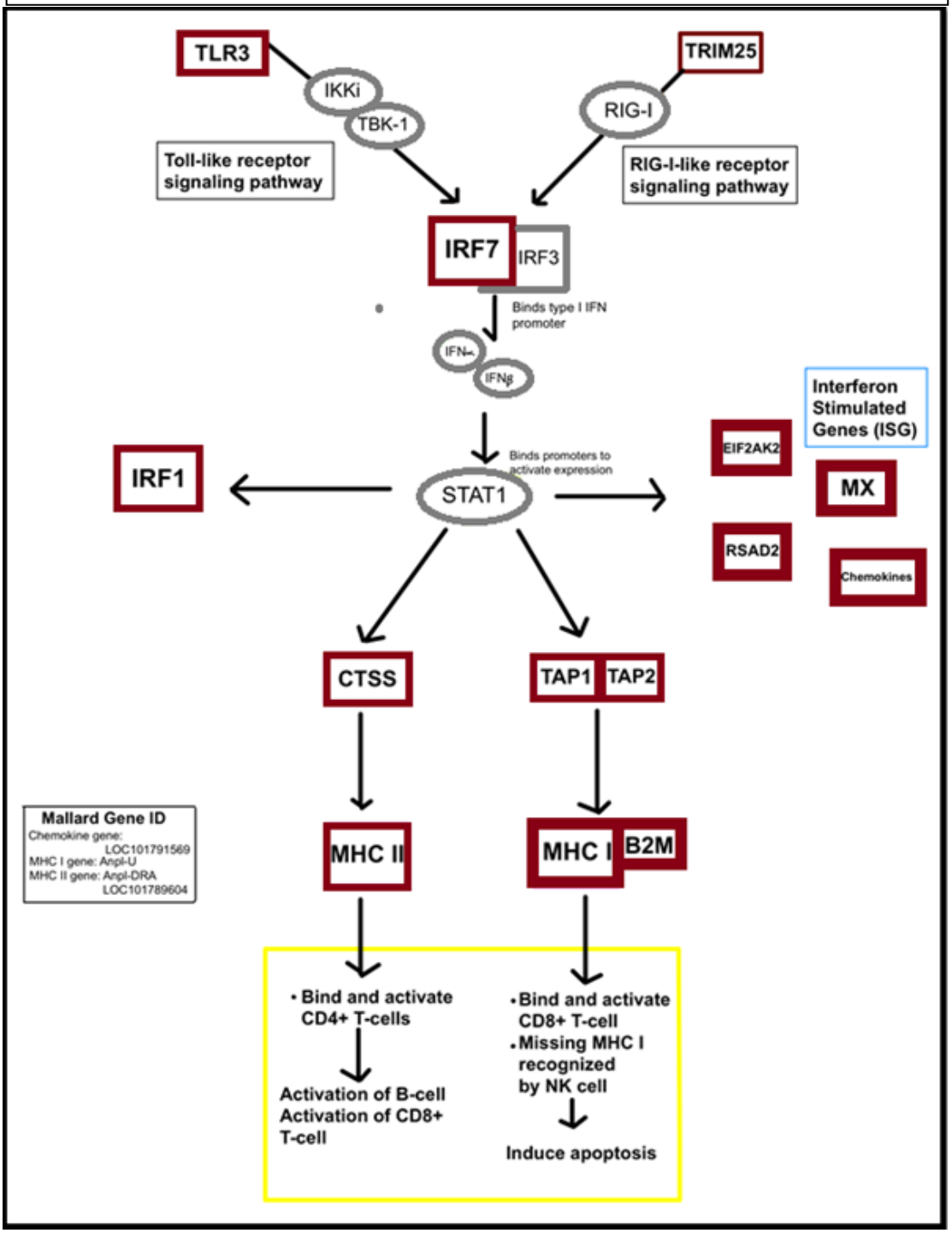

4.1.1.4. Interferon Regulatory Factor 1

Interferon regulatory factor 1 (IRF1) is not induced by the PRR signaling pathways like IRF7. IRF1 is activated later in the viral replication cycle than IRF7. Interferon regulatory factor 1 is essential to inducing the antiviral effects of IFNγ which is released by natural killer cells (Figure 6). It is postulated that IRF1 induces a second wave of type I interferons through activation of the Jak/STAT pathway (Figure 4), which feedback into inducing genes through IRF7. This aids in maintaining an antiviral state in the host cell. [149, 150] Interferon regulatory factor 1 can be induced by IFNγ interferons released by natural killer cells. Upon activation, IRF1 binds to the IRF1 responsive element (IRF-E) which promotes expression of TAP1 and subsequently MHC I [151]. Interferon regulatory factor 1 knockout mice are deficient in natural killer cells and cytotoxic T-cells. [151, 152] Several important disease causing viruses are inhibited in cell culture by IRF1, possible through IRF1 effect on inducible transcripts that overlap with interferon induced transcripts (Figure 6). [153]

Interferon regulatory factor 1 has recently been isolated in mallard ducks, and its function is not dissimilar from human IRF1 as it is able to induce IFNβ. [154] In ducks, IRF1 is an essential regulatory factor for the host antiviral response. When ducks were infected with avian influenza A, IRF1 was significantly activated, induced production of type I interferons and inhibited viral replication. [154] Additionally while it is expressed in the spleen, liver, brain, and pancreas, upon stimulation with avian influenza virus, expression of IRF1 was found to be highest in the brain. [154] Vesicular stomatitis virus (VSV) infected mice cleared the infection, however IRF1 knockout mice succumbed to encephalitis caused by VSV infecting the central nervous system. Researchers postulate that IRF1 protects the host cell

later in the viral replication cycle, after the initial induction of type I interferons, and inhibits inflammation of the central nervous system in response to a VSV infection. [151, 155]

4.1.2. Interferon Stimulated Genes

The Interferon-induced myxovirus resistance dynamin like GTPase (MX), viperin (RSAD2), and the eukaryotic translation initiation factor 2 alpha kinase 2 (EIF2AK2) genes are constituently expressed in cells and are further induced by type I interferons. LOC101791569 is described as a C-C motif chemokine-4 like gene, which is expressed by innate immune cells (Figure 4). These genes produce chemokines induced by inflammation and an antiviral state in host cells.

Figure 5. Viral Interactions with the Top 15 Genes. Rabies virus phosphoprotein (P-protein) is able to inhibit phosphorylation of IRF7, via IKKi and TBK-1, and STAT1. The mammalian BV genome has a monophosphate 5' end which is not recognized by the RIG-I receptor. Both mammalian and avian BV are able to inhibit RIG-I via the non-structural X protein in cell culture. The mammalian BV nucleoprotein (N-protein)protein can inhibit IRF7 function. The mammalian BV phosphoprotein (P-protein) can inhibit IRF3, which forms a dimer with IRF7.

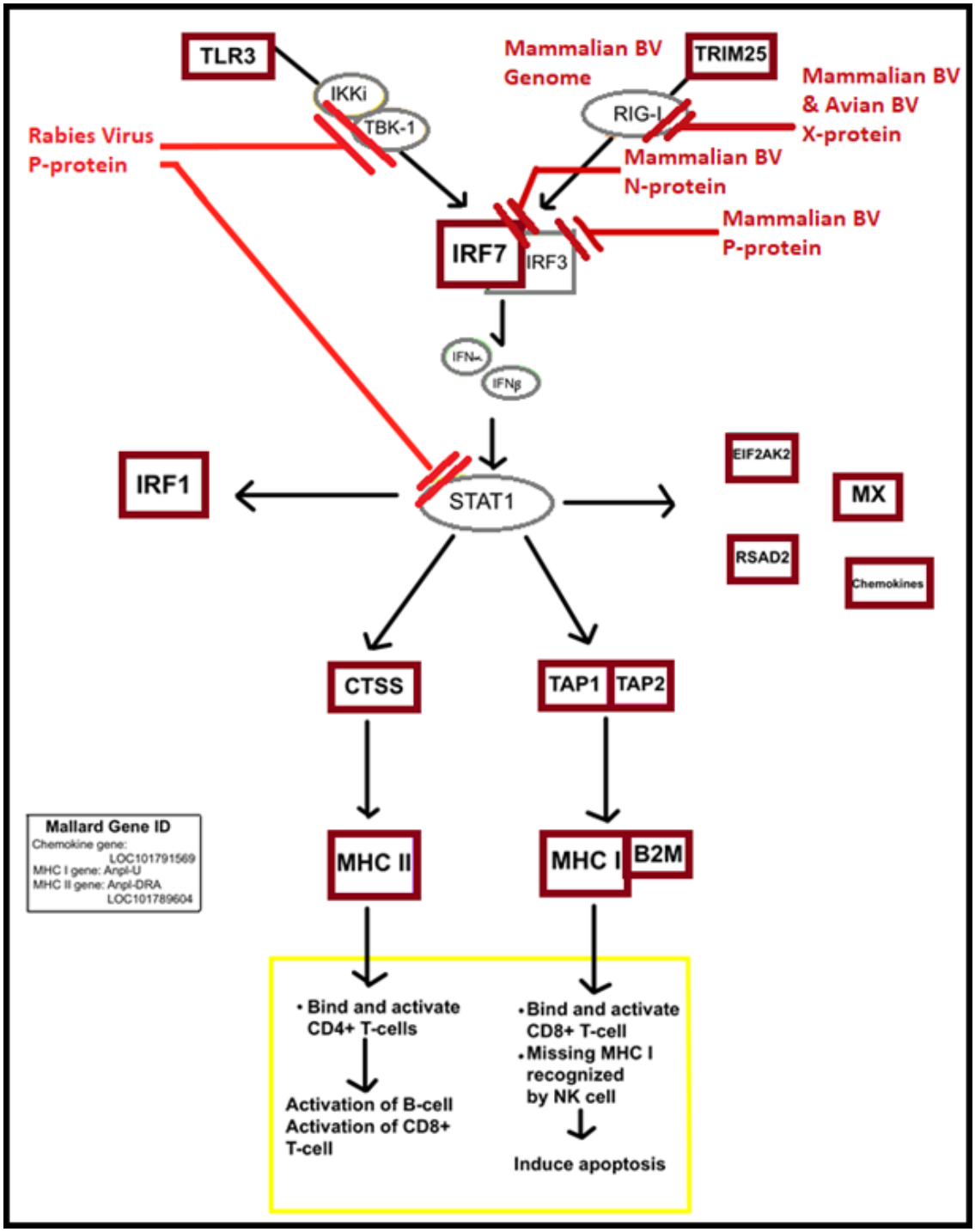

4.1.2.1. Interferon-induced myxovirus resistance dynamin like GTPase

The Interferon-induced myxovirus resistance dynamin like GTPase (MX) gene is known to protect against negative-stranded RNA by inhibiting viral replication or viral entry. By controlling vesicle trafficking in the cell, the MX protein is able to trap essential viral replicating proteins. [156, 157] The MX gene is further expressed by both type I and type II interferons (Figure 6). [158] The control of vesicle transport stimulates a broad antiviral response. MX restricts viral replication of viruses through blocking viral RNA from entering the nucleus, attacking viral nucleocapsids to prevent cytoplasmic mRNA replication, sequestering viral N proteins, and inhibiting viral integration into the host DNA. [158] Influenza virus replication is specifically blocked by MX inhibiting assembly of viral ribonucleoprotein complexes via the polymerase basic protein 2 (PB2) and nucleoprotein (NP) viral proteins necessary for viral replication in the host cell. [159] Both RIG-I and MX are upregulated in ducks when infected with a low pathogenic form of avian influenza virus. This is interesting as mallard ducks are a reservoir for avian influenza, a disease that is lethal to chickens and humans. [128, 160] The nucleoprotein is a main determinant of influenza A virus vulnerability to MX, but the nucleoproteins can vary amongst influenza A virus strains which causes variability in MX sensitivity. [161, 162] Increased sensitivity to MX may account for decreased virus success in mammals. [161, 162] Other than influenza A virus, MX is able to target rabies virus and inhibit replication similar to how MX is able to inhibit replication of VSV, two viruses in the same family. [163]

4.1.2.2. Viperin

Viperin (RSAD2) is associated with the endoplasmic reticulum and protects the host cell against enveloped and RNA viruses. Viperin targets viruses to both inhibit initial viral replication, packaging, and release from the host cell. [157] Viperin in the duck is expressed in the brain, and is highly similar to other species including mammals. [164] Viperin expression is able to impair viral transmission in respiratory syncytial virus (RSV) infected cells by possibly inhibiting virus formation. [165]

4.1.2.3. Eukaryotic Translation Initiation Factor 2 Alpha Kinase 2

Eukaryotic translation initiation factor 2 alpha kinase 2 (EIF2AK2), also called PKR, functions to phosphorylate eIF2α which stops mRNA translation. It also has the ability to act as a cytosolic PRR and activate the RIG-I signaling pathway when it directly interacts with viral RNA (Figure 6). [166, 167] Other than RIG-I, EIF2AK2 interacts with multiple pattern recognition receptor pathways that regulate apoptosis, inflammation, and possibly the adaptive immune response. [156] While it is constitutively being expressed in cells, its expression is upregulated by type I and type II interferons (Figure 4). [156, 166, 167] Influenza A and B non-structural protein 1 inhibits EIF2AK2, however this same protein downregulated RIG-I signaling. [166] Ebola virus polymerase cofactor VP35 inhibits EIF2AK2 activation and inhibits IRF7 activation. [166] Both viruses inhibit EIF2AK3 expression by blocking proteins which signal the production of type I interferons. [166] Sendai virus C and human

parainfluenza virus type 1 produces proteins that limit RNA replication to avoid activation of antiviral EIF2AK2. [168]

The downregulation of these genes may be due to PaBV-2 inhibiting the function of STAT1. After STAT1 and STAT2 are activated by IFNα and IFNβ, the rabies virus phosphoprotein inhibits STAT1 and STAT2 function (Figure 5). Specifically, the phosphoprotein is able to bind to STAT1 so that the STAT complex cannot enter the nucleus, and the phosphoprotein can block the DNA promoters that STAT binds to activate. This blocks the host cell from carrying out an antiviral response by interferon stimulated genes, MX, EIF2AK2, and RSAD2. Interestingly, STAT1 is consistently upregulated in central nervous system infections of Japanese encephalitis virus, rabies virus, and sindbus virus. [140, 144, 169]

4.1.2.4. LOC101791569 (C-C Motif Chemokine-like)

Chemokines, including LOC101791569, function to attract leukocyte or proinflammatory cells. [170] TLR3 activation mediates the inflammatory response as it regulates the production of cytokines and chemokines through the downstream proteins TNF receptor associated factor 6, inhibitor of nuclear factor kappa B kinase subunit epsilon, and nuclear factor kappa-light-chain-enhancer (Figure 4). Additionally, TLR3 mediates the infection of the brain by West Nile virus due to the increased expression of cytokines and chemokines increasing the permeability of the blood brain barrier. [133, 134] Expression of chemokines in rabies infection increases the permeability of the blood brain barrier to allow migration of immune cells including natural killer cells and T-cells. [171] In mammalian borna

disease virus (BDV) infected mice, there was significant upregulation of chemokines before leukocyte infiltration or neurological disease was seen in the central nervous system. However, the production of cytokines did not significantly occur from the abundantly infected astrocytes in the central nervous system of infected mice. Investigators theorize that the infection of BDV may be affecting the gene expression of chemokines. [172]

4.1.3. Antigen Presentation Processing

Transporter associated with antigen processing 1(TAP1), transporter associated with antigen processing 2 (TAP2), and cathepsin S (CTSS) are essential genes in the antigen presentation pathway. These genes control the expression of Anpl-U (MHCI), Anpl-DRA (MHCII), LOC101789604 (MHCII), and beta-2-microglobulin (B2M)(Figure 4). Without both TAPs, no MHC I would reach the cell surface, and CTSS is necessary to release MHC II, including B2M, proteins to the cell surface. Additionally, expression of these genes begins to overlap with previously mentioned downregulated genes of the immune system response.

4.1.3.1. Transporter associated with antigen processing 1 and 2

Expressed on the endoplasmic reticulum, TAP1 and TAP2 are two proteins of the TAP heterodimer that function to transport degraded peptides in the antigen presentation process. MHC I (Anpl-U) complex is bound to TAP which loads digested antigen peptides onto it. Only then can the MHC I be displayed on the cell membrane. [151, 173] Transporter associated with antigen processing genes are in close proximity to MHC I, MHC II, B2M

genes on the duck genome, and IRF1 is able to induce expression of the TAP gene (Figure 6). [151, 174] Additionally, upregulation of TAP1 gene expression is associated to an upregulation in the expression of MHC I in cell culture. This mechanism was used to avoid cell death via natural killer cells during a hepatitis C virus infection. [175]

4.1.3.2. Cathepsin S

Cathepsin S (CTSS) performs proteolysis on the bond between CD74 and MHC II, and frees MHC II (Anpl-DRA, LOC101789604, and B2M) to migrate to the cell surface. [176] Cathepsin S gene expression does not change when chemokines and cytokines, including IFNγ, TNFα, are released, indicating that CTSS expression is independent of interferon expression. Additonally, cathepsin S is not expressed in astrocytes but is expressed in the microglia of the central nervous system in mice. [177] The antigen presentation process in the central nervous system is significantly hindered when CTSS is impaired. Additionally, expression of CD74 is able to regulate the expression of CTSS, but chemokines and cytokines do not in the central nervous system. [177] Finally, cathepsin S is upregulated across 3 different neurotropic viral infections in mice including rabies virus, Japanese encephalitis, and sindbis virus. [169]

Figure 6. Cross Interactions with the Top 15 Genes. EIF2AK2 recognizes viral genomes and in turn can activate the RIG-I signaling pathway. Natural killer cells and CD8+ cytotoxic T-cells release IFNγ which is able to activate both IRF1 and IRF7. IRF1 can in turn activate interferon stimulated genes and TAP1. The induction of type I interferons interact with IRF7 through positive feedback.

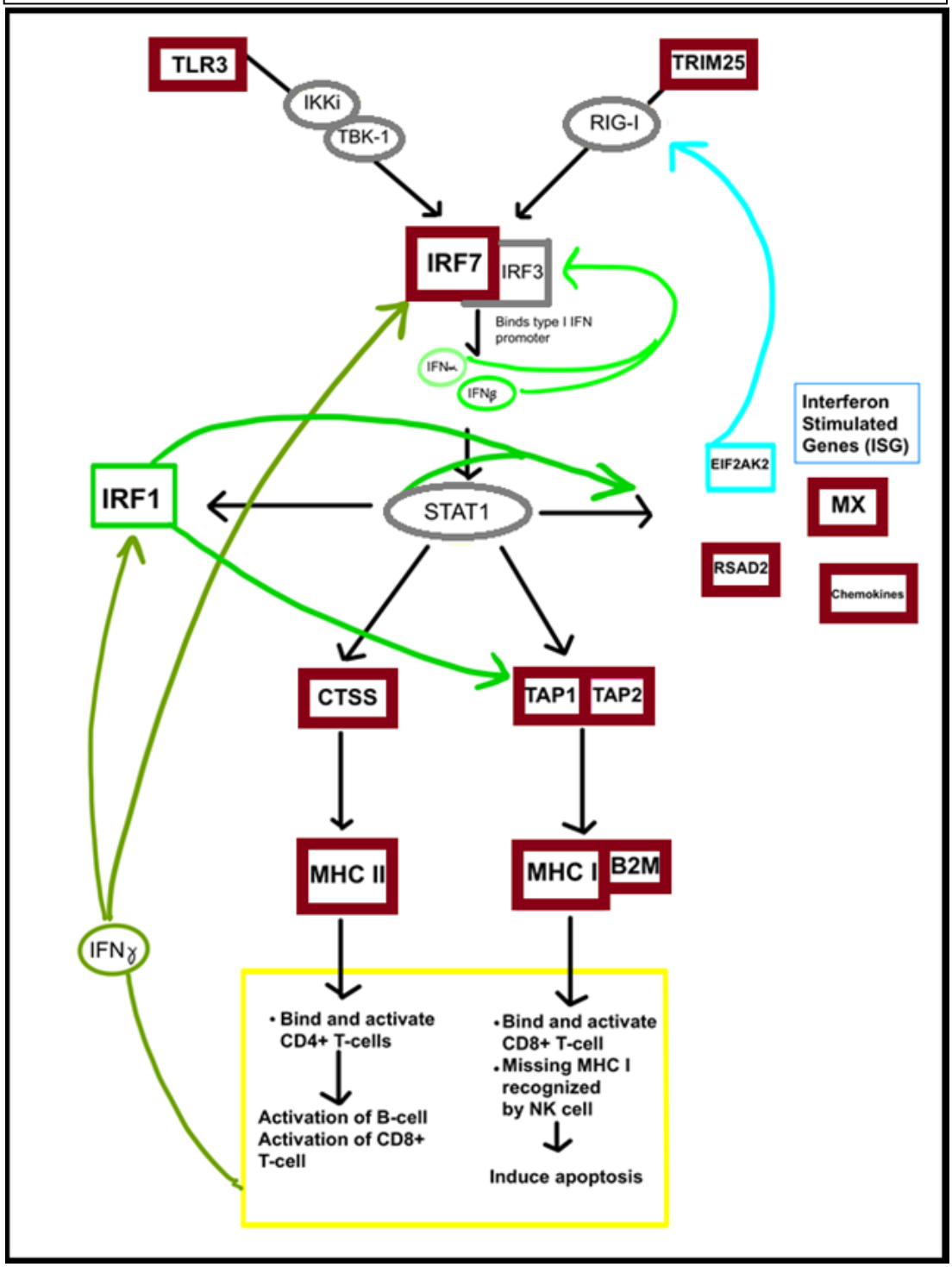

CHAPTER V

CONCLUSION

In our study, we identified differentially expressed genes in ducks infected with PaBV-2. Of these differentially expressed genes, a majority of the genes downregulated at least by 4-fold change from the infected ducks were related to immunology and viral recognition. Unexpectedly, we were able to obtain differentially expressed genes from an infected duck that also exhibited severe ataxia. Clinical signs in ducks due to PaBV-2 infection have not been previously observed in North America. This is the first observation of PDD-like clinical signs with neurological involvement in avian bornavirus infected waterfowl.

While significant, this study is not without its limitations. First, the duck genome is not fully annotated and functions of certain genes are still to be fully elucidated. Secondly, while this study used PaBV-2 infected mallard ducks, PaBV-2 is not known to naturally infect mallard ducks. Noting these limitations, this study is relevant as ducks can be experimentally infected with PaBV-2, PDD is an avian disease, and most importantly, there is not a standard reference genome in other PaBV bird model such as conures or cockatiels. With this study, precedence has been set for the use of RNA-Seq in the research of PaBV infection. This study showed immunologically relevant genes are differentially expressed in ducks infected with PaBV-2 and this study is the first of its kind to use RNA-Seq in the study of PaBV.

REFERENCES

1. Gray, P., et al., *Use of avian bornavirus isolates to induce proventricular dilatation disease in conures.* Emerg Infect Dis, 2010. **16**(3): p. 473-9.

2. Hoppes, S.M., I. Tizard, and H.L. Shivaprasad, *Avian bornavirus and proventricular dilatation disease: diagnostics, pathology, prevalence, and control.* Vet Clin North Am Exot Anim Pract, 2013. **16**(2): p. 339-55.

3. Stenglein, M.D., et al., *Genome Sequence of a Bornavirus Recovered from an African Garter Snake (Elapsoidea loveridgei).* Genome Announcements, 2014. **2**(5): p. e00779-14.

4. Guo, J. and I. Tizard, *The genome sequence of parrot bornavirus 5.* Virus Genes, 2015. **51**(3): p. 430-3.

5. Kuhn, J.H., et al., *Taxonomic reorganization of the family Bornaviridae.* Arch Virol, 2015. **160**(2): p. 621-32.

6. Schlottau, K., et al., *Variegated Squirrel Bornavirus 1 in Squirrels, Germany and the Netherlands.* Emerging Infectious Diseases, 2017. **23**(3): p. 477-481.

7. Kuhn, J.H., et al., *Taxonomic reorganization of the family Bornaviridae.* Archives of Virology, 2015. **160**(2): p. 621-632.

8. Kistler, A.L., et al., *Recovery of divergent avian bornaviruses from cases of proventricular dilatation disease: identification of a candidate etiologic agent.* Virol J, 2008. **5**: p. 88.

9. Honkavuori, K.S., et al., *Novel borna virus in psittacine birds with proventricular dilatation disease.* Emerg Infect Dis, 2008. **14**(12): p. 1883-6.

10. Reuter, A., et al., *Avian bornaviruses escape recognition by the innate immune system.* Viruses, 2010. **2**(4): p. 927-38.

11. Leal de Araujo, J., et al., *Are anti-ganglioside antibodies associated with proventricular dilatation disease in birds?* PeerJ, 2017. **5**: p. e3144.

12. Bourque, L., et al., *Identification of avian bornavirus in a Himalayan monal (Lophophorus impejanus) with neurological disease.* Avian Pathol, 2015. **44**(4): p. 323-7.

13. Guo, J., et al., *Avian Bornaviruses in North American Gulls.* J Wildl Dis, 2015. **51**(3): p. 754-8.

14. Last, R.D., et al., *Avian bornavirus genotype 4 recovered from naturally infected psittacine birds with proventricular dilatation disease in South Africa.* J S Afr Vet Assoc, 2012. **83**(1): p. 938.

15. Weissenbock, H., et al., *Avian bornaviruses in psittacine birds from Europe and Australia with proventricular dilatation disease.* Emerg Infect Dis, 2009. **15**(9): p. 1453-9.

16. Weissenbock, H., et al., *Novel avian bornavirus in a nonpsittacine species (Canary; Serinus canaria) with enteric ganglioneuritis and encephalitis.* J Virol, 2009. **83**(21): p. 11367-71.

17. Payne, S.L., et al., *Birds and bornaviruses.* Anim Health Res Rev, 2012. **13**(2): p. 145-56.

18. Hoppes, S., et al., *The isolation, pathogenesis, diagnosis, transmission, and control of avian bornavirus and proventricular dilatation disease.* Vet Clin North Am Exot Anim Pract, 2010. **13**(3): p. 495-508.

19. Mirhosseini, N., et al., *Proventricular dilatation disease in cockatiels (Nymphicus hollandicus) after infection with a genotype 2 avian bornavirus.* J Avian Med Surg, 2011. **25**(3): p. 199-204.

20. Piepenbring, A.K., et al., *Pathogenesis of avian bornavirus in experimentally infected cockatiels.* Emerg Infect Dis, 2012. **18**(2): p. 234-41.

21. Rubbenstroth, D., et al., *Avian bornaviruses are widely distributed in canary birds (Serinus canaria f. domestica).* Vet Microbiol, 2013. **165**(3-4): p. 287-95.

22. Monaco, E., et al., *The detection of avian bornavirus within psittacine eggs.* J Avian Med Surg, 2012. **26**(3): p. 144-8.

23. Delnatte, P., et al., *Investigation into the possibility of vertical transmission of avian bornavirus in free-ranging Canada geese (Branta canadensis).* Avian Pathol, 2014. **43**(4): p. 301-4.

24. Kerski, A., A.H. de Kloet, and S.R. de Kloet, *Vertical transmission of avian bornavirus in Psittaciformes: avian bornavirus RNA and anti-avian bornavirus antibodies in eggs, embryos, and hatchlings obtained from infected sun conures (Aratinga solstitialis).* Avian Dis, 2012. **56**(3): p. 471-8.

25. Lierz, M., et al., *Vertical transmission of avian bornavirus in psittacines.* Emerg Infect Dis, 2011. **17**(12): p. 2390-1.

26. Heckmann, J., et al., *Investigation of Different Infection Routes of Parrot Bornavirus in Cockatiels.* Avian Dis, 2017. **61**(1): p. 90-95.

27. Delnatte, P., et al., *Detection of Avian bornavirus in multiple tissues of infected psittacine birds using real-time reverse transcription polymerase chain reaction.* J Vet Diagn Invest, 2014. **26**(2): p. 266-71.

28. Zimmermann, V., et al., *Impact of antigenic diversity on laboratory diagnosis of Avian bornavirus infections in birds.* J Vet Diagn Invest, 2014. **26**(6): p. 769-77.

29. Delnatte, P., et al., *Avian bornavirus in free-ranging waterfowl: prevalence of antibodies and cloacal shedding of viral RNA.* J Wildl Dis, 2014. **50**(3): p. 512-23.

30. Raghav, R., et al., *Avian bornavirus is present in many tissues of psittacine birds with histopathologic evidence of proventricular dilatation disease.* J Vet Diagn Invest, 2010. **22**(4): p. 495-508.

31. Heffels-Redmann, U., et al., *Follow-up investigations on different courses of natural avian bornavirus infections in psittacines.* Avian Dis, 2012. **56**(1): p. 153-9.

32. Leal de Araujo, J., et al., *From nerves to brain to gastrointestinal tract: A time-based study of parrot bornavirus 2 (PaBV-2) pathogenesis in cockatiels (Nymphicus hollandicus).* PLoS ONE, 2017. **12**(11): p. e0187797.

33. Rinder, M., et al., *Broad tissue and cell tropism of avian bornavirus in parrots with proventricular dilatation disease.* J Virol, 2009. **83**(11): p. 5401-7.

34. Guo, J., et al., *Characterization of a new genotype of avian bornavirus from wild ducks.* Virol J, 2014. **11**: p. 197.

35. Horie, M., et al., *Isolation of avian bornaviruses from psittacine birds using QT6 quail cells in Japan.* J Vet Med Sci, 2016. **78**(2): p. 305-8.

36. Villanueva, I., et al., *The diagnosis of proventricular dilatation disease: Use of a Western blot assay to detect antibodies against avian Borna virus.* Veterinary Microbiology, 2010. **143**(2): p. 196-201.

37. de Kloet, A.H., A. Kerski, and S.R. de Kloet, *Diagnosis of Avian bornavirus infection in psittaciformes by serum antibody detection and reverse transcription polymerase chain reaction assay using feather calami.* J Vet Diagn Invest, 2011. **23**(3): p. 421-9.

38. Weissenbock, H., et al., *Localization of avian bornavirus RNA by in situ hybridization in tissues of psittacine birds with proventricular dilatation disease.* Vet Microbiol, 2010. **145**(1-2): p. 9-16.

39. Herzog, S., et al., *Indirect immunofluorescence assay for intra vitam diagnosis of avian bornavirus infection in psittacine birds.* J Clin Microbiol, 2010. **48**(6): p. 2282-4.

40. Gancz, A.Y., et al., *Experimental induction of proventricular dilatation disease in cockatiels (Nymphicus hollandicus) inoculated with brain homogenates containing avian bornavirus 4.* Virol J, 2009. **6**: p. 100.

41. Piepenbring, A.K., et al., *Parrot Bornavirus (PaBV)-2 isolate causes different disease patterns in cockatiels than PaBV-4.* Avian Pathol, 2016. **45**(2): p. 156-68.

42. Payne, S., et al., *Unusual and severe lesions of proventricular dilatation disease in cockatiels (Nymphicus hollandicus) acting as healthy carriers of avian bornavirus (ABV) and subsequently infected with a virulent strain of ABV.* Avian Pathol, 2011. **40**(1): p. 15-22.

43. Kistler, A.L., et al., *Analysis of naturally occurring avian bornavirus infection and transmission during an outbreak of proventricular dilatation disease among captive psittacine birds.* J Virol, 2010. **84**(4): p. 2176-9.

44. Delnatte, P., et al., *Pathology and diagnosis of avian bornavirus infection in wild Canada geese (Branta canadensis), trumpeter swans (Cygnus buccinator) and mute swans (Cygnus olor) in Canada: a retrospective study.* Avian Pathol, 2013. **42**(2): p. 114-28.

45. Rubbenstroth, D., et al., *Discovery of a new avian bornavirus genotype in estrildid finches (Estrildidae) in Germany.* Vet Microbiol, 2014. **168**(2-4): p. 318-23.

46. Sassa, Y., et al., *Parrot bornavirus-2 and -4 RNA detected in wild bird samples in Japan are phylogenetically adjacent to those found in pet birds in Japan.* Virus Genes, 2015. **51**(2): p. 234-43.

47. Encinas-Nagel, N., et al., *Avian bornavirus in free-ranging psittacine birds, Brazil.* Emerg Infect Dis, 2014. **20**(12): p. 2103-6.

48. De Kloet, S.R. and G.M. Dorrestein, *Presence of avian bornavirus RNA and anti-avian bornavirus antibodies in apparently healthy macaws.* Avian Dis, 2009. **53**(4): p. 568-73.

49. Delnatte, P., et al., *New genotype of avian bornavirus in wild geese and trumpeter swans in Canada.* Vet Rec, 2011. **169**(4): p. 108.

50. Payne, S., et al., *Detection and characterization of a distinct bornavirus lineage from healthy Canada geese (Branta canadensis).* J Virol, 2011. **85**(22): p. 12053-6.

51. Lierz, M., et al., *Anatomical distribution of avian bornavirus in parrots, its occurrence in clinically healthy birds and ABV-antibody detection.* Avian Pathol, 2009. **38**(6): p. 491-6.

52. Ouyang, N., et al., *Histopathology and the detection of avian bornavirus in the nervous system of birds diagnosed with proventricular dilatation disease.* Avian Pathol, 2009. **38**(5): p. 393-401.

53. Hoppes, S., et al., *Meloxicam Treatment in Cockatiels (Nymphicus hollandicus) Infected With Avian Bornavirus.* Journal of Exotic Pet Medicine, 2013. **22**(3): p. 275-279.

54. Runge, S., et al., *Viral vector vaccines protect cockatiels from inflammatory lesions after heterologous parrot bornavirus 2 challenge infection.* Vaccine, 2017. **35**(4): p. 557-563.

55. Kapgate, S.S., S.B. Barbuddhe, and K. Kumanan, *Next generation sequencing technologies: tool to study avian virus diversity.* Acta Virol, 2015. **59**(1): p. 3-13.

56. Marton, S., et al., *Coding-complete sequencing classifies parrot bornavirus 5 into a novel virus species.* Arch Virol, 2015. **160**(11): p. 2763-8.

57. Van Goor, A., et al., *Unique genetic responses revealed in RNA-seq of the spleen of chickens stimulated with lipopolysaccharide and short-term heat.* PLoS One, 2017. **12**(2): p. e0171414.

58. Zhang, J., C.J. Schmidt, and S.J. Lamont, *Transcriptome analysis reveals potential mechanisms underlying differential heart development in fast- and slow-growing broilers under heat stress.* BMC Genomics, 2017. **18**(1): p. 295.

59. Yi, B., et al., *Transcriptome Profile Analysis of Breast Muscle Tissues from High or Low Levels of Atmospheric Ammonia Exposed Broilers (Gallus gallus).* PLoS One, 2016. **11**(9): p. e0162631.

60. Nie, Q., et al., *Deep sequencing-based transcriptome analysis of chicken spleen in response to avian pathogenic Escherichia coli (APEC) infection.* PLoS One, 2012. **7**(7): p. e41645.

61. Hamzic, E., et al., *RNA sequencing-based analysis of the spleen transcriptome following infectious bronchitis virus infection of chickens selected for different mannose-binding lectin serum concentrations.* BMC Genomics, 2016. **17**(82).

62. Yang, F., et al., *Transcriptome Analysis and Gene Identification in the Pulmonary Artery of Broilers with Ascites Syndrome.* PLoS One, 2016. **11**(6): p. e0156045.

63. Kong, L., et al., *The transcriptome sequencing analysis of ciprofloxacin-resistant avian Pasteurella multocida.* Zhongguo Yufang Shouyi Xuebao / Chinese Journal of Preventive Veterinary Medicine, 2017. **39**(4): p. 262-266.

64. Chen, Y., et al., *Gene expression profile after activation of RIG-I in 5'ppp-dsRNA challenged DF1.* Developmental and Comparative Immunology, 2016.

65. Ogiwara, H., et al., *Histopathological evaluation of the diversity of cells susceptible to H5N1 virulent avian influenza virus.* Am J Pathol, 2014. **184**(1): p. 171-83.

66. Wang, Y., et al., *RNA-seq analysis revealed novel genes and signaling pathway associated with disease resistance to avian influenza virus infection in chickens.* Poult Sci, 2014. **93**(2): p. 485-93.

67. Wang, Y., et al., *Integrated analysis of microRNA expression and mRNA transcriptome in lungs of avian influenza virus infected broilers.* BMC Genomics, 2012. **13**: p. 278.

68. McKinley, E.T., et al., *Attenuated live vaccine usage affects accurate measures of virus diversity and mutation rates in avian coronavirus infectious bronchitis virus.* Virus Res, 2011. **158**(1-2): p. 225-34.

69. Huang, Y., et al., *The duck genome and transcriptome provide insight into an avian influenza virus reservoir species.* Nat Genet, 2013. **45**(7): p. 776-783.

70. Huang, Y., et al., *A 4-year study of avian influenza virus prevalence and subtype diversity in ducks of Newfoundland, Canada.* Can J Microbiol, 2013. **59**(10): p. 701-8.

71. Moon, D.A., et al., *The MHC of the duck (Anas platyrhynchos) contains five differentially expressed class I genes.* J Immunol, 2005. **175**(10): p. 6702-12.

72. Xia, C., et al., *cDNA cloning and genomic structure of the duck (Anas platyrhynchos) MHC class I gene.* Immunogenetics, 2004. **56**(4): p. 304-9.

73. Wang, Q., et al., *Spleen Transcriptome Profile of Muscovy Ducklings in Response to Infection With Muscovy Duck Reovirus.* Avian Diseases, 2015. **59**(2): p. 282-290.

74. Xu, Q., et al., *The CD8alpha gene in duck (Anatidae): cloning, characterization, and expression during viral infection.* Mol Biol Rep, 2015. **42**(2): p. 431-9.

75. Zeng, D.W., et al., *Serum HBsAg and HBeAg levels are associated with liver pathological stages in the immune clearance phase of hepatitis B virus chronic infection.* Mol Med Rep, 2015. **11**(5): p. 3465-72.

76. Zeng, T., et al., *De novo assembly and characterization of Muscovy duck liver transcriptome and analysis of differentially regulated genes in response to heat stress.* Cell Stress & Chaperones, 2015. **20**(3): p. 483-493.

77. Reinisova, M., et al., *Genetic Diversity of NHE1, Receptor for Subgroup J Avian Leukosis Virus, in Domestic Chicken and Wild Anseriform Species.* PLoS One, 2016. **11**(3): p. e0150589.

78. Huang, Y., et al., *The duck genome and transcriptome provide insight into an avian influenza virus reservoir species.* Nature Genetics, 2013. **45**: p. 776.

79. Formisano, S., et al., *Central Nervous System Infection with Borna Disease Virus Causes Kynurenine Pathway Dysregulation and Neurotoxic Quinolinic Acid Production.* J Virol, 2017. **91**(14).

80. Marguerat, S. and J. Bähler, *RNA-seq: from technology to biology.* Cellular and molecular life sciences, 2010. **67**(4): p. 569-579.

81. Marguerat, S., Brian T. Wilhelm, and J. Bähler, *Next-generation sequencing: applications beyond genomes.* Biochemical Society Transactions, 2008. **36**(Pt 5): p. 1091-1096.

82. Kumar, R., et al., *A High-Throughput Method for Illumina RNA-Seq Library Preparation.* Frontiers in Plant Science, 2012. **3**: p. 202.

83. Wilhelm, B.T. and J.-R. Landry, *RNA-Seq—quantitative measurement of expression through massively parallel RNA-sequencing.* Methods, 2009. **48**(3): p. 249-257.

84. Lister, R., B.D. Gregory, and J.R. Ecker, *Next is now: new technologies for sequencing of genomes, transcriptomes and beyond.* Current opinion in plant biology, 2009. **12**(2): p. 107-118.

85. Morrissy, A.S., et al., *Next-generation tag sequencing for cancer gene expression profiling.* Genome Res, 2009. **19**.

86. Caragata, E.P., et al., *The transcriptome of the mosquito Aedes fluviatilis (Diptera: Culicidae), and transcriptional changes associated with its native Wolbachia infection.* BMC Genomics, 2017. **18**(1): p. 6.

87. Matochko, W.L., et al., *Deep sequencing analysis of phage libraries using Illumina platform.* Methods, 2012. **58**(1): p. 47-55.

88. Smith, D.R., *Buying in to bioinformatics: an introduction to commercial sequence analysis software.* Briefings in Bioinformatics, 2015. **16**(4): p. 700-709.

89. Robinson, M.D., D.J. McCarthy, and G.K. Smyth, *edgeR: a Bioconductor package for differential expression analysis of digital gene expression data.* Bioinformatics, 2010. **26**.

90. Robinson, M.D. and A. Oshlack, *A scaling normalization method for differential expression analysis of RNA-seq data.* Genome Biol, 2010. **11**.

91. Dillies, M.-A., et al., *A comprehensive evaluation of normalization methods for Illumina high-throughput RNA sequencing data analysis.* Briefings in Bioinformatics, 2013. **14**(6): p. 671-683.

92. Anders, S. and W. Huber, *Differential expression analysis for sequence count data.* Genome Biology, 2010. **11**(10): p. R106.

93. Wang, L., et al., *DEGseq: an R package for identifying differentially expressed genes from RNA-seq data.* Bioinformatics, 2010. **26**.

94. Huang, D.W., B.T. Sherman, and R.A. Lempicki, *Systematic and integrative analysis of large gene lists using DAVID bioinformatics resources.* Nature Protocols, 2008. **4**: p. 44.

95. Huang, D.W., B.T. Sherman, and R.A. Lempicki, *Bioinformatics enrichment tools: paths toward the comprehensive functional analysis of large gene lists.* Nucleic Acids Research, 2009. **37**(1): p. 1-13.

96. Kanehisa, M., et al., *KEGG: new perspectives on genomes, pathways, diseases and drugs.* Nucleic Acids Research, 2017. **45**(Database issue): p. D353-D361.

97. Kanehisa, M. and S. Goto, *KEGG: Kyoto Encyclopedia of Genes and Genomes.* Nucleic Acids Research, 2000. **28**(1): p. 27-30.

98. Kanehisa, M., et al., *KEGG as a reference resource for gene and protein annotation.* Nucleic Acids Research, 2016. **44**(Database issue): p. D457-D462.

99. Kim, J.O., et al., *Characterization of the Transcriptome and Gene Expression of Brain Tissue in Sevenband Grouper (Hyporthodus septemfasciatus) in Response to NNV Infection.* Genes (Basel), 2017. **8**(1).

100. Wang, Q., et al., *Transcriptome analysis reveals the molecular mechanism of hepatic fat metabolism disorder caused by Muscovy duck reovirus infection.* Avian Pathology, 2017: p. 1-13.

101. Wille, M., et al., *Temporal dynamics, diversity, and interplay in three components of the virodiversity of a Mallard population: influenza A virus, avian paramyxovirus and avian coronavirus.* Infect Genet Evol, 2015. **29**: p. 129-37.

102. Guo, J., et al., *Avian Bornaviruses: Diagnosis, Isolation, and Genotyping*, in *Current Protocols in Microbiology*. 2005, John Wiley & Sons, Inc.

103. Cui, L., et al., *Characterization of melanin-concentrating hormone (MCH) and its receptor in chickens: Tissue expression, functional analysis, and fasting-induced up-regulation of hypothalamic MCH expression.* Gene, 2017. **615**: p. 57-67.

104. Guo, J.T., et al., *Characterization of serum amyloid A protein mRNA expression and secondary amyloidosis in the domestic duck.* Proc Natl Acad Sci U S A, 1996. **93**(25): p. 14548-53.

105. Hendriks, W., et al., *Duck lens epsilon-crystallin and lactate dehydrogenase B4 are identical: a single-copy gene product with two distinct functions.* Proc Natl Acad Sci U S A, 1988. **85**(19): p. 7114-8.

106. Hodin, J. and G. Wistow, *5'-RACE PCR of mRNA for three taxon-specific crystallins: for each gene one promoter controls both lens and non-lens expression.* Biochem Biophys Res Commun, 1993. **190**(2): p. 391-6.

107. Jeong, J., et al., *Molecular identification of duck and quail common cytokine receptor gamma chain genes.* Vet Immunol Immunopathol, 2011. **140**(1-2): p. 159-65.

108. Lowe, T.M. and S.R. Eddy, *tRNAscan-SE: a program for improved detection of transfer RNA genes in genomic sequence.* Nucleic Acids Res, 1997. **25**(5): p. 955-64.

109. Martin, C., et al., *The avian XPR1 gammaretrovirus receptor is under positive selection and is disabled in bird species in contact with virus-infected wild mice.* J Virol, 2013. **87**(18): p. 10094-104.

110. Takada, S., et al., *Nucleotide sequence and embryonic expression of quail and duck Sox9 genes.* Gen Comp Endocrinol, 2006. **145**(2): p. 208-13.

111. Wang, C., et al., *Cloning and expression profiling of the VLDLR gene associated with egg performance in duck (Anas platyrhynchos).* Genet Sel Evol, 2011. **43**: p. 29.

112. Wang, J., et al., *Molecular cloning of prolactin receptor of the Peking duck.* Poult Sci, 2009. **88**(5): p. 1016-22.

113. Wistow, G.J. and J. Piatigorsky, *Gene conversion and splice-site slippage in the argininosuccinate lyases/delta-crystallins of the duck lens: members of an enzyme superfamily.* Gene, 1990. **96**(2): p. 263-70.

114. Xia, J., et al., *Immune gene discovery by expressed sequence tag analysis of spleen in the duck (Anas platyrhynchos).* Dev Comp Immunol, 2007. **31**(3): p. 272-85.

115. Xu, Q., et al., *Identification and expression analysis of the leukocyte cell-derived chemotaxin-2 (LECT2) gene in duck (Anas platyrhynchos).* Gene, 2014. **533**(1): p. 280-5.

116. Yao, Q., et al., *cDNA cloning, genomic structure, molecular characterization and mRNA expression analysis of the Pekin duck interleukin-10 receptor 1.* Int J Immunogenet, 2012. **39**(1): p. 55-67.

117. Yen, C.F., et al., *Cloning and expression of the genes associated with lipid metabolism in Tsaiya ducks.* Poult Sci, 2005. **84**(1): p. 67-74.

118. Zhan, K., et al., *Molecular cloning and expression of the duplicated thyroid hormone responsive spot 14 (THRSP) genes in ducks.* Poult Sci, 2006. **85**(10): p. 1746-54.

119. Incorporated, Q. *CLC Genomics Workbench* [Internet] [cited 2018 May 3]; 8.0.1:[Qiagen CLC Genomics Workbench Company Website]. Available from: https://www.qiagenbioinformatics.com/.

120. Clark, K., et al., *GenBank.* Nucleic Acids Research, 2016. **44**(D1): p. D67-D72.

121. The UniProt Consortium, *UniProt: the universal protein knowledgebase.* Nucleic Acids Research, 2017. **45**(D1): p. D158-D169.

122. Baxevanis, A.D. and B.F.F. Ouellette, *Bioinformatics : a practical guide to the analysis of genes and proteins*. 2nd ed. Methods of biochemical analysis. 2001, New York: Wiley-Interscience. xviii, 470 p., 16 p. of plates.

123. Martín-Vicente, M., et al., *TRIM25 in the Regulation of the Antiviral Innate Immunity.* Frontiers in Immunology, 2017. **8**: p. 1187.

124. Sanchez, J.G., et al., *Mechanism of TRIM25 Catalytic Activation in the Antiviral RIG-I Pathway.* Cell reports, 2016. **16**(5): p. 1315-1325.

125. Meyerson, N.R., et al., *Nuclear TRIM25 Specifically Targets Influenza Virus Ribonucleoproteins to Block the Onset of RNA Chain Elongation.* Cell Host & Microbe, 2017. **22**(5): p. 627-638.e7.

126. Hu, Y., et al., *The Severe Acute Respiratory Syndrome Coronavirus Nucleocapsid Inhibits Type I Interferon Production by Interfering with TRIM25-Mediated RIG-I Ubiquitination.* Journal of Virology, 2017. **91**(8): p. e02143-16.

127. Manokaran, G., et al., *Dengue subgenomic RNA binds TRIM25 to inhibit interferon expression for epidemiological fitness.* Science (New York, N.Y.), 2015. **350**(6257): p. 217-221.

128. Helin, A.S., et al., *A rapid and transient innate immune response to avian influenza infection in mallards.* Molecular Immunology, 2018. **95**: p. 64-72.

129. Wensman, J.J., et al., *The X proteins of bornaviruses interfere with type I interferon signalling.* J Gen Virol, 2013. **94**(Pt 2): p. 263-9.

130. Zhang, M., et al., *Molecular cloning of Peking duck Toll-like receptor 3 (duTLR3) gene and its responses to reovirus infection.* Virology Journal, 2015. **12**: p. 207.

131. Verma, R. and K. Bharti, *Toll like receptor 3 and viral infections of nervous system.* Journal of the Neurological Sciences, 2017. **372**: p. 40-48.

132. Li, Y., et al., *Host Avian Beta-Defensin and Toll-Like Receptor Responses of Pigeons following Infection with Pigeon Paramyxovirus Type 1.* Appl Environ Microbiol, 2015. **81**(18): p. 6415-24.

133. Wang, T., et al., *Toll-like receptor 3 mediates West Nile virus entry into the brain causing lethal encephalitis.* Nature Medicine, 2004. **10**: p. 1366.

134. Xagorari, A. and K. Chlichlia, *Toll-Like Receptors and Viruses: Induction of Innate Antiviral Immune Responses.* The Open Microbiology Journal, 2008. **2**: p. 49-59.

135. Wilson, J.R., et al., *West Nile Virus Nonstructural Protein 1 Inhibits TLR3 Signal Transduction.* Journal of Virology, 2008. **82**(17): p. 8262-8271.

136. Garcia-Sastre, A., *Ten Strategies of Interferon Evasion by Viruses.* Cell Host Microbe, 2017. **22**(2): p. 176-184.

137. Reinert, L.S., et al., *TLR3 deficiency renders astrocytes permissive to herpes simplex virus infection and facilitates establishment of CNS infection in mice.* J Clin Invest, 2012. **122**(4): p. 1368-76.

138. McKimmie, C.S., et al., *Viruses selectively upregulate Toll-like receptors in the central nervous system.* Biochemical and Biophysical Research Communications, 2005. **336**(3): p. 925-933.

139. Ménager, P., et al., *Toll-Like Receptor 3 (TLR3) Plays a Major Role in the Formation of Rabies Virus Negri Bodies.* PLoS Pathogens, 2009. **5**(2): p. e1000315.

140. Blondel, D., et al., *Resistance to Rhabdoviridae Infection and Subversion of Antiviral Responses.* Viruses, 2015. **7**(7): p. 3675-3702.

141. Daffis, S., et al., *Interferon Regulatory Factor IRF-7 Induces the Antiviral Alpha Interferon Response and Protects against Lethal West Nile Virus Infection.* Journal of Virology, 2008. **82**(17): p. 8465-8475.

142. Honda, K., A. Takaoka, and T. Taniguchi, *Type I Inteferon Gene Induction by the Interferon Regulatory Factor Family of Transcription Factors.* Immunity, 2006. **25**(3): p. 349-360.

143. Vabret, N. and J.M. Blander, *Sensing Microbial RNA in the Cytosol.* Frontiers in Immunology, 2013. **4**: p. 468.

144. Brzózka, K., S. Finke, and K.-K. Conzelmann, *Inhibition of Interferon Signaling by Rabies Virus Phosphoprotein P: Activation-Dependent Binding of STAT1 and STAT2.* Journal of Virology, 2006. **80**(6): p. 2675-2683.

145. Rieder, M., et al., *Genetic Dissection of Interferon-Antagonistic Functions of Rabies Virus Phosphoprotein: Inhibition of Interferon Regulatory Factor 3 Activation Is Important for Pathogenicity.* Journal of Virology, 2011. **85**(2): p. 842-852.

146. Unterstab, G., et al., *Viral targeting of the interferon-β-inducing Traf family member-associated NF-κB activator (TANK)-binding kinase-1.* Proceedings of the National Academy of Sciences of the United States of America, 2005. **102**(38): p. 13640.

147. Song, W., et al., *Borna disease virus nucleoprotein inhibits type I interferon induction through the interferon regulatory factor 7 pathway.* Biochemical and Biophysical Research Communications, 2013. **438**(4): p. 619-623.

148. Marsili, G., et al., *IFN Regulatory Factors and Antiviral Innate Immunity: How Viruses Can Get Better.* Journal of Interferon & Cytokine Research, 2016. **36**(7): p. 414-432.

149. Schroder, K., et al., *Interferon-γ: an overview of signals, mechanisms and functions.* Journal of Leukocyte Biology, 2003. **75**(2): p. 163-189.

150. Rhein, B.A., et al., *Interferon-γ Inhibits Ebola Virus Infection.* PLOS Pathogens, 2015. **11**(11): p. e1005263.

151. White, L.C., et al., *Regulation of LMP2 and TAP1 Genes by IRF-1 Explains the Paucity of CD8+ T Cells in IRF-1−/− Mice.* Immunity, 1996. **5**(4): p. 365-376.

152. Ogasawara, K., et al., *Requirement for IRF-1 in the microenvironment supporting development of natural killer cells.* Nature, 1998. **391**: p. 700.

153. Schoggins, J.W., et al., *A diverse range of gene products are effectors of the type I interferon antiviral response.* Nature, 2011. **472**: p. 481.

154. Qian, W., et al., *Duck interferon regulatory factor 1 acts as a positive regulator in duck innate antiviral response.* Developmental & Comparative Immunology, 2018. **78**: p. 1-13.

155. Nair, S., et al., *Interferon Regulatory Factor-1 Protects from Fatal Neurotropic Infection with Vesicular Stomatitis Virus by Specific Inhibition of Viral Replication in Neurons.* PLOS Pathogens, 2014. **10**(3): p. e1003999.

156. Sadler, A.J. and B.R.G. Williams, *Interferon-inducible antiviral effectors.* Nature reviews. Immunology, 2008. **8**(7): p. 559-568.

157. Schneider, W.M., M.D. Chevillotte, and C.M. Rice, *Interferon-Stimulated Genes: A Complex Web of Host Defenses.* Annual review of immunology, 2014. **32**: p. 513-545.

158. Haller, O., et al., *Mx GTPases: dynamin-like antiviral machines of innate immunity.* Trends Microbiol, 2015. **23**(3): p. 154-63.

159. Verhelst, J., et al., *Interferon-Inducible Protein Mx1 Inhibits Influenza Virus by Interfering with Functional Viral Ribonucleoprotein Complex Assembly.* Journal of Virology, 2012. **86**(24): p. 13445-13455.

160. Helin, A.S., et al., *Expression of immune genes RIG-I and Mx in mallard ducks infected with low pathogenic avian influenza (LPAI): A dataset.* Data in Brief, 2018. **18**: p. 1562-1566.

161. Dittmann, J., et al., *Influenza A Virus Strains Differ in Sensitivity to the Antiviral Action of Mx-GTPase.* Journal of Virology, 2008. **82**(7): p. 3624-3631.

162. Zimmermann, P., et al., *The Viral Nucleoprotein Determines Mx Sensitivity of Influenza A Viruses.* Journal of Virology, 2011. **85**(16): p. 8133-8140.

163. Leroy, M., et al., *Expression of the interferon-alpha/beta-inducible bovine Mx1 dynamin interferes with replication of rabies virus.* Neurobiology of Disease, 2006. **21**(3): p. 515-521.

164. Zhong, Z., et al., *Molecular characterization and expression analysis of the duck viperin gene.* Gene, 2015. **570**(1): p. 100-107.

165. Jumat, M.R., et al., *Viperin protein expression inhibits the late stage of respiratory syncytial virus morphogenesis.* Antiviral Research, 2015. **114**: p. 11-20.

166. Dauber, B. and T. Wolff, *Activation of the Antiviral Kinase PKR and Viral Countermeasures.* Viruses, 2009. **1**(3): p. 523-44.

167. Chatterjee, S., et al., *Molecular mechanisms of innate immune inhibition by non-segmented negative-sense RNA viruses.* Journal of molecular biology, 2016. **428**(17): p. 3467-3482.

168. Gerlier, D. and D.S. Lyles, *Interplay between Innate Immunity and Negative-Strand RNA Viruses: towards a Rational Model.* Microbiology and Molecular Biology Reviews : MMBR, 2011. **75**(3): p. 468-490.

169. Saha, S. and P.N. Rangarajan, *Common host genes are activated in mouse brain by Japanese encephalitis and rabies viruses.* Journal of General Virology, 2003. **84**(7): p. 1729-1735.

170. Kaiser, P. and P. Stäheli, *Chapter 10 - Avian Cytokines and Chemokines*, in *Avian Immunology (Second Edition)*. 2014, Academic Press: Boston. p. 189-204.

171. Chai, Q., et al., *Expression of Neuronal CXCL10 Induced by Rabies Virus Infection Initiates Infiltration of Inflammatory Cells, Production of Chemokines and Cytokines, and Enhancement of Blood-Brain Barrier Permeability.* Journal of Virology, 2015. **89**(1): p. 870-876.

172. Sauder, C., et al., *Chemokine Gene Expression in Astrocytes of Borna Disease Virus-Infected Rats and Mice in the Absence of Inflammation.* Journal of Virology, 2000. **74**(19): p. 9267-9280.

173. Abele, R. and R. Tampé, *The ABCs of Immunology: Structure and Function of TAP, the Transporter Associated with Antigen Processing.* Physiology, 2004. **19**(4): p. 216-224.

174. Kaufman, J., *Antigen processing and presentation: Evolution from a bird's eye view().* Molecular Immunology, 2013. **55**(2): p. 159-161.

175. Herzer, K., et al., *Upregulation of Major Histocompatibility Complex Class I on Liver Cells by Hepatitis C Virus Core Protein via p53 and TAP1 Impairs Natural Killer Cell Cytotoxicity.* Journal of Virology, 2003. **77**(15): p. 8299-8309.

176. Faure-André, G., et al., *Regulation of Dendritic Cell Migration by CD74, the MHC Class II-Associated Invariant Chain.* Science, 2008. **322**(5908): p. 1705.

177. Gresser, O., et al., *Immunocompetent astrocytes and microglia display major differences in the processing of the invariant chain and in the expression of active cathepsin L and cathepsin S.* European Journal of Immunology, 2001. **31**(6): p. 1813-1824.

APPENDIX A

Figure.A1: Original RNA isolation protocol and troubleshooting (Macheney-Nagel Inc.)

RNA isolation

Protocol-at-a-glance (Rev. 03)

NucleoSpin® RNA Plus

1	**Homogenize sample and lyse sample**		350 µL LBP
2	**Remove gDNA and filtrate lysate**		11,000 x *g*, 30 s
3	**Adjust RNA binding conditions**		100 µL BS Mix
4	**Bind RNA**		Load sample 11,000 x *g*, 15 s
5	**Wash and dry silica membrane**	1st wash 2nd wash 3rd wash	200 µL WB1 600 µL WB2 250 µL WB2
		1st and 2nd 3rd	11,000 x *g*, 15 s 11,000 x *g*, 2 min
6	**Elute RNA**		30 µL RNase-free H_2O 11,000 x *g*, 1 min 30 µL RNase-free H_2O 11,000 x *g*, 1 min

MACHEREY-NAGEL GmbH & Co. KG · Neumann-Neander-Str. 6–8 · 52355 Düren · Germany
Tel.: +49 24 21 969-270 · Fax: +49 24 21 969-199 · tech-bio@mn-net.com · **www.mn-net.com**

5 NucleoSpin® RNA Plus protocol

Before starting the preparation:

- Check if Wash Buffer WB2 was prepared according to section 3.

1 Homogenize and lyse sample

Add **350 µL Buffer LBP** per sample and disrupt the sample according to one of the methods described in section 2.3.

Note: Lysis tube is not included in the kit. Addition of reducing agent (e.g. ß-mercaptoethanol, DTT, or TCEP) is not necessary. The sample material should be broken up and lysed as completely as possible.

Note: If considerable amounts of non-lysed sample material is still visible after sample disruption (which might occur with certain plant material), briefly centrifuge the lysate (approx. 3 s at 2,000 x g) in order to sediment the sample debris. If the sediment represents e.g., > 20 % of the total lysate volume, do not transfer the sediment onto the NucleoSpin® gDNA Removal Column.

For certain sample types (e.g., some plant types) it can be beneficial to use 500 µL lysis buffer instead of 350 µL, especially, if a lot of sample debris remains are observed after sample disintegration.

+ 350 µL LBP

2 Remove gDNA and filtrate lysate

Place NucleoSpin® gDNA Removal Column (yellow ring) in a Collection Tube (2 mL; provided), transfer the homogenized lysate to the NucleoSpin® gDNA Removal Column, and centrifuge for **30 s** at **11,000 x *g***.

Discard the column and **continue with the flow-through**.

Note: Ensure that no liquid remains on the column membrane after centrifugation. If necessary, repeat the centrifugation until all liquid has passed through the membrane.

If (in rare cases) the flow-through contains obvious undissolved sediment, recover flow-through without sediment. Optimize mechanical sample disruption for subsequent preparations.

11,000 x *g*, 30 s

3 Ajust RNA binding conditions

Add **100 µL Binding Solution BS** to the flow-through and mix well by moderate vortexing or by pipetting up and down several times.

Note: If mixing is done by vortexing, be careful in order to avoid spilling, because the Collection Tube does not contain a lid.

Note: If another volume than 350 µL of Lysis Buffer LBP has been used for lysis (e.g., 500 µL), make sure to add approximately 0.3 volume of Binding Buffer BS to the cleared lysate in order to adjust RNA binding conditions.

After addition of Binding Solution BS a stringy precipitate may become visible which will not affect the RNA isolation. Be sure to disaggregate any precipitate by mixing and load all of the precipitate on the column as described in the following step. Do not centrifuge the lysate after addition of Binding Solution before loading it onto the column in order to avoid pelleting the precipitate.

+ 100 µL BS Mix

4 Bind RNA

Transfer the whole lysate (~ 450 µL) to the NucleoSpin® RNA Plus Column (light blue ring) pre-assembled with a Collection Tube. Centrifuge for **15 s** at **11,000 x *g***.

Note: Flow-through (~ 450 µL) may stay in the Collection Tube. Alternatively, discard the flow-through and reuse collection tube or place the column into a new 2 mL collection tube (not provided).

Load lysate

11,000 x *g*, 15 s

5 Wash and dry silica membrane

1st wash

Add **200 µL Buffer WB1** to the NucleoSpin® RNA Plus Column. Centrifuge for **15 s** at **11,000 x *g***. Discard the flow-through with collection tube and place the column into a new 2 mL Collection Tube (provided).

+ 200 µL WB1

11,000 x *g*, 15 s

2nd wash

Add **600 µL Buffer WB2** to the NucleoSpin® RNA Plus Column. Centrifuge for **15 s** at **11,000 x *g***. Discard flow-through and place the column back into the Collection Tube.

Note: Make sure that residual buffer from the previous steps is washed away with Buffer WB2 especially if the lysate has been in contact with the inner rim of the column during loading of the lysate onto the column. For efficient washing of the inner rim flush it with Buffer WB2.

+ 600 µL WB2

11,000 x *g*, 15 s

3rd wash

Add **250 µL Buffer WB2** to the NucleoSpin® RNA Plus Column. Centrifuge for **2 min** at **11,000 x *g*** to dry the membrane completely. Place the column into a nuclease-free Collection Tube (1.5 mL, provided).

If for any reason, the liquid level in the Collection Tube has reached the NucleoSpin® RNA Plus Column after centrifugation, discard flow-through, and centrifuge again.

+ 250 µL WB2

11,000 x *g*, 2 min

6 Elute RNA

Add **30 µL RNase-free H_2O** and centrifuge at **11,000 x *g*** for **1 min**.

Add again **30 µL RNase-free H_2O** and centrifuge at **11,000 x *g*** for **1 min**.

Alternatively, elution can be performed with 1 x 60 µL, but yield can be slightly reduced compared to elution with 2 x 30 µL. For alternative elution procedures see section 2.4.

+ 30 µL RNase-free H_2O

11,000 x *g*, 1 min

+ 30 µL RNase-free H_2O

11,000 x *g*, 1 min

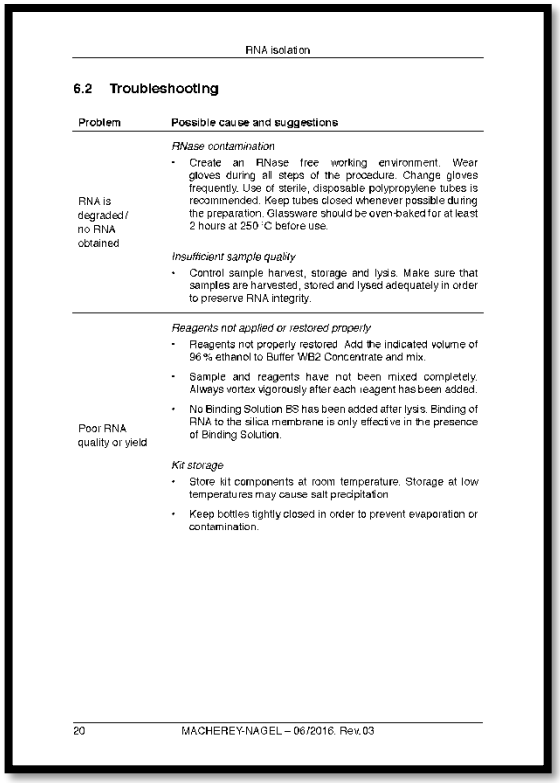

6.2 Troubleshooting

Problem	Possible cause and suggestions
RNA is degraded / no RNA obtained	*RNase contamination* • Create an RNase free working environment. Wear gloves during all steps of the procedure. Change gloves frequently. Use of sterile, disposable polypropylene tubes is recommended. Keep tubes closed whenever possible during the preparation. Glassware should be oven-baked for at least 2 hours at 250 °C before use. *Insufficient sample quality* • Control sample harvest, storage and lysis. Make sure that samples are harvested, stored and lysed adequately in order to preserve RNA integrity.
Poor RNA quality or yield	*Reagents not applied or restored properly* • Reagents not properly restored. Add the indicated volume of 96 % ethanol to Buffer WB2 Concentrate and mix. • Sample and reagents have not been mixed completely. Always vortex vigorously after each reagent has been added. • No Binding Solution BS has been added after lysis. Binding of RNA to the silica membrane is only effective in the presence of Binding Solution. *Kit storage* • Store kit components at room temperature. Storage at low temperatures may cause salt precipitation • Keep bottles tightly closed in order to prevent evaporation or contamination.

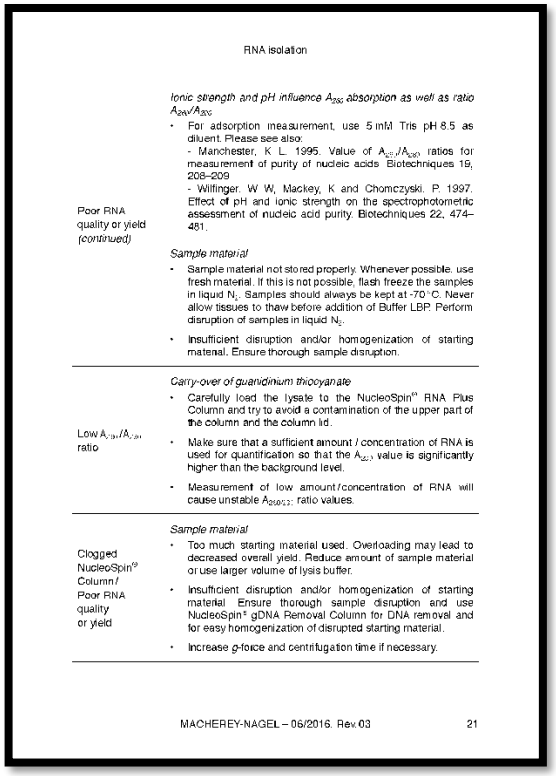

Poor RNA quality or yield *(continued)*	*Ionic strength and pH influence A_{260} absorption as well as ratio A_{260}/A_{320}* • For adsorption measurement, use 5 mM Tris pH 8.5 as diluent. Please see also: - Manchester, K. L. 1995. Value of A_{260}/A_{280} ratios for measurement of purity of nucleic acids. Biotechniques 19, 208–209 - Wilfinger, W. W, Mackey, K. and Chomczynski, P. 1997. Effect of pH and ionic strength on the spectrophotometric assessment of nucleic acid purity. Biotechniques 22, 474–481. *Sample material* • Sample material not stored properly. Whenever possible, use fresh material. If this is not possible, flash freeze the samples in liquid N_2. Samples should always be kept at -70 °C. Never allow tissues to thaw before addition of Buffer LBP. Perform disruption of samples in liquid N_2. • Insufficient disruption and/or homogenization of starting material. Ensure thorough sample disruption.
Low A_{260}/A_{230} ratio	*Carry-over of guanidinium thiocyanate* • Carefully load the lysate to the NucleoSpin® RNA Plus Column and try to avoid a contamination of the upper part of the column and the column lid. • Make sure that a sufficient amount / concentration of RNA is used for quantification so that the A_{230} value is significantly higher than the background level. • Measurement of low amount / concentration of RNA will cause unstable $A_{260}/_{230}$ ratio values.
Clogged NucleoSpin® Column / Poor RNA quality or yield	*Sample material* • Too much starting material used. Overloading may lead to decreased overall yield. Reduce amount of sample material or use larger volume of lysis buffer. • Insufficient disruption and/or homogenization of starting material. Ensure thorough sample disruption and use NucleoSpin® gDNA Removal Column for DNA removal and for easy homogenization of disrupted starting material. • Increase *g*-force and centrifugation time if necessary.

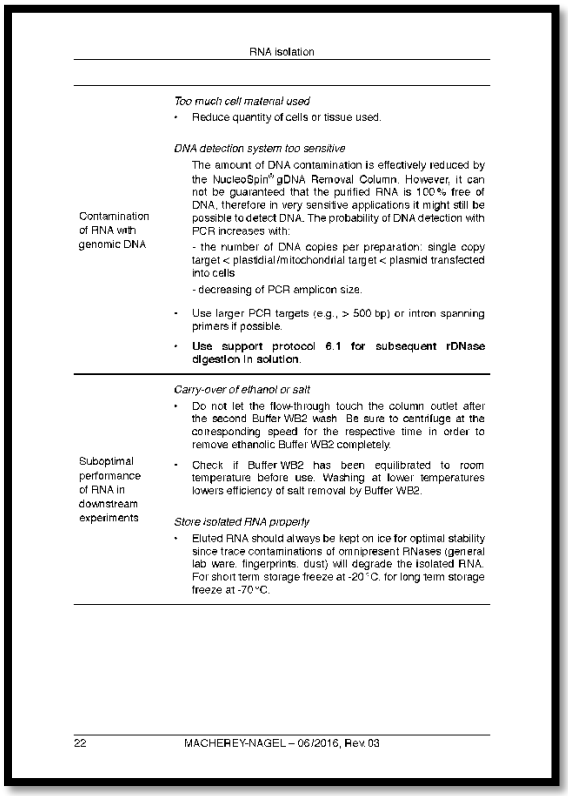

Contamination of RNA with genomic DNA	*Too much cell material used* • Reduce quantity of cells or tissue used. *DNA detection system too sensitive* The amount of DNA contamination is effectively reduced by the NucleoSpin® gDNA Removal Column. However, it can not be guaranteed that the purified RNA is 100 % free of DNA, therefore in very sensitive applications it might still be possible to detect DNA. The probability of DNA detection with PCR increases with: - the number of DNA copies per preparation: single copy target < plastidial / mitochondrial target < plasmid transfected into cells - decreasing of PCR amplicon size. • Use larger PCR targets (e.g., > 500 bp) or intron spanning primers if possible. • **Use support protocol 6.1 for subsequent rDNase digestion in solution.**
Suboptimal performance of RNA in downstream experiments	*Carry-over of ethanol or salt* • Do not let the flow-through touch the column outlet after the second Buffer WB2 wash. Be sure to centrifuge at the corresponding speed for the respective time in order to remove ethanolic Buffer WB2 completely. • Check if Buffer WB2 has been equilibrated to room temperature before use. Washing at lower temperatures lowers efficiency of salt removal by Buffer WB2. *Store isolated RNA properly* • Eluted RNA should always be kept on ice for optimal stability since trace contaminations of omnipresent RNases (general lab ware, fingerprints, dust) will degrade the isolated RNA. For short term storage freeze at -20 °C, for long term storage freeze at -70 °C.

(Macherey-Nagel Inc.)

Table A1. List of tissues taken for PCR and histopathology

PCR samples	Histopathology Samples
Cerebellum	Lung
Hindbrain	Heart
Forebrain	Liver
Midbrain	Small intestine
Spinal cord	Proventriculus
Eye	Adrenal gland
Optic nerve	Sciatic nerve
Aqueous humor	Brachial plexus
Intestine	Optic nerve
Adrenal gland	Cerebrum
Kidney	Cerebellum
Proventriculus	Bursa of Fabricious
Ventriculus	Cloaca
Crop	Uterus
	Muscle
	Ventriculus
	Spleen
	Pancreas

Table A2. Mallard duck genome contigs and annotations

Total Annotated Contigs	78488
Contigs Size <= 100	943
Contigs with >1 annotation added	2313
Total Annotations Added	131444
Contigs with Mallard Gene Annotations	2313
Total Annotations Added to Contigs	55270
Total Mapped Genes	18146
Mallard Genes Size < 500	1403
Total Annotations Added	
All Contigs	131444
Contigs =1 Annotations Added	76174
Mallard Gene Contigs	55270
% of All Contigs with Gene Annotations	42.05%

Table A3. Normal Reads Checks

RNAseq Normal Reads Checks:	Reference Sequences		
	References	Length	Genes
	2,313	985,842,582	18,146

Control Samples					Infected Samples							
C4 A	C4 B		C4 C		I4 A		I4 B		I4 C			
Sum of Total gene reads	7221200	Sum of total gene reads	8293570	Sum of total gene reads	1038198	Sum of total gene reads	8435331	Sum of total gene reads	7099475	Sum of total gene reads	9972592	
Input reads	24111497	Input reads	27,015,149	Input reads	3,586,458	Input reads	27962596	Input reads	24,833,763	Input reads	34,355,784	
total -input	16890279	total -input	18,721,579	total -input	2,548,260	total -input	19527265	total -input	17,734,288	total -input	24,383,192	
% difference	70.05072725	% difference	69.30029888	% difference	71.05227497	% difference	69.83351975	% difference	71.41200477	% difference	70.97259664	
Sum/input %	29.94919809	Sum/input %	30.69970112	Sum/input %	28.94772503	Sum/input %	30.16648025	Sum/input %	28.5879953	Sum/input %	29.02740336	
C5 A	C5 B		C5 C		I3 A		I3 B		I3 C			
Sum of Total gene reads	22299844	Sum of Total gene reads	10817885	Sum of Total gene reads	4072082	Sum of total gene reads	2610557	Sum of total gene reads	5725383	Sum of total gene reads	4764654	
Input reads	82,143,336	Input reads	41,110,198	Input reads	14,718,424	Input reads	12,647,034	Input reads	26,888,460	Input reads	22,704,880	
total -input	59,843,492	total -input	30,292,313	total -input	10,646,342	total -input	10,036,477	total -input	21,163,077	total - input	17,940,226	
% difference	72.85252208	% difference	73.68564121	% difference	72.33343733	% difference	79.358346	% difference	78.7069137	% difference	79.01484615	
Sum/input %	27.14747792	Sum/input %	26.31435879	Sum/input %	27.66656267	Sum/input %	20.641654	Sum/input %	21.2930863	Sum/input %	20.98515385	
C1 A	C1 B		C1 C		I2 A		I2 B		I2 C			
Sum of total gene reads	6899104	Sum of total gene reads	6735338	Sum of total gene reads	5534772	Sum of total gene reads	6119624	Sum of total gene reads	5282788	Sum of total gene reads	5569272	
Input reads	21,418,609	Input reads	19,826,175	Input reads	17,226,595	Input reads	19,783,670	Input reads	17,263,151	Input reads	18,028,551	
total -input	14,519,505	total -input	13,090,837	total -input	11691823	total -input	13,664,046	total -input	11,980,363	total - input	12459279	
% difference	67.78920611	% difference	66.0280513	% difference	67.87077191	% difference	69.06729641	% difference	69.3984719	% difference	69.10859891	
Sum/input %	32.21079389	Sum/input %	33.9719487	Sum/input %	32.12922809	Sum/input %	30.93270359	Sum/input %	30.6015281	Sum/input %	30.89140109	
C2 A	C2 B		C2 C		I1 A		I1 B		I1 C			
Sum of Total gene reads	6883819	Sum of Total gene reads	3573853	Sum of Total gene reads	4424030	Sum of total gene reads	4302107	Sum of total gene reads	4232872	Sum of total gene reads	4197260	
Input reads	25,226,606	Input reads	13,819,703	Input reads	18,233,114	Input reads	17,777,771	Input reads	17,694,834	Input reads	18,153,668	
total -input	18342787	total -input	10245850	total -input	13809084	total -input	13475664	total -input	13461962	total - input	13956408	
% difference	72.71206836	% difference	74.13943701	% difference	75.73628948	% difference	75.8006389	% difference	76.0784871	% difference	76.8792731	
Sum/input %	27.28793164	Sum/input %	25.86056299	Sum/input %	24.26371052	Sum/input %	24.1993611	Sum/input %	23.9215129	Sum/input %	23.1207269	
C3 A	C3 B		C3 C		C5 A		C5 B		C5 C			
Sum of Total gene reads	3850743	Sum of Total gene reads	5514079	Sum of Total gene reads	5668676	Sum of total gene reads	6441462	Sum of total gene reads	6046518	Sum of total gene reads	4639313	
Input reads	14,050,472	Input reads	20,068,646	Input reads	19,271,782	Input reads	20,516,546	Input reads	19,953,060	Input reads	15,308,778	
total -input	10199729	total -input	14,554,567	total -input	13,603,106	total -input	14075084	total -input	13,906,542	total - input	10,669,465	
% difference	72.59349721	% difference	72.52391118	% difference	70.5856158	% difference	68.60357489	% difference	69.6962872	% difference	69.69507952	
Sum/input %	27.40650279	Sum/input %	27.47608882	Sum/input %	29.4143842	Sum/input %	31.39642511	Sum/input %	30.3037128	Sum/input %	30.30492048	

Figure A2. CLC Importation parameters: RNA (Qiagen Inc.)

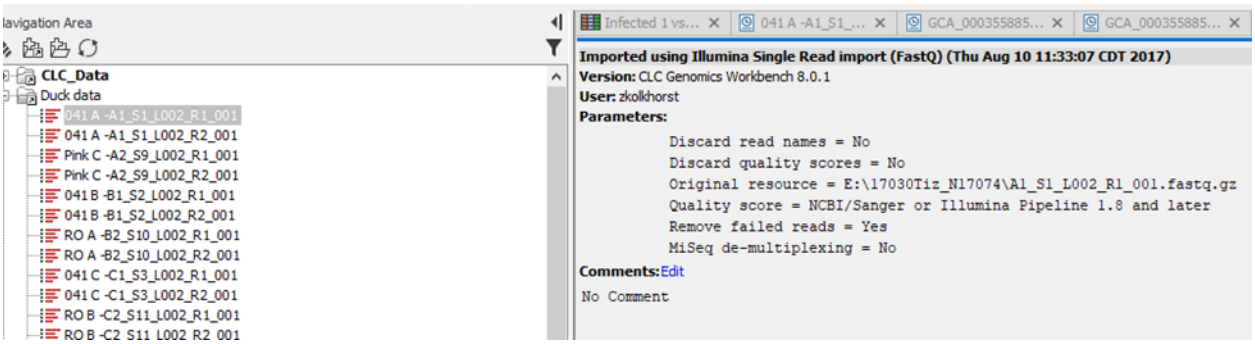

Figure A3. CLC tool: RNA-Seq Analysis (Qiagen Inc.)

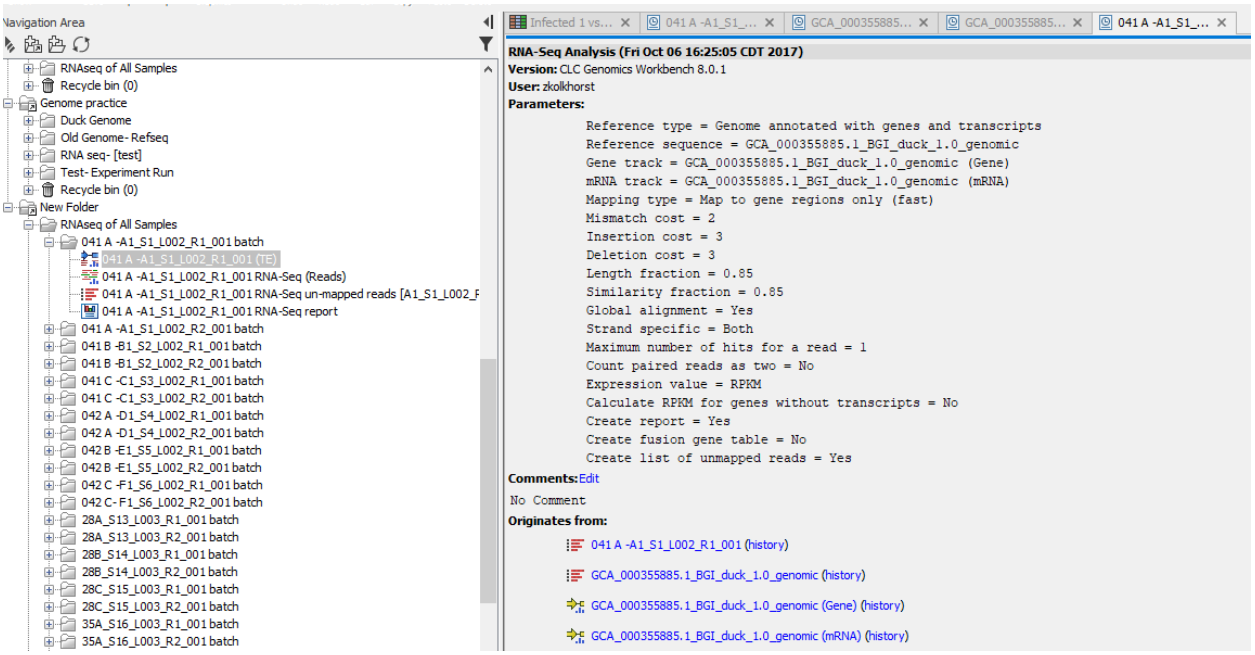

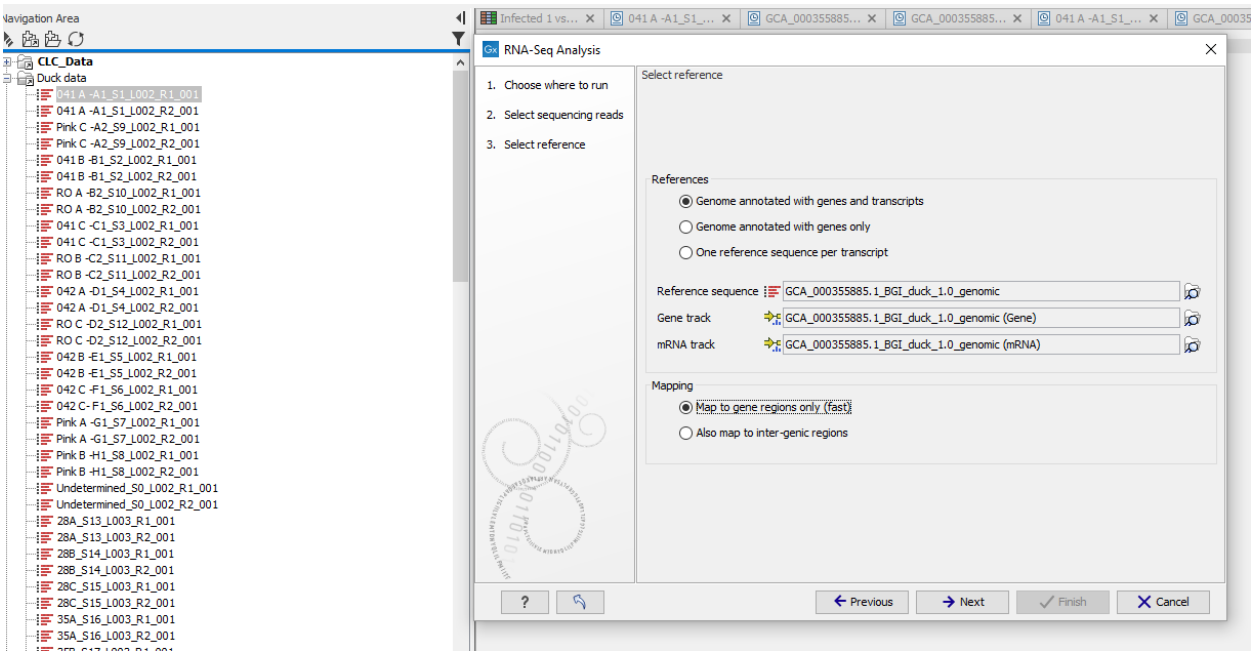
Navigation Area
CLC_Data
Duck data
041 A -A1_S1_L002_R1_001
041 A -A1_S1_L002_R2_001
Pink C -A2_S9_L002_R1_001
Pink C -A2_S9_L002_R2_001
041 B -B1_S2_L002_R1_001
041 B -B1_S2_L002_R2_001
RO A -B2_S10_L002_R1_001
RO A -B2_S10_L002_R2_001
041 C -C1_S3_L002_R1_001
041 C -C1_S3_L002_R2_001
RO B -C2_S11_L002_R1_001
RO B -C2_S11_L002_R2_001
042 A -D1_S4_L002_R1_001
042 A -D1_S4_L002_R2_001
RO C -D2_S12_L002_R1_001
RO C -D2_S12_L002_R2_001
042 B -E1_S5_L002_R1_001
042 B -E1_S5_L002_R2_001
042 C -F1_S6_L002_R1_001
042 C- F1_S6_L002_R2_001
Pink A -G1_S7_L002_R1_001
Pink A -G1_S7_L002_R2_001
Pink B -H1_S8_L002_R1_001
Pink B -H1_S8_L002_R2_001
Undetermined_S0_L002_R1_001
Undetermined_S0_L002_R2_001
28A_S13_L003_R1_001
28A_S13_L003_R2_001
28B_S14_L003_R1_001
28B_S14_L003_R2_001
28C_S15_L003_R1_001
28C_S15_L003_R2_001
35A_S16_L003_R1_001
35A_S16_L003_R2_001
RNA-Seq Analysis
1. Choose where to run
2. Select sequencing reads
3. Select reference
Select reference
References
Genome annotated with genes and transcripts
Genome annotated with genes only
One reference sequence per transcript
Reference sequence
GCA_000355885.1_BGI_duck_1.0_genomic
Gene track
GCA_000355885.1_BGI_duck_1.0_genomic (Gene)
mRNA track
GCA_000355885.1_BGI_duck_1.0_genomic (mRNA)
Mapping
Map to gene regions only (fast)
Also map to inter-genic regions
Previous
Next
Finish
Cancel

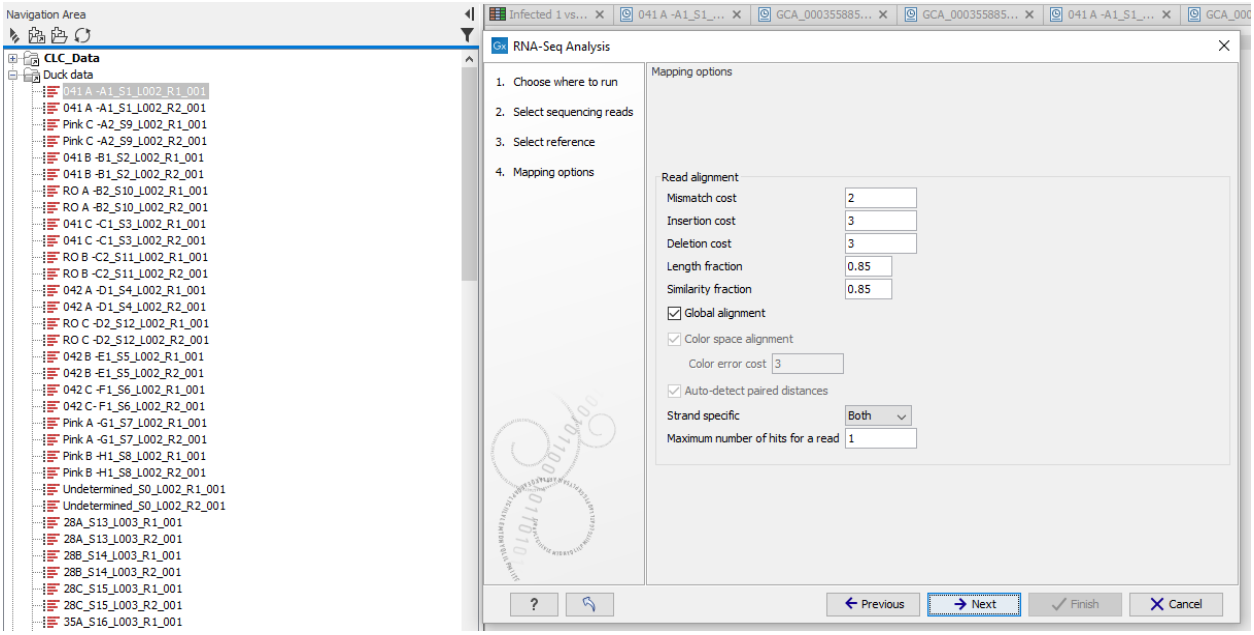
Navigation Area
CLC_Data
Duck data
041 A -A1_S1_L002_R1_001
041 A -A1_S1_L002_R2_001
Pink C -A2_S9_L002_R1_001
Pink C -A2_S9_L002_R2_001
041 B -B1_S2_L002_R1_001
041 B -B1_S2_L002_R2_001
RO A -B2_S10_L002_R1_001
RO A -B2_S10_L002_R2_001
041 C -C1_S3_L002_R1_001
041 C -C1_S3_L002_R2_001
RO B -C2_S11_L002_R1_001
RO B -C2_S11_L002_R2_001
042 A -D1_S4_L002_R1_001
042 A -D1_S4_L002_R2_001
RO C -D2_S12_L002_R1_001
RO C -D2_S12_L002_R2_001
042 B -E1_S5_L002_R1_001
042 B -E1_S5_L002_R2_001
042 C -F1_S6_L002_R1_001
042 C- F1_S6_L002_R2_001
Pink A -G1_S7_L002_R1_001
Pink A -G1_S7_L002_R2_001
Pink B -H1_S8_L002_R1_001
Pink B -H1_S8_L002_R2_001
Undetermined_S0_L002_R1_001
Undetermined_S0_L002_R2_001
28A_S13_L003_R1_001
28A_S13_L003_R2_001
28B_S14_L003_R1_001
28B_S14_L003_R2_001
28C_S15_L003_R1_001
28C_S15_L003_R2_001
35A_S16_L003_R1_001
RNA-Seq Analysis
1. Choose where to run
2. Select sequencing reads
3. Select reference
4. Mapping options
Mapping options
Read alignment
Mismatch cost
2
Insertion cost
3
Deletion cost
3
Length fraction
0.85
Similarity fraction
0.85
Global alignment
Color space alignment
Color error cost
3
Auto-detect paired distances
Strand specific
Both
Maximum number of hits for a read
1
Previous
Next
Finish
Cancel

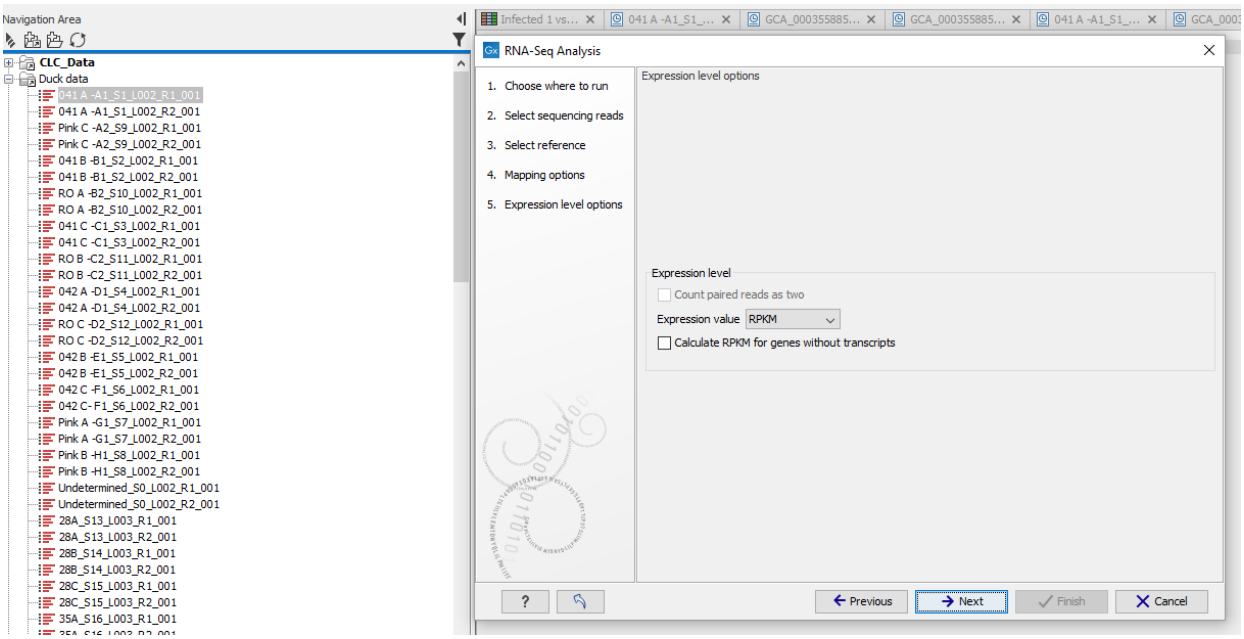
Navigation Area
CLC_Data
Duck data
041 A -A1_S1_L002_R1_001
041 A -A1_S1_L002_R2_001
Pink C -A2_S9_L002_R1_001
Pink C -A2_S9_L002_R2_001
041 B -B1_S2_L002_R1_001
041 B -B1_S2_L002_R2_001
RO A -B2_S10_L002_R1_001
RO A -B2_S10_L002_R2_001
041 C -C1_S3_L002_R1_001
041 C -C1_S3_L002_R2_001
RO B -C2_S11_L002_R1_001
RO B -C2_S11_L002_R2_001
042 A -D1_S4_L002_R1_001
042 A -D1_S4_L002_R2_001
RO C -D2_S12_L002_R1_001
RO C -D2_S12_L002_R2_001
042 B -E1_S5_L002_R1_001
042 B -E1_S5_L002_R2_001
042 C -F1_S6_L002_R1_001
042 C- F1_S6_L002_R2_001
Pink A -G1_S7_L002_R1_001
Pink A -G1_S7_L002_R2_001
Pink B -H1_S8_L002_R1_001
Pink B -H1_S8_L002_R2_001
Undetermined_S0_L002_R1_001
Undetermined_S0_L002_R2_001
28A_S13_L003_R1_001
28A_S13_L003_R2_001
28B_S14_L003_R1_001
28B_S14_L003_R2_001
28C_S15_L003_R1_001
28C_S15_L003_R2_001
35A_S16_L003_R1_001
Infected 1 vs...
041 A -A1_S1_...
GCA_000355885...
GCA_000355885...
041 A -A1_S1_...
RNA-Seq Analysis
1. Choose where to run
2. Select sequencing reads
3. Select reference
4. Mapping options
5. Expression level options
Expression level options
Expression level
Count paired reads as two
Expression value
RPKM
Calculate RPKM for genes without transcripts
Previous
Next
Finish
Cancel

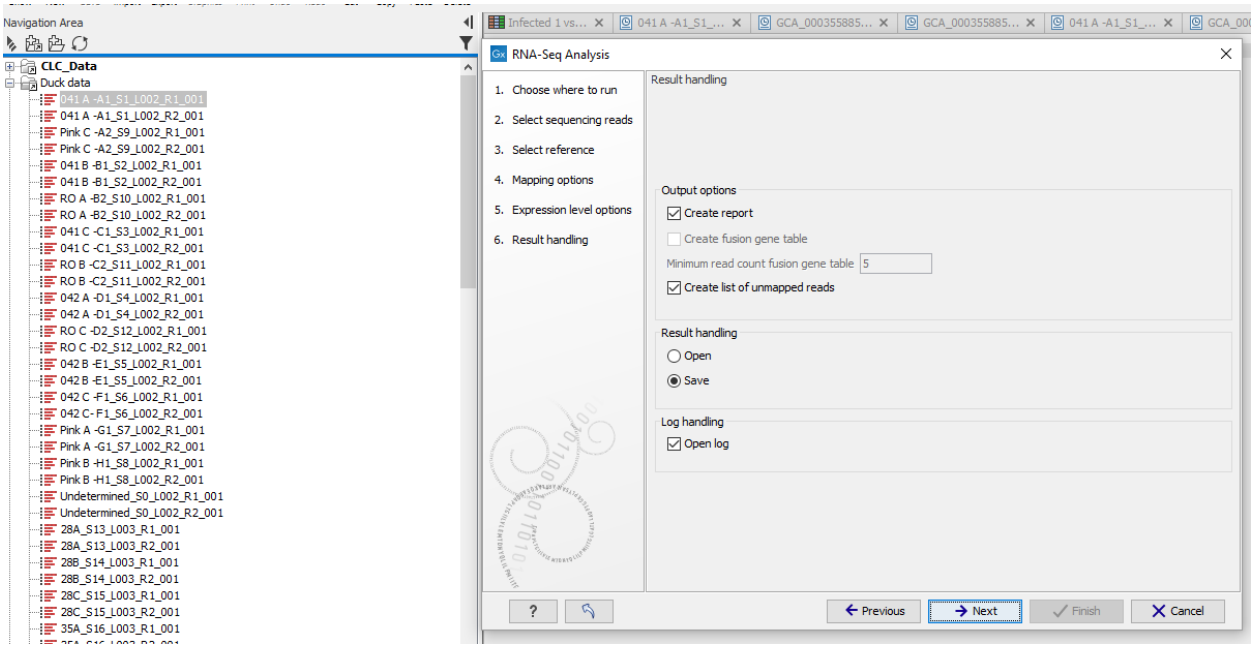
Navigation Area
CLC_Data
Duck data
041 A -A1_S1_L002_R1_001
041 A -A1_S1_L002_R2_001
Pink C -A2_S9_L002_R1_001
Pink C -A2_S9_L002_R2_001
041 B -B1_S2_L002_R1_001
041 B -B1_S2_L002_R2_001
RO A -B2_S10_L002_R1_001
RO A -B2_S10_L002_R2_001
041 C -C1_S3_L002_R1_001
041 C -C1_S3_L002_R2_001
RO B -C2_S11_L002_R1_001
RO B -C2_S11_L002_R2_001
042 A -D1_S4_L002_R1_001
042 A -D1_S4_L002_R2_001
RO C -D2_S12_L002_R1_001
RO C -D2_S12_L002_R2_001
042 B -E1_S5_L002_R1_001
042 B -E1_S5_L002_R2_001
042 C -F1_S6_L002_R1_001
042 C- F1_S6_L002_R2_001
Pink A -G1_S7_L002_R1_001
Pink A -G1_S7_L002_R2_001
Pink B -H1_S8_L002_R1_001
Pink B -H1_S8_L002_R2_001
Undetermined_S0_L002_R1_001
Undetermined_S0_L002_R2_001
28A_S13_L003_R1_001
28A_S13_L003_R2_001
28B_S14_L003_R1_001
28B_S14_L003_R2_001
28C_S15_L003_R1_001
28C_S15_L003_R2_001
35A_S16_L003_R1_001
Infected 1 vs...
041 A -A1_S1_...
GCA_000355885...
GCA_000355885...
041 A -A1_S1_...
RNA-Seq Analysis
1. Choose where to run
2. Select sequencing reads
3. Select reference
4. Mapping options
5. Expression level options
6. Result handling
Result handling
Output options
Create report
Create fusion gene table
Minimum read count fusion gene table
5
Create list of unmapped reads
Result handling
Open
Save
Log handling
Open log
Previous
Next
Finish
Cancel

Figure A4. CLC tool: Annotation with GFF file (Qiagen Inc.)

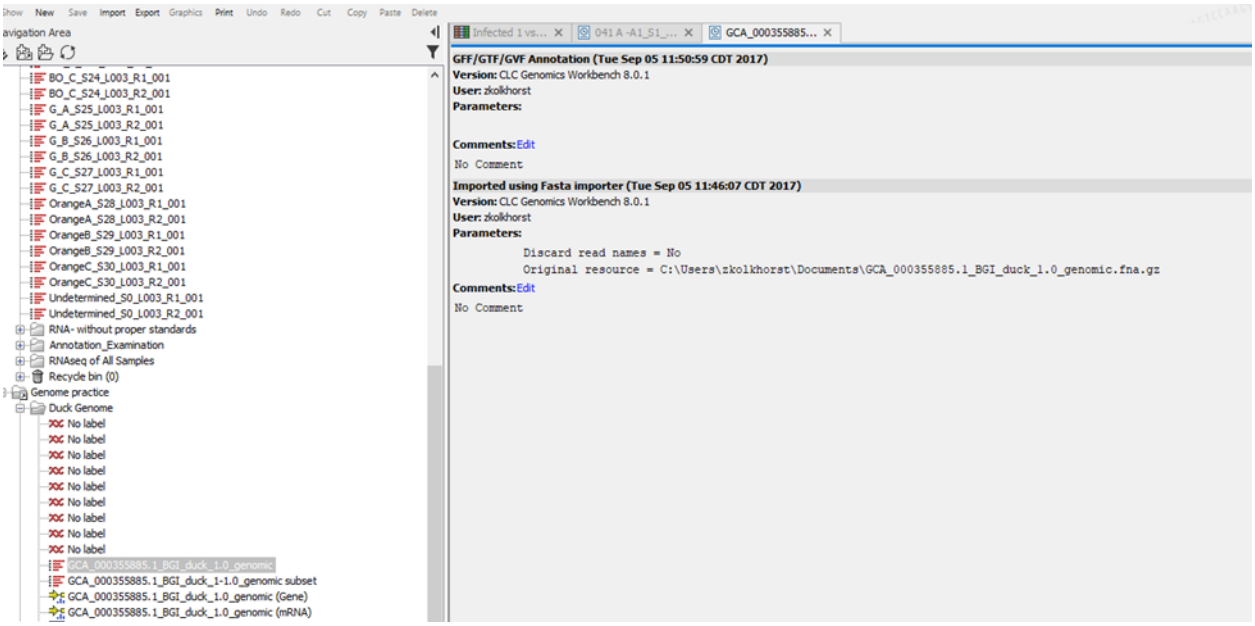

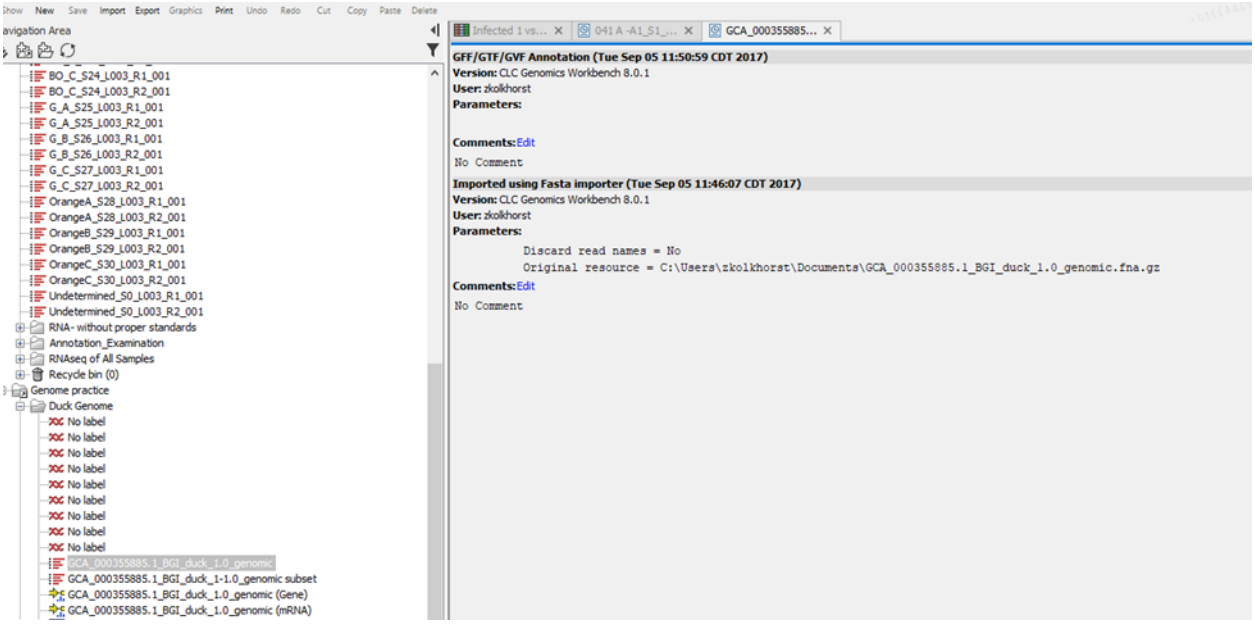
Navigation Area
BO_C_S24_L003_R1_001
BO_C_S24_L003_R2_001
G_A_S25_L003_R1_001
G_A_S25_L003_R2_001
G_B_S26_L003_R1_001
G_B_S26_L003_R2_001
G_C_S27_L003_R1_001
G_C_S27_L003_R2_001
OrangeA_S28_L003_R1_001
OrangeA_S28_L003_R2_001
OrangeB_S29_L003_R1_001
OrangeB_S29_L003_R2_001
OrangeC_S30_L003_R1_001
OrangeC_S30_L003_R2_001
Undetermined_S0_L003_R1_001
Undetermined_S0_L003_R2_001
RNA- without proper standards
Annotation_Examination
RNAseq of All Samples
Recycle bin (0)
Genome practice
Duck Genome
No label
GCA_000355885.1_BGI_duck_1.0_genomic
GCA_000355885.1_BGI_duck_1-1.0_genomic subset
GCA_000355885.1_BGI_duck_1.0_genomic (Gene)
GCA_000355885.1_BGI_duck_1.0_genomic (mRNA)
Infected 1 vs...
041 A -A1_S1_...
GCA_000355885...
GFF/GTF/GVF Annotation (Tue Sep 05 11:50:59 CDT 2017)
Version: CLC Genomics Workbench 8.0.1
User: zkolkhorst
Parameters:
Comments: Edit
No Comment
Imported using Fasta importer (Tue Sep 05 11:46:07 CDT 2017)
Version: CLC Genomics Workbench 8.0.1
User: zkolkhorst
Parameters:
Discard read names = No
Original resource = C:\Users\zkolkhorst\Documents\GCA_000355885.1_BGI_duck_1.0_genomic.fna.gz
Comments: Edit
No Comment

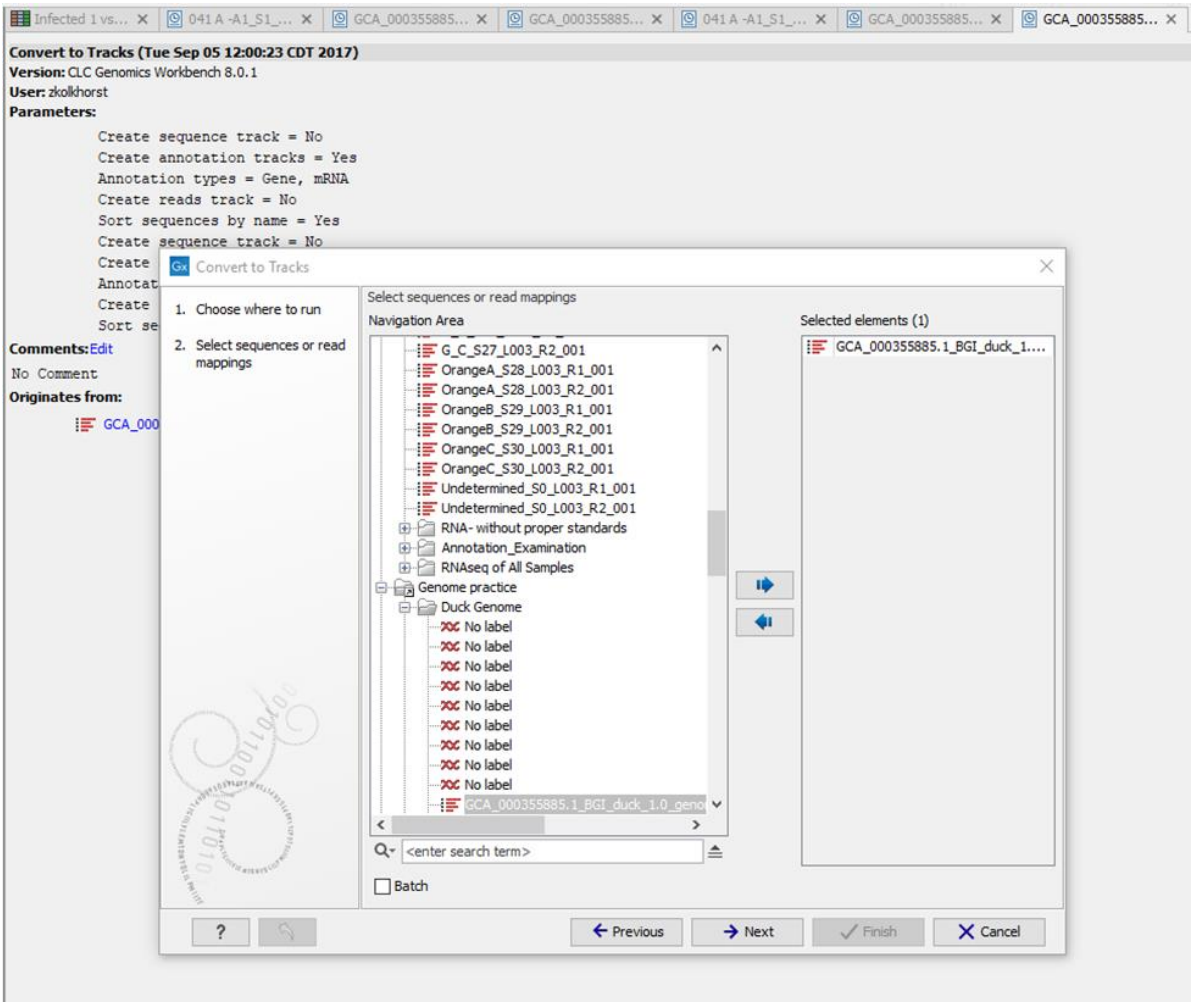
Infected 1 vs...
041 A -A1_S1_...
GCA_000355885...
GCA_000355885...
041 A -A1_S1_...
GCA_000355885...
GCA_000355885...
Convert to Tracks (Tue Sep 05 12:00:23 CDT 2017)
Version: CLC Genomics Workbench 8.0.1
User: zkolkhorst
Parameters:
Create sequence track = No
Create annotation tracks = Yes
Annotation types = Gene, mRNA
Create reads track = No
Sort sequences by name = Yes
Create sequence track = No
Comments: Edit
No Comment
Originates from:
Convert to Tracks
1. Choose where to run
2. Select sequences or read mappings
Select sequences or read mappings
Navigation Area
Selected elements (1)
GCA_000355885.1_BGI_duck_1....
<enter search term>
Batch
Previous
Next
Finish
Cancel

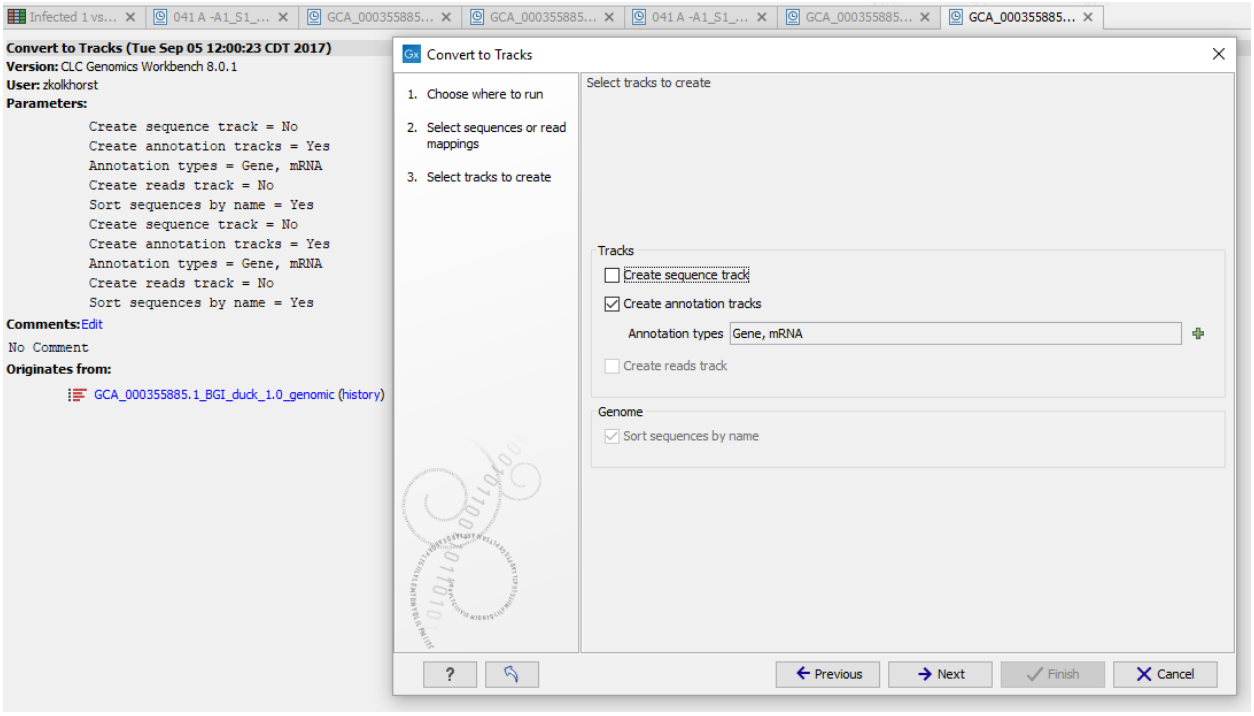

Figure A5. CLC tool: Set Up Experiment (Qiagen Inc.)

appendix

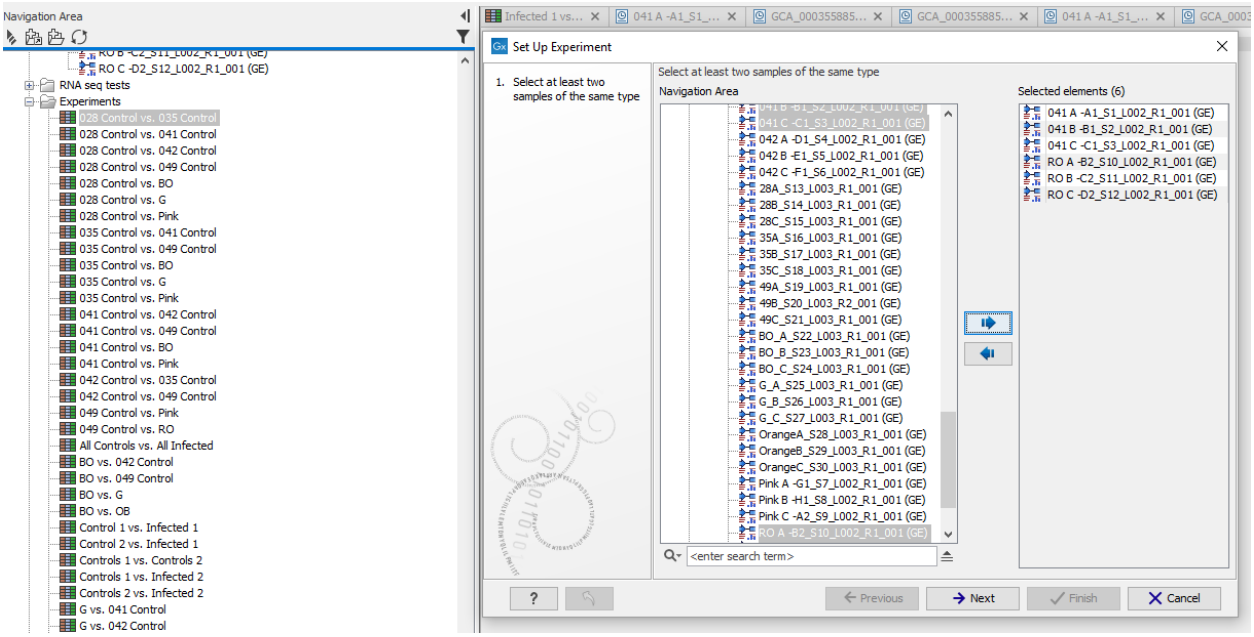

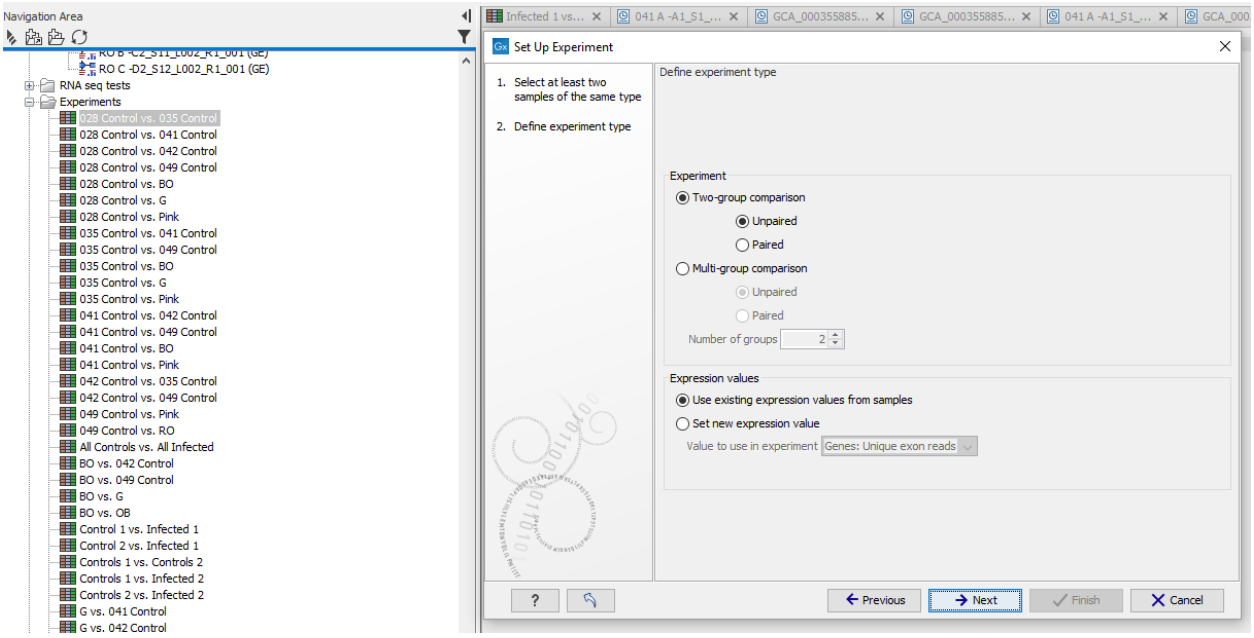
Navigation Area
RO C -D2_S12_L002_R1_001 (GE)
RNA seq tests
Experiments
028 Control vs. 035 Control
028 Control vs. 041 Control
028 Control vs. 042 Control
028 Control vs. 049 Control
028 Control vs. BO
028 Control vs. G
028 Control vs. Pink
035 Control vs. 041 Control
035 Control vs. 049 Control
035 Control vs. BO
035 Control vs. G
035 Control vs. Pink
041 Control vs. 042 Control
041 Control vs. 049 Control
041 Control vs. BO
041 Control vs. Pink
042 Control vs. 035 Control
042 Control vs. 049 Control
049 Control vs. Pink
049 Control vs. RO
All Controls vs. All Infected
BO vs. 042 Control
BO vs. 049 Control
BO vs. G
BO vs. OB
Control 1 vs. Infected 1
Control 2 vs. Infected 1
Controls 1 vs. Controls 2
Controls 1 vs. Infected 2
Controls 2 vs. Infected 2
G vs. 041 Control
G vs. 042 Control
Set Up Experiment
1. Select at least two samples of the same type
2. Define experiment type
Define experiment type
Experiment
Two-group comparison
Unpaired
Paired
Multi-group comparison
Unpaired
Paired
Number of groups
2
Expression values
Use existing expression values from samples
Set new expression value
Value to use in experiment
Genes: Unique exon reads
Previous
Next
Finish
Cancel

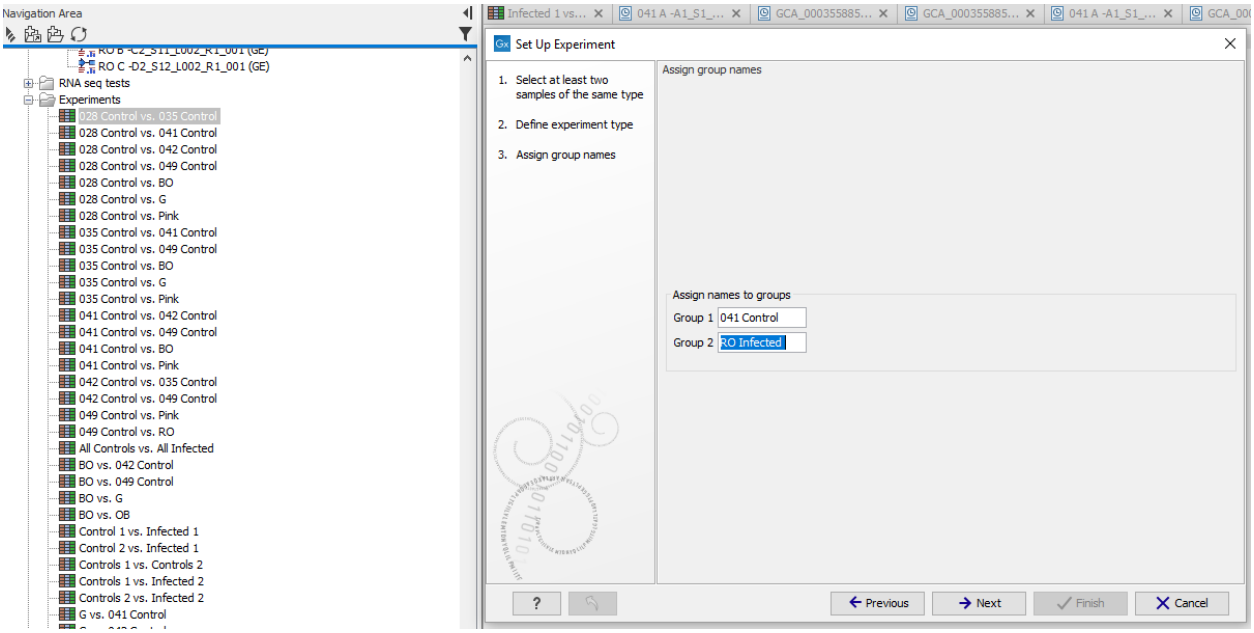
Navigation Area
RO C -D2_S12_L002_R1_001 (GE)
RNA seq tests
Experiments
028 Control vs. 035 Control
028 Control vs. 041 Control
028 Control vs. 042 Control
028 Control vs. 049 Control
028 Control vs. BO
028 Control vs. G
028 Control vs. Pink
035 Control vs. 041 Control
035 Control vs. 049 Control
035 Control vs. BO
035 Control vs. G
035 Control vs. Pink
041 Control vs. 042 Control
041 Control vs. 049 Control
041 Control vs. BO
041 Control vs. Pink
042 Control vs. 035 Control
042 Control vs. 049 Control
049 Control vs. Pink
049 Control vs. RO
All Controls vs. All Infected
BO vs. 042 Control
BO vs. 049 Control
BO vs. G
BO vs. OB
Control 1 vs. Infected 1
Control 2 vs. Infected 1
Controls 1 vs. Controls 2
Controls 1 vs. Infected 2
Controls 2 vs. Infected 2
G vs. 041 Control
Set Up Experiment
1. Select at least two samples of the same type
2. Define experiment type
3. Assign group names
Assign group names
Assign names to groups
Group 1
041 Control
Group 2
RO Infected
Previous
Next
Finish
Cancel

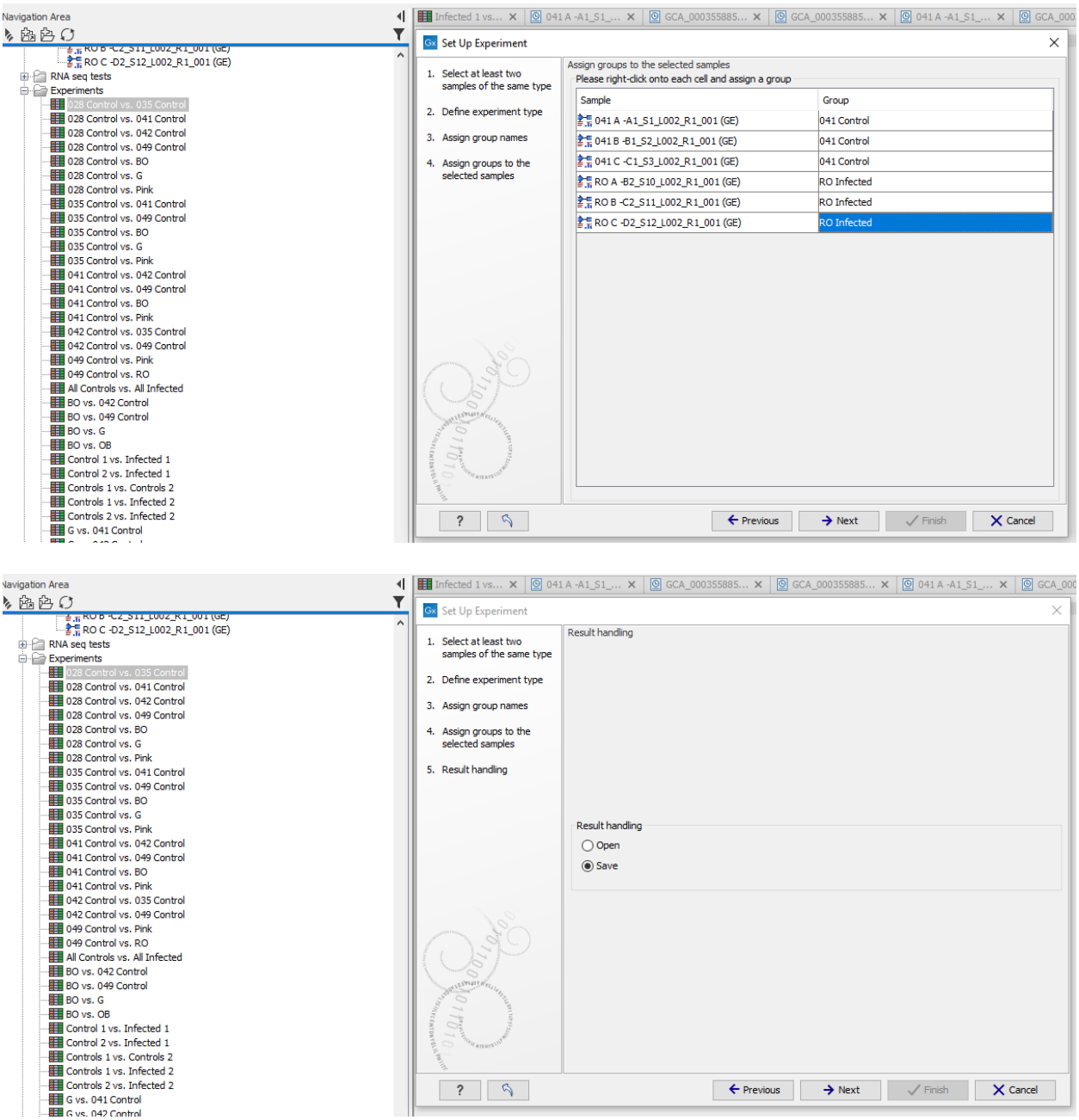

Figure A6. CLC tool: Empirical Analysis by DGE (Qiagen Inc.)

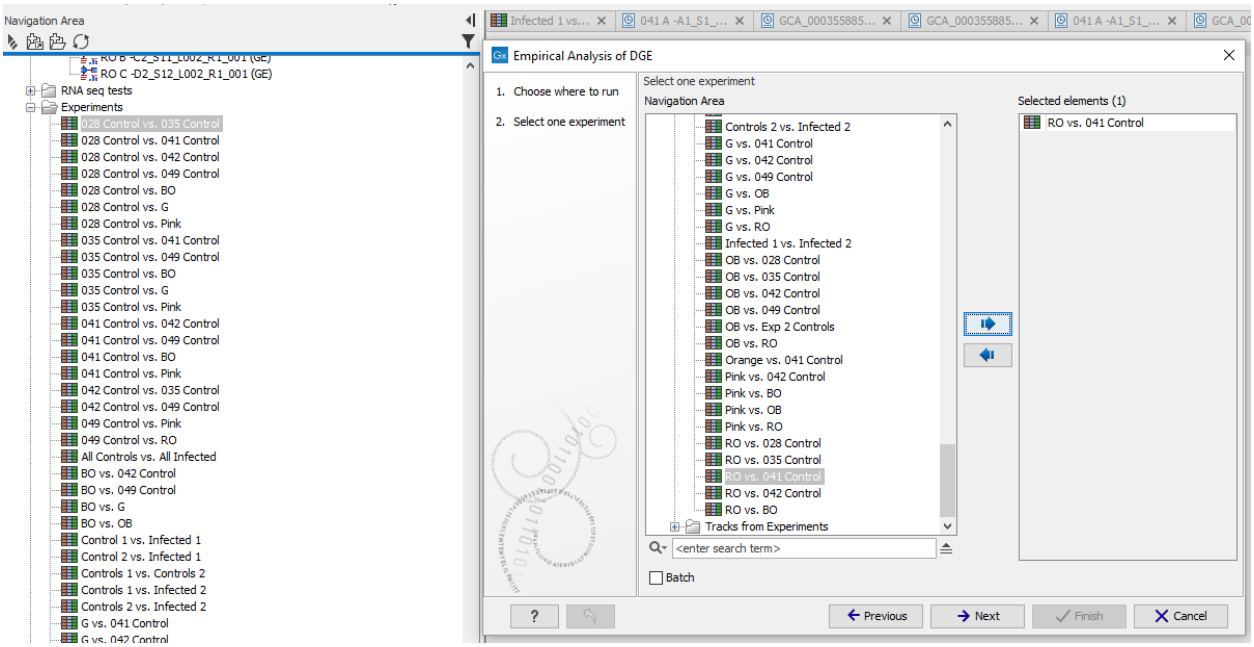
Navigation Area
RO C -D2_S12_L002_R1_001 (GE)
RNA seq tests
Experiments
028 Control vs. 035 Control
028 Control vs. 041 Control
028 Control vs. 042 Control
028 Control vs. 049 Control
028 Control vs. BO
028 Control vs. G
028 Control vs. Pink
035 Control vs. 041 Control
035 Control vs. 049 Control
035 Control vs. BO
035 Control vs. G
035 Control vs. Pink
041 Control vs. 042 Control
041 Control vs. 049 Control
041 Control vs. BO
041 Control vs. Pink
042 Control vs. 035 Control
042 Control vs. 049 Control
049 Control vs. Pink
049 Control vs. RO
All Controls vs. All Infected
BO vs. 042 Control
BO vs. 049 Control
BO vs. G
BO vs. OB
Control 1 vs. Infected 1
Control 2 vs. Infected 1
Controls 1 vs. Controls 2
Controls 1 vs. Infected 2
Controls 2 vs. Infected 2
G vs. 041 Control
G vs. 042 Control
Empirical Analysis of DGE
1. Choose where to run
2. Select one experiment
Select one experiment
Navigation Area
Controls 2 vs. Infected 2
G vs. 041 Control
G vs. 042 Control
G vs. 049 Control
G vs. OB
G vs. Pink
G vs. RO
Infected 1 vs. Infected 2
OB vs. 028 Control
OB vs. 035 Control
OB vs. 042 Control
OB vs. 049 Control
OB vs. Exp 2 Controls
OB vs. RO
Orange vs. 041 Control
Pink vs. 042 Control
Pink vs. BO
Pink vs. OB
Pink vs. RO
RO vs. 028 Control
RO vs. 035 Control
RO vs. 041 Control
RO vs. 042 Control
RO vs. BO
Tracks from Experiments
<enter search term>
Batch
Selected elements (1)
RO vs. 041 Control
Previous
Next
Finish
Cancel

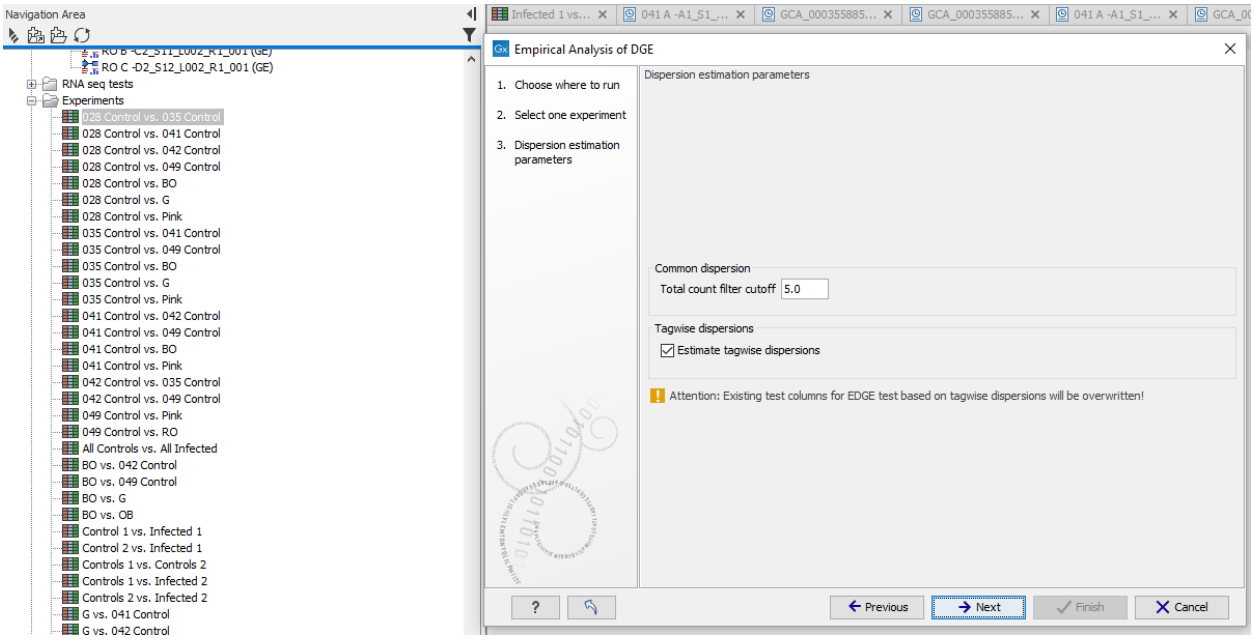
Navigation Area
RO C -D2_S12_L002_R1_001 (GE)
RNA seq tests
Experiments
028 Control vs. 035 Control
028 Control vs. 041 Control
028 Control vs. 042 Control
028 Control vs. 049 Control
028 Control vs. BO
028 Control vs. G
028 Control vs. Pink
035 Control vs. 041 Control
035 Control vs. 049 Control
035 Control vs. BO
035 Control vs. G
035 Control vs. Pink
041 Control vs. 042 Control
041 Control vs. 049 Control
041 Control vs. BO
041 Control vs. Pink
042 Control vs. 035 Control
042 Control vs. 049 Control
049 Control vs. Pink
049 Control vs. RO
All Controls vs. All Infected
BO vs. 042 Control
BO vs. 049 Control
BO vs. G
BO vs. OB
Control 1 vs. Infected 1
Control 2 vs. Infected 1
Controls 1 vs. Controls 2
Controls 1 vs. Infected 2
Controls 2 vs. Infected 2
G vs. 041 Control
G vs. 042 Control
Empirical Analysis of DGE
1. Choose where to run
2. Select one experiment
3. Dispersion estimation parameters
Dispersion estimation parameters
Common dispersion
Total count filter cutoff 5.0
Tagwise dispersions
Estimate tagwise dispersions
Attention: Existing test columns for EDGE test based on tagwise dispersions will be overwritten!
Previous
Next
Finish
Cancel

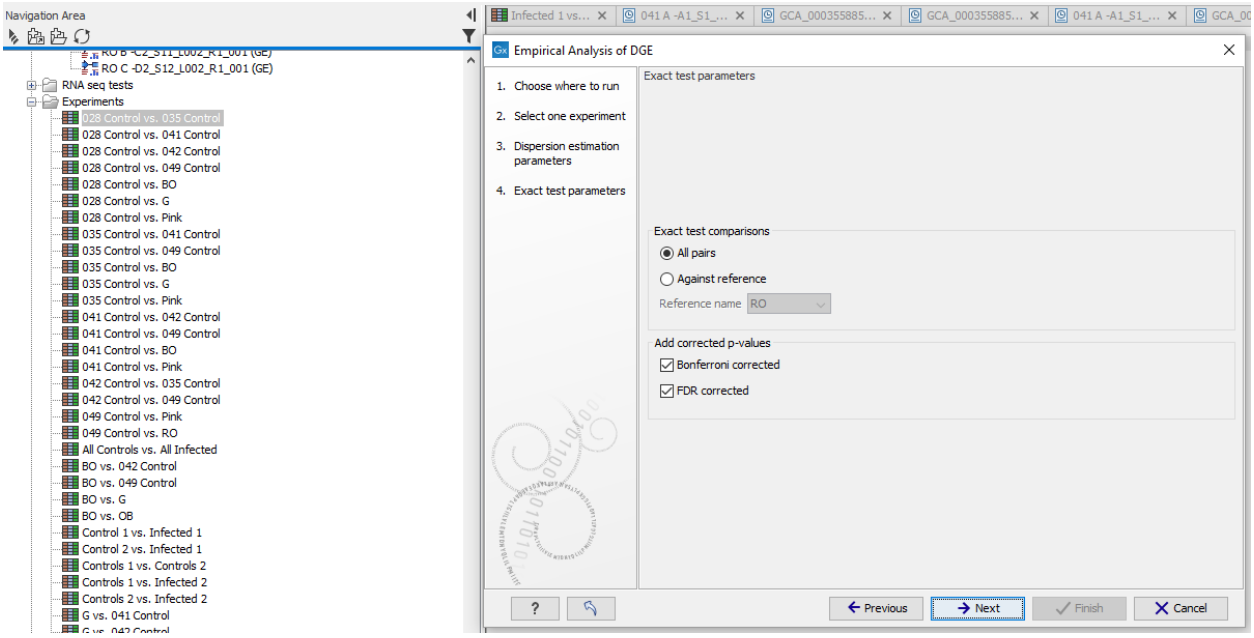
Navigation Area
RO C -D2_S12_L002_R1_001 (GE)
RNA seq tests
Experiments
028 Control vs. 035 Control
028 Control vs. 041 Control
028 Control vs. 042 Control
028 Control vs. 049 Control
028 Control vs. BO
028 Control vs. G
028 Control vs. Pink
035 Control vs. 041 Control
035 Control vs. 049 Control
035 Control vs. BO
035 Control vs. G
035 Control vs. Pink
041 Control vs. 042 Control
041 Control vs. 049 Control
041 Control vs. BO
041 Control vs. Pink
042 Control vs. 035 Control
042 Control vs. 049 Control
049 Control vs. Pink
049 Control vs. RO
All Controls vs. All Infected
BO vs. 042 Control
BO vs. 049 Control
BO vs. G
BO vs. OB
Control 1 vs. Infected 1
Control 2 vs. Infected 1
Controls 1 vs. Controls 2
Controls 1 vs. Infected 2
Controls 2 vs. Infected 2
G vs. 041 Control
Empirical Analysis of DGE
1. Choose where to run
2. Select one experiment
3. Dispersion estimation parameters
4. Exact test parameters
Exact test parameters
Exact test comparisons
All pairs
Against reference
Reference name
RO
Add corrected p-values
Bonferroni corrected
FDR corrected
Previous
Next
Finish
Cancel

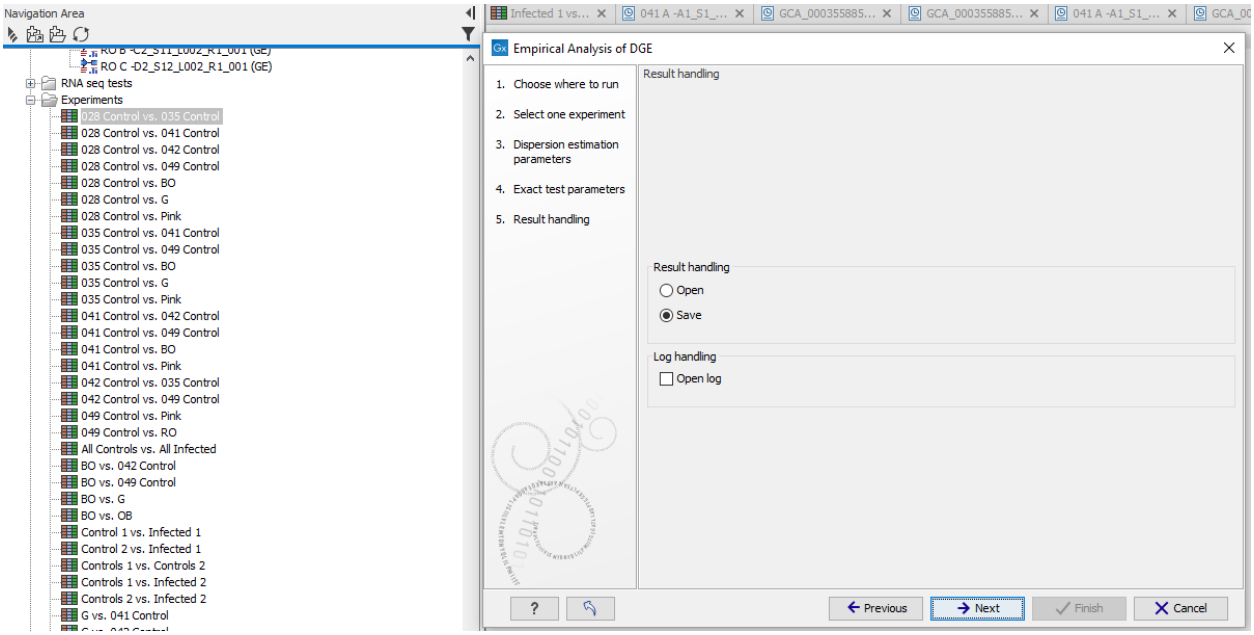
Navigation Area
RO C -D2_S12_L002_R1_001 (GE)
RNA seq tests
Experiments
028 Control vs. 035 Control
028 Control vs. 041 Control
028 Control vs. 042 Control
028 Control vs. 049 Control
028 Control vs. BO
028 Control vs. G
028 Control vs. Pink
035 Control vs. 041 Control
035 Control vs. 049 Control
035 Control vs. BO
035 Control vs. G
035 Control vs. Pink
041 Control vs. 042 Control
041 Control vs. 049 Control
041 Control vs. BO
041 Control vs. Pink
042 Control vs. 035 Control
042 Control vs. 049 Control
049 Control vs. Pink
049 Control vs. RO
All Controls vs. All Infected
BO vs. 042 Control
BO vs. 049 Control
BO vs. G
BO vs. OB
Control 1 vs. Infected 1
Control 2 vs. Infected 1
Controls 1 vs. Controls 2
Controls 1 vs. Infected 2
Controls 2 vs. Infected 2
G vs. 041 Control
Empirical Analysis of DGE
1. Choose where to run
2. Select one experiment
3. Dispersion estimation parameters
4. Exact test parameters
5. Result handling
Result handling
Result handling
Open
Save
Log handling
Open log
Previous
Next
Finish
Cancel

APPENDIX B

Table B1. Cloacal swab PCR and Mass of Ducks Results

Infected Duck Cloacal swabs and mass

Cloacal Swabs

Infected	Day 7	Day 14	Day 29	Day 43	Day 57	Day 71	Day 83
I1	-	-	-	-	-	-	-
I2	-	-	-	+	-	+	-
CS (Clinical Sign)	+	+	-	-	+		

Mass

Infected	Sex	Day 7/Dec 15, 2016	Day 14/Dec 22	Day 29/Jan 6, 2017	Day 43/Jan 20	Day 58/Feb 4	Day 71/Feb 17	Harvest Date
I1	Male	190.3	350	820	1110.00	1250	1260	1220
I2	Male	102.5	231	580	850.00	980	1020	1030
CS	Male	152.6	298.6	630	850.00	950	770	

Control Duck Cloacal swabs and mass

Cloacal Swabs

Control	Day 7	Day 14	Day 29	Day 43	Day 57	Day 71	Day 83
C1	-	-	-	-	-	-	-
C2	-	-	-	-	-	-	-
C3	-	-	-	-	-	-	-

Mass

Control	Sex	Day 7/Dec 15, 2016	Day 14/Dec 22	Day 29/Jan 6, 2017	Day 43/Jan 20	Day 58/Feb 4	Day 71/Feb 17	Harvest Date
C1	Female	140.5	326	710	900	950	1000	920
C2	Female	99.3	225	520	820	890	900	850
C3	Female	165.5	373	740	860	930	980	920

Table B2. Detailed RT-PCR and Western Blot Results

PCR and Western Blot Results						
	Controls			Infected		
	C1	C2	C3	I1	I2	CS
Western Blot Results						
Serum	-	-	-	+	-	+
PCR Results						
Cerebellum	-	-	-	+	+	+
Hindbrain	-	-	-	+	+	+
Forebrain						+
Midbrain						+
Spinal cord						+
Eye						+
Optic Nerve						+
Aqueous Humor						+
Intestine						+
Adrenal Gland						+
Kidney						+
Proventriculus						+
Ventriculus						+
Crop						+
Bursa						